1)For (2,1,3) convolutional code, $g^{(0)}$ = [1 0 1 1] and $g^{(1)}$ = [1 1 1 1] the generator polynomials are

$g^{(0)}(X) = 1 + X^2 + X^3$
$g^{(1)}(X) = 1 + X + X^2 + X^3$

and the information sequence d(X) = $1 + X^2 + X^3 + X^4$,find the code word

Ans:$C^{(0)}(X) = g^{(0)}(X).\ d(X)$

$C^{(0)}(X) = (1 + X^2 + X^3 + X^4)(1 + X^2 + X^3)$
$C^{(0)}(X) = (1 + X^2 + X^3 + X^4 + X^2 + X^4 + X^5 + X^6 + X^3 + X^5 + X^6 + X^7)$ $C^{(0)}(X) = (1 + X^2 + X^2 + X^3 + X^3 + X^4 + X^4 + X^5 + X^5 + X^6 + X^6 + X^7)$ $C^{(0)}(X) = (1 + X^7)$

$C^{(1)}(X) = g^{(1)}(X).\ d(X)$
$C^{(1)}(X) = (1 + X^2 + X^3 + X^4)(1 + X + X^2 + X^3)$
$C^{(1)}(X) = (1 + X^2 + X^3 + X^4 + X + X^3 + X^4 + X^5 + X^2 + X^4 + X^5 + X^6 = +X^3 + X^5 + X^6 + X^7)$
$C^{(1)}(X) = 1 + X + X^3 + X^4 + X^5 + X^7$

and the code word is
$C(X) = [1 + X^7,\ 1 + X + X^3 + X^4 + X^5 + X^7]$

After multiplexing, the code word become

$C(X) = C^{(0)}(X^2) + XC^{(1)}(X^2)$

$C^{(0)}(X^2) = (1 + X^{14})$
$C^{(1)}(X^2) = XC^{(1)}(X^2) = X(1 + X^2 + X^6 + X^8 + X^{10} + +X^{14})$
$C^{(1)}(X^2) = XC^{(1)}(X^2) = X + X^3 + X^7 + X^9 + X^{11} + +X^{15}$

$C(X) = C^{(0)}(X^2) + XC^{(1)}(X^2)$
$C(X) = 1 + X + X^3 + X^7 + X^9 + X^{11} + X^{14} + X^{15}$
C = [11 01 00 01 01 01 01 11]

The result is the same as convolution and matrix multiplication.

2)For (3,2,3) convolutional encoder
$g^{(0)}{}_1 = (1\ 1)$, $g^{(1)}{}_1 = (0\ 1)$, $g^{(2)}{}_1 = (1\ 1)$
$g^{(0)}{}_2 = (0\ 1)$, $g^{(1)}{}_2 = (1\ 0)$, $g^{(2)}{}_2 = (1\ 0)$

$$\begin{bmatrix} 1+X & X & 1+X \\ X & 1 & 1 \end{bmatrix}$$

and the information sequence $d^{(1)}(X) = 1 + X^2$, $d^{(2)}(X) = 1 + X$, find the encoding equations of the codeword
Ans:

$$C(X) = [C^{(0)}(X), C^{(1)}(X), C^{(2)}(X)]$$

$$\begin{bmatrix} 1+X & X & 1+X \\ X & 1 & 1 \end{bmatrix}$$

$C(X) = [1 + X^2, 1 + X]$

$C(X) = [(1 + X^2).(1 + X) + (1 + X)X, (1 + X^2).X + (1 + X)1,$
$= (1 + X^2).(1 + X) + (1 + X)1]$
$C(X) = [1 + X^3, 1 + X^3, X^2 + X^3]$

After multiplexing, the code word become

$C(X) = C^{(0)}(X^n) + XC^{(1)}(X^n) + \ldots + X^{(n-1)}C^{(n-1)}(X^n)$
$C(X) = (1 + X^3)^3 + X(1 + X^3)^3 + X^2(X^2 + X^3)^3$
$C(X) = (1 + X^9) + X(1 + X^9) + X^2(X^6 + X^9)$
$C(X) = 1 + X + X^8 + X^9 + X^{10} + X^{11}$

C=[11 00 00 00 11 11 00 00]

Coherent binary modulation techniques

Coherent binary PSK

In coherent binary PSK system, the pair of signals, $s_1(t)$ and $s_2(t)$ used to represent binary symbols 1 and 0 respectively

$$s_1(t) = \sqrt{\frac{2E_b}{T_b}} \cos 2\pi f_c t \quad \text{—— For symbol 1}$$

$$s_2(t) = \sqrt{\frac{2E_b}{T_b}} [\cos 2\pi f_c t + \pi) \quad \text{—— For symbol 0}$$

$$s_2(t) = -\sqrt{\frac{2E_b}{T_b}} \cos 2\pi f_c t. \qquad 0 \le t \le T_b$$

Where E_b is the transmitted signal energy per bit and f_c is the carrier frequency.

$$f_c = \frac{n_c}{T_b}$$

The basis function of unit energy is given by

$$\phi_1(t) = \sqrt{\frac{2}{T_b}} \cos 2\pi f_c t \qquad 0 \le t \le T_b.$$

then

$$s_1(t) = \sqrt{E_b}\, \phi_1(t) \qquad 0 \le t \le T_b$$

$$s_2(t) = -\sqrt{E_b}\, \phi_1(t) \qquad 0 \le t \le T_b$$

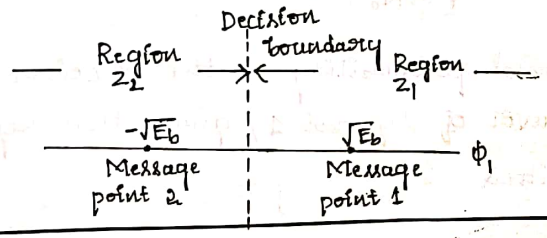

Figure shows Signal space for the coherent binary PSK with one dimensional [N=1] & with two message points [M=2].

The co-ordinates of the message points are.

$$S_{11} = \int_0^{T_b} S_1(t)\,\phi_1(t).\,dt = +\sqrt{E_b}$$

$$S_{21} = \int_0^{T_b} S_2(t)\,\phi_1(t).\,dt = -\sqrt{E_b}$$

To calculate the probability of error, decision region associated with symbol 1 or $S_1(t)$ is given by.

$$Z_1 : 0 \leq x_1 \leq +\infty$$

where x_1 is the observation vector.

$$x_1 = \int_0^{T_b} x(t)\,\phi_1(t).\,dt.$$

Where $x(t)$ is the received signal.

The maximum likelihood function when symbol 0 or $S_2(t)$ is transmitted is defined by

$$f_{X_1}(x_1|0) = \frac{1}{\sqrt{\pi N_0}} \exp\left[-\frac{1}{N_0}(x_1 - S_{21})^2\right]$$

$$= \frac{1}{\sqrt{\pi N_0}}\, e^{\left[-\frac{1}{N_0}(x_1 + \sqrt{E_b})^2\right]}$$

The conditional probability of the receiver deciding in favor of symbol 1, given that symbol 0 was transmitted is

$$P_e(0) = \int_0^{\infty} f_{X_1}(x_1|0).\, dx_1$$

$$= \frac{1}{\sqrt{\pi N_0}} \int_0^{\infty} e^{\left(-\frac{1}{N_0}(x_1+\sqrt{E_b})^2\right)} .\, dx_1$$

put $Z = \dfrac{(x_1+\sqrt{E_b})}{\sqrt{N_0}}$

$$dz = \frac{dx_1 + 0}{\sqrt{N_0}}$$

$$dx_1 = dz\sqrt{N_0}$$

when $x_1 = 0$ $\quad x_1 = \infty$

$Z = \dfrac{x_1+\sqrt{E_b}}{\sqrt{N_0}}$ $\quad Z = \infty$

$Z = \dfrac{0+\sqrt{E_b}}{\sqrt{N_0}}$

$Z = \sqrt{\dfrac{E_b}{N_0}}$

Then

$$P_e(0) = \frac{1}{\sqrt{\pi N_0}} \int_{\sqrt{Eb/No}}^{\infty} e^{-z^2} .\, dz .\sqrt{N_0}$$

$$P_e(0) = \frac{1}{\sqrt{\pi}} \cdot \frac{2}{2} \int_{\sqrt{Eb/No}}^{\infty} e^{-z^2} .\, dz.$$

$$P_e(0) = \frac{1}{2}\left[\frac{2}{\sqrt{\pi}} \int_{\sqrt{Eb/No}}^{\infty} e^{-z^2} .\, dz\right]$$

$$\operatorname{erfc}(u) = \frac{1}{\sqrt{\pi}} \int_u^{\infty} e^{-u^2} .\, du$$

$$P_e(0) = \frac{1}{2} \operatorname{erfc}\left[\sqrt{\frac{E_b}{N_0}}\right]$$

Similarly we can calculate $P_e(1)$, the conditional probability of receiver deciding in favour of symbol 0 given that symbol 1 was transmitted.

$$P_e(1) = \frac{1}{2} \operatorname{erfc}\left[\sqrt{Eb/No}\right)$$

Then average probability of error

$$P_e = P(0)\,P_e(0) + P(1)\,P_e(1)$$

$$= \frac{1}{2}\left[\frac{1}{2}\operatorname{erfc}\sqrt{E_b/N_0}\right] + \frac{1}{2}\left[\frac{1}{2}\operatorname{erfc}\sqrt{E_b/2}\right]$$

$$\left\langle P_e = \frac{1}{2}\operatorname{erfc}\sqrt{\frac{E_b}{N_0}} \right\rangle$$

Binary PSK transmitter

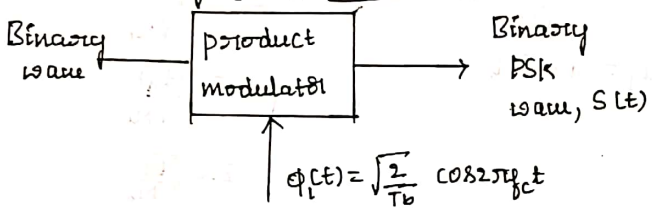

Coherent binary PSK receiver

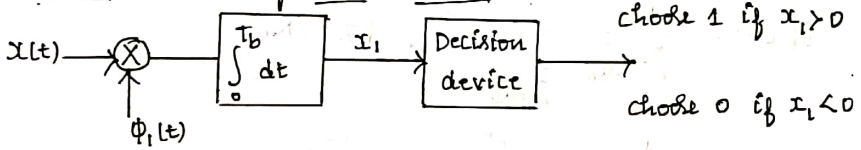

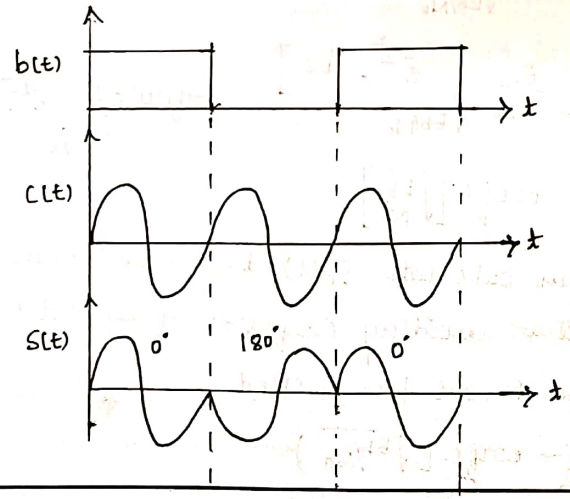

Coherent Binary FSK.

In binary FSK system, symbols 1 and 0 are distinguished from each other by transmitting one of two sinusoidal waves that differ in frequency by a fixed amount.

Binary FSK transmitter.

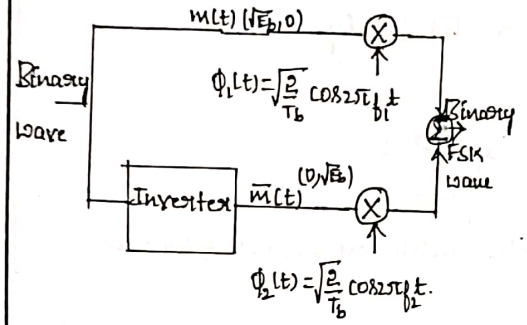

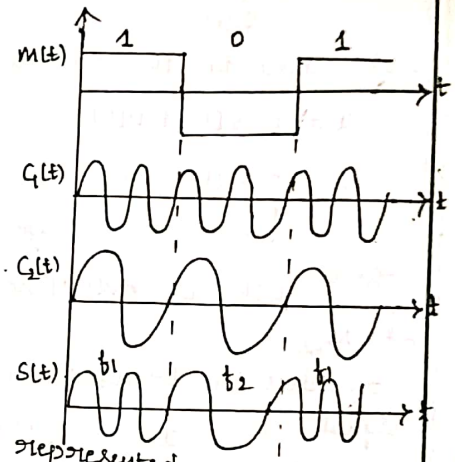

* The binary FSK wave can be represented as follows

$$S(t) = \begin{cases} S_1(t) = \sqrt{\frac{2E_b}{T_b}} \cos 2\pi f_1 t & 0 \le t \le T_b \text{ for symbol '1'} \\ S_2(t) = \sqrt{\frac{2E_b}{T_b}} \cos 2\pi f_2 t & 0 \le t \le T_b \text{ for symbol '0'.} \end{cases}$$

* The basis function $\phi_1(t)$ and $\phi_2(t)$ are defined by

$$\phi_1(t) = \sqrt{2/T_b} \cos 2\pi f_1 t \quad \text{and} \quad \phi_2(t) = \sqrt{2/T_b} \cos 2\pi f_2 t$$

$$\therefore S(t) = \begin{cases} S_1(t) = \sqrt{E_b}\, \phi_1(t) & \text{for symbol 1} \\ S_2(t) = \sqrt{E_b}\, \phi_2(t) & \text{for symbol 0} \end{cases}$$

Where $\phi_1(t)$ and $\phi_2(t)$ are two orthonormal basis functions. It is seen that signal space is two dimensional and there are two message points. [N=2 & M=2]

Coherent detection of BFSK.

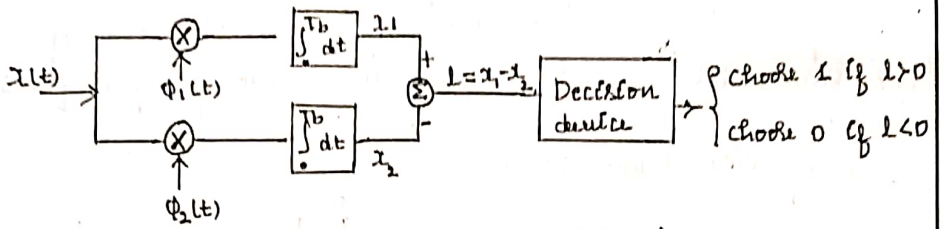

Let $x(t)$ be the received BFSK signal.

$$x(t) = s(t) + w(t)$$

$$x = \begin{cases} s_1(t) + w(t) & \text{for symbol 1} \\ s_2(t) + w(t) & \text{for symbol 0} \end{cases}$$

Where $w(t)$ is AWGN noise with mean $\mu = 0$ & Variance $\sigma^2 = N_0/2$

Consider the transmission of symbol '0' then the received signal is $x(t) = s_2(t) + w(t)$

The output of top correlator is

$$x_1 = \int_0^{T_b} x(t)\, \phi_1(t)\, dt.$$

$$x_1 = \int_0^{T_b} [s_2(t) + w(t)]\, \phi_1(t)\, dt.$$

$$= \int_0^{T_b} s_2(t).\, \phi_1(t)\, dt + \int_0^{T_b} w(t)\, \phi_1(t)\, dt.$$

$$x_1 = s_{21} + w_1$$

$$x_1 = 0 + w_1$$

Mean is given by

$$E[X_1] = E[0 + W_1]$$

$$= 0 + 0$$

$$\langle E[X_1] = 0 \rangle$$

Variance of x_1 is

$$\text{Var}[X_1] = \text{Var}[0 + W_1]$$

$$= 0 + N_0/2$$

$$\langle \text{Var}[X_1] = N_0/2 \rangle$$

* The output of bottom correlator is

$$x_2 = \int_0^{T_b} x(t)\, \phi_2(t)\, dt.$$

$$= \int_0^{T_b} [s_2(t) + w(t)]\, \phi_2(t)\, dt$$

$$x_2 = \int_0^{T_b} s_2(t)\, \phi_2(t)\, dt + \int_0^{T_b} w(t)\, \phi_2(t)\, dt$$

$$x_2 = s_{2,2} + w_2$$

$$\langle x_2 = \sqrt{E_b} + w_2 \rangle$$

* Mean of x_2 is

$$E[X_2] = E[\sqrt{E_b} + w_2] = \sqrt{E_b}.$$

* Variance of x_2 is

$$\text{Var}[X_2] = \text{Var}[\sqrt{E_b} + w_2] = \frac{N_0}{2}$$

* Let l be the random variable defined as the difference of two random variables x_1 and x_2 i.e $l = x_1 - x_2$

Mean of l

$$E[L] = E[X_1] - E[X_2]$$

$$= 0 - \sqrt{E_b}$$

$$\boxed{E[L] = -\sqrt{E_b}}$$

Variance of l

$$\text{Var}[L] = \text{Var}[X_1] + \text{Var}[X_2]$$

$$= \frac{N_0}{2} + \frac{N_0}{2}$$

$$\boxed{\text{Var}[L] = N_0}$$

* The conditional probability density function [PDF] when symbol '0' is transmitted is given by

$$f_L(l/0) = \frac{1}{\sqrt{2\pi\sigma^2}} \exp\left[-\frac{(l-\mu)^2}{2\sigma^2}\right]$$

$\sigma^2 = N_0$, $\mu = -\sqrt{E_b}$

$$f_L(l/0) = \frac{1}{\sqrt{2\pi N_0}} \exp\left[-\frac{(l+\sqrt{E_b})^2}{2N_0}\right]$$

$$f_L(l/0) = \frac{1}{\sqrt{2\pi N_0}} \exp\left[-\left(\frac{l+\sqrt{E_b}}{\sqrt{2N_0}}\right)^2\right]$$

* $P_e(0)$ denote the probability of symbol error when receiver decides in favour of symbol '1' when symbol '0' was transmitted

$\therefore$ Region Z_1 : $0 \le x \le \infty$

$$P_e(0) = \int_0^\infty f_L(l/0)\, dl$$

$$= \int_0^\infty \frac{1}{\sqrt{2\pi N_0}} \cdot e^{-\left(\frac{l+\sqrt{E_b}}{\sqrt{2N_0}}\right)^2} \cdot dl.$$

Let $Z = \frac{l+\sqrt{E_b}}{\sqrt{2N_0}}$

$dz = \frac{dl + 0}{\sqrt{2N_0}}$

$dl = dz \cdot \sqrt{2N_0}$

when $l = 0$

$Z = \frac{l+\sqrt{E_b}}{\sqrt{2N_0}}$

$Z = \frac{0+\sqrt{E_b}}{\sqrt{2N_0}}$

$Z = \sqrt{\frac{E_b}{2N_0}}$

when $l = \infty$

$Z = \infty$

When,

$$P_e(0) = \int_{\sqrt{E_b/2N_0}}^{\infty} \frac{1}{\sqrt{2\pi N_0}} \cdot e^{-(z)^2} \cdot dz \cdot \sqrt{2N_0}.$$

$$= \frac{1}{\sqrt{\pi}} \cdot \int_{\sqrt{\frac{E_b}{2N_0}}}^{\infty} e^{-(z)^2} \cdot dz$$

$$P_e(0) = \frac{1}{\sqrt{\pi}} \times \frac{1}{2} \int_{\sqrt{E_b/N_0}}^{\infty} e^{-(z)^2} \cdot dz.$$

W.K.T complementary error function is

$$erfc(u) = \frac{2}{\sqrt{\pi}} \int_{u}^{\infty} \exp(-t^2) \cdot dt.$$

then

$$P_e(0) = \frac{1}{2} erfc\left[\sqrt{\frac{E_b}{2N_0}}\right]$$

Similarly we can calculate $P_e(1)$

$P_e(1)$ denote the probability of symbol error when symbol 1 is transmitted & decision is taken in favour of symbol 0.

$$P_e(1) = \frac{1}{2} erfc\left[\sqrt{\frac{E_b}{2N_0}}\right]$$

$$P_e(0) = P_e(1)$$

The average probability of error is

$$P_e = P(0) P_e(0) + P(1) P_e(1)$$

$$= \frac{1}{2}\left[\frac{1}{2} erfc\left(\sqrt{\frac{E_b}{N_0}}\right)\right] + \frac{1}{2}\left[\frac{1}{2} erfc\left(\sqrt{\frac{E_b}{N_0}}\right)\right]$$

$$P_e = \frac{1}{2} erfc\left[\sqrt{\frac{E_b}{N_0}}\right]$$

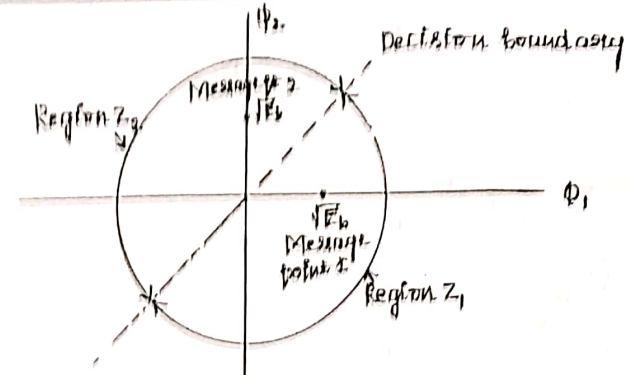

Signal space diagram for coherent binary FSK system
[N=2, M=2]

$$S_{ij} = \int_0^{T_b} S_i(t)\, \phi_j(t)\, dt$$

$$= \int_0^{T_b} \sqrt{\frac{2E_b}{T_b}} \cos 2\pi f_i t \cdot \sqrt{\frac{2}{T_b}} \cos 2\pi f_j t \cdot dt.$$

$$S_{ij} = \begin{cases} \sqrt{E_b} & i=j \\ 0 & i \neq j \end{cases}$$

$$S_1 = \begin{bmatrix} S_{11} \\ S_{12} \end{bmatrix} = \begin{bmatrix} \sqrt{E_b} \\ 0 \end{bmatrix}$$

$$S_2 = \begin{bmatrix} S_{21} \\ S_{22} \end{bmatrix} = \begin{bmatrix} 0 \\ \sqrt{E_b} \end{bmatrix}$$

Minimum shift keying

Minimum shift keying is a form of continous phase frequency shift keying, providing spectrum efficiency & enabling efficient RF power amplifier operation

MSK is a form of frequency modulation based on system called continous-phase frequency-shift keying.

The continous-phase frequency-shift keying [CPFSK] signal for the interval $0 \le t \le T_b$ is given by

$$S(t) = \begin{cases} \sqrt{\frac{2E_b}{T_b}} \cos[2\pi f_1 t + \theta(0)] & \text{for symbol 1} \\ \sqrt{\frac{2E_b}{T_b}} \cos[2\pi f_2 t + \theta(0)] & \text{for symbol 0} \end{cases} \rightarrow (1)$$

Where $E_b \rightarrow$ Transmitted signal energy per bit.

$T_b \rightarrow$ Bit duration

$\theta(0) \rightarrow$ Value of the phase at time $t=0$

The frequencies f_1 and f_2 are sent in response to binary symbols 1 and 0 respectively.

Another way of representing the CPFSK signal S(t) as

$$S(t) = \sqrt{\frac{2E_b}{T_b}} \cos[2\pi f_c t + \theta(t)] \quad \text{---------- (2)}$$

Where $\theta(t) \rightarrow$ phase of S(t). It is continous function of time

$f_c \rightarrow$ carrier frequency.

$$f_c = \frac{1}{2}[f_1 + f_2] \quad \text{---------- (3)}$$

* The phase $\theta(t)$ of CPFSK signal increases or decreases linearly with time

$$\theta(t) = \theta(0) \pm \frac{\pi h}{T_b} t \qquad 0 \le t \le T_b \quad \text{——— (1)}$$

'+' sign corresponds to sending symbol '1'

'−' sign corresponds to sending symbol '0'

$h \rightarrow$ deviation ratio

$$h = T_b [f_1 - f_2]$$

* At time $t = T_b$

$$\theta(T_b) - \theta(0) = \begin{cases} \pi h & \text{for symbol 1} \\ -\pi h & \text{for symbol 0} \end{cases}$$

The eqn (2) $S(t) = \sqrt{\frac{2E_b}{T_b}} \cos[2\pi f_c t + \theta(t)]$ is written as

$$S(t) = \sqrt{\frac{2E_b}{T_b}} \cos[\theta(t)] \cdot \cos 2\pi f_c t - \sqrt{\frac{2E_b}{T_b}} \sin[\theta(t)] \sin 2\pi f_c t.$$

$$S(t) = S_I(t) \cos 2\pi f_c t - S_Q(t) \sin 2\pi f_c t.$$

With deviation ration $h = 1/2$, equation (1) can be written as

$$\theta(t) = \theta(0) \pm \frac{\pi}{2T_b} t \qquad 0 \le t \le T_b$$

* The In-phase component $S_I(t)$

$$S_I(t) = \sqrt{\frac{2E_b}{T_b}} \cos[\theta(t)] = \sqrt{\frac{2E_b}{T_b}} \cos\left[\theta(0) \pm \frac{\pi}{2T_b} t\right]$$

$$S_I(t) = \sqrt{\frac{2E_b}{T_b}} \cos[\theta(0)] \cos\left[\frac{\pi}{2T_b} t\right]$$

$$S_I(t) = \pm\sqrt{\frac{2E_b}{T_b}} \cos\left[\frac{\pi}{2T_b} t\right] \qquad -T_b \le t \le T_b$$

$+ \rightarrow \theta(0) = 0$ & $- \rightarrow \theta(0) = \pi$

The Quadrature component $S_Q(t)$

$$S_Q(t) = \sqrt{\frac{2E_b}{T_b}} \sin[\theta(t)] = \sqrt{\frac{2E_b}{T_b}} \sin(\theta(T_b) \pm [\pi/2T_b]t)$$

$$S_Q(t) = \sqrt{\frac{2E_b}{T_b}} \sin[\theta(T_b)] \sin[\pi/2T_b]t$$

$$S_Q(t) = \pm\sqrt{\frac{2E_b}{T_b}} \sin\left(\frac{\pi}{2T_b}t\right) \qquad 0 \le t \le 2T_b$$

$+ \longrightarrow \theta(T_b) = \pi/2$

$- \longrightarrow \theta(T_b) = -\pi/2$

* The orthonormal basis functions are

$$\phi_1(t) = \sqrt{\frac{2}{T_b}} \cos\left(\frac{\pi}{2T_b}t\right) \cos 2\pi f_c t \qquad -T_b \le t \le T_b$$

and

$$\phi_2(t) = \sqrt{\frac{2}{T_b}} \sin\left[\frac{\pi}{2T_b}t\right] \sin 2\pi f_c t \qquad 0 \le t \le 2T_b$$

Then MSK signal is given by

$$\langle S(t) = S_1\phi_1(t) + S_2\phi_2(t) \rangle \qquad 0 \le t \le T_b$$

$S_1 \rightarrow$ Inphase component of $S(t)$

$$S_1 = \int_{-T_b}^{T_b} S(t)\,\phi_1(t)\,dt \qquad S_1 = \sqrt{E_b}\cos[\theta(0)] \qquad -T_b \le t \le T_b$$

$S_2 \rightarrow$ Quadrature component of $S(t)$

$$S_2 = \int_{0}^{2T_b} S(t)\,\phi_2(t)\,dt$$

$$S_2 = -\sqrt{E_b} \sin[\theta(T_b)] \qquad 0 \le t \le 2T_b$$

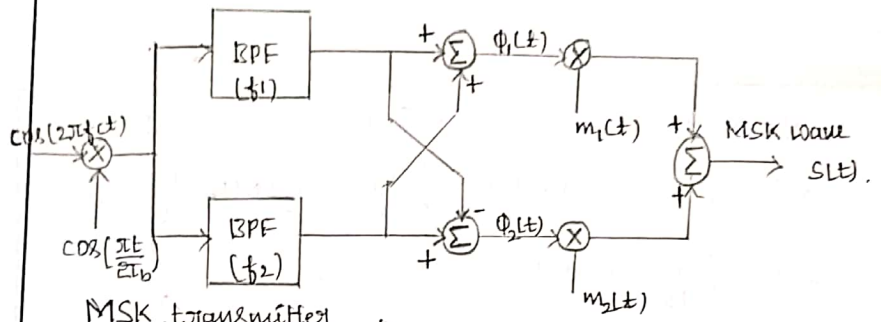

MSK transmitter

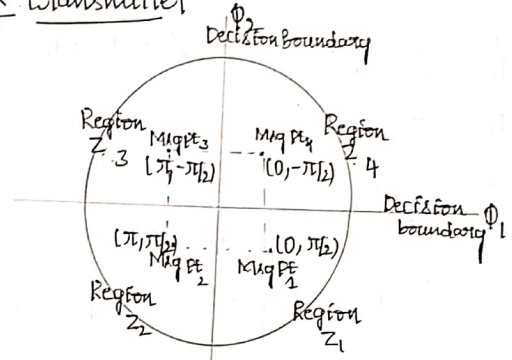

Signal space diagram for MSK system

Transmitted binary symbol $0 \le t \le T_b$	Phase states $\theta(0)$	$\theta(T_b)$	Co-ordinates of message points s_1	s_2
1	0	$\pi/2$	$+\sqrt{E_b}$	$-\sqrt{E_b}$
0	π	$\pi/2$	$-\sqrt{E_b}$	$-\sqrt{E_b}$
1	π	$-\pi/2$	$-\sqrt{E_b}$	$+\sqrt{E_b}$
0	0	$-\pi/2$	$+\sqrt{E_b}$	$+\sqrt{E_b}$

Signal-space characterization.

MSK Receiver

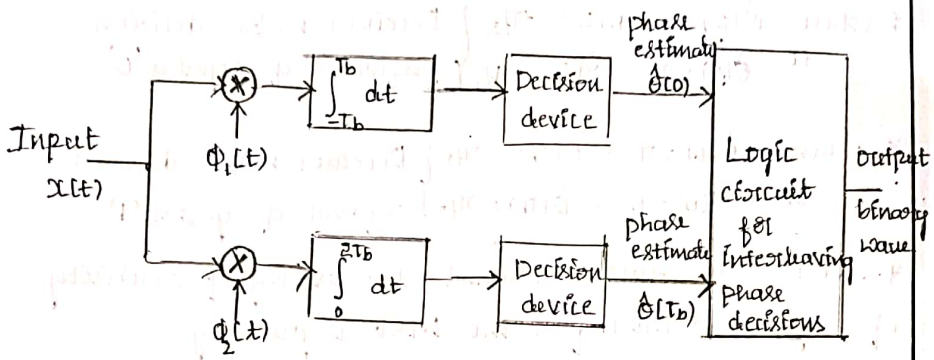

* In case of an AWGN channel, the received signal is given by

$$x(t) = s(t) + w(t)$$

For the optimum detection of $\theta(0)$, the projection of received signal onto the reference signal $\phi_1(t)$ is given by

$$x_1 = \int_{-T_b}^{T_b} x(t)\,\phi_1(t).dt.$$

$$x_1 = s_1 + w_1 \qquad -T_b \le t \le T_b$$

If $x_1 > 0 \longrightarrow \hat{\theta}(0) = 0$

$x_1 < 0 \longrightarrow \hat{\theta}(0) = \pi$

Now for the optimum detection $\theta(T_b)$, the projection of received signal onto the second reference signal $\phi_2(t)$ is given by

$$x_2 = \int_{0}^{2T_b} x(t)\,\phi_2(t).dt$$

$$x_2 = s_2 + w_2 \qquad 0 \le t \le 2T_b$$

If $x_2 > 0 \longrightarrow \hat{\theta}(T_b) = -\pi/2$ & $x_2 < 0 \longrightarrow \hat{\theta}(T_b) = \pi/2$

* When $\hat{\theta}(0) = 0$ & $\hat{\theta}(T_b) = \pi/2$ } Receiver makes decision
or $\hat{\theta}(0) = \pi$ & $\hat{\theta}(T_b) = \pi/2$ } infavour of symbol '0'.

* When $\hat{\theta}(0) = \pi$ & $\hat{\theta}(T_b) = -\pi/2$ } Receiver makes decision
or $\hat{\theta}(0) = 0$ & $\hat{\theta}(T_b) = \pi/2$ } infavour of symbol '1'

* For the AWGN channel, the average probability of symbol error for the MSK is given by

$$P_e = \text{erfc}\left[\sqrt{\frac{E_b}{N_0}}\right] - \frac{1}{\pi}\text{erfc}^2\left[\sqrt{\frac{E_b}{N_0}}\right]$$

In the second term $E_b/N_0 \gg 1$, ignoring the second term.

$$\left\langle P_e = \text{erfc}\left[\sqrt{\frac{E_b}{N_0}}\right] \right\rangle$$

Coherent Quadriphase Shift Keying

[Quadrature Shift Keying] QPSK.

In QPSK, the phase of the carrier takes on the one of four equally spaced values i.e $\frac{\pi}{4}, \frac{3\pi}{4}, \frac{5\pi}{4}, \frac{7\pi}{4}$ as shown by.

$$S_i(t) = \begin{cases} \sqrt{\frac{2E}{T}} \cos\left[2\pi f_c t + (2i-1)\frac{\pi}{4}\right] & 0 \le t \le T_b \\ 0 & \text{elsewhere} \end{cases} \rightarrow 1$$

where $i = 1, 2, 3, 4$

E → transmitted signal energy per symbol.

T → Symbol duration

f_c → carrier frequency, $f_c = \frac{n_c}{T}$

* Using trignometric relation

$\cos[A+B] = \cos A.\cos B - \sin A.\sin B$. The equation 1 can be written as

$$S_i(t) = \sqrt{\frac{2E}{T}} \cos(2i-1)\frac{\pi}{4}.\cos 2\pi f_c t - \sqrt{\frac{2E}{T}}.\sin(2i-1)\frac{\pi}{4}.\sin 2\pi f_c t. \quad \rightarrow 2$$

* $\phi_1(t)$ and $\phi_2(t)$ be the two orthonormal basis functions represented as.

$$\phi_1(t) = \sqrt{\frac{2}{T}} \cos 2\pi f_c t \qquad 0 \le t \le T \qquad \text{——— 3}$$

$$\phi_2(t) = \sqrt{\frac{2}{T}} \sin 2\pi f_c t. \qquad 0 \le t \le T \qquad \text{——— 4}$$

* There are four message points and the associated signal vectors are

$$S_i = \begin{bmatrix} \sqrt{E}\cos(2i-1)\pi/4 \\ -\sqrt{E}\sin(2i-1)\pi/4 \end{bmatrix} \qquad i = 1, 2, 3, 4$$

The elements of signal vectors are Si_1 and Si_2

* QPSK signal is characterized by two-dimensional signal constellation [M=2] and four message points (M=4)

Input dibit pattern	Phase of the QPSK signal [Radians]	Co-ordinates of message points	
		Si_1	Si_2
10	$\pi/4$	$+\sqrt{E/2}$	$-\sqrt{E/2}$
00	$3\pi/4$	$-\sqrt{E/2}$	$+\sqrt{E/2}$
01	$5\pi/4$	$-\sqrt{E/2}$	$+\sqrt{E/2}$
11	$7\pi/4$	$+\sqrt{E/2}$	$+\sqrt{E/2}$

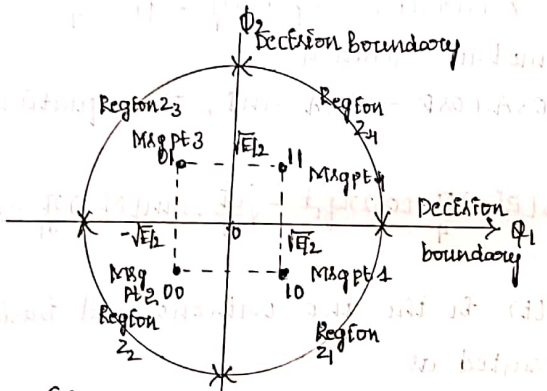

Signal space diagram for coherent QPSK system

QPSK transmitter

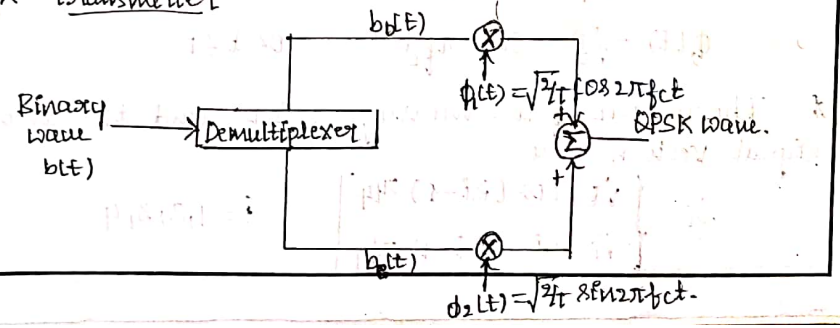

QPSK receiver

Coherent detection of QPSK signal.

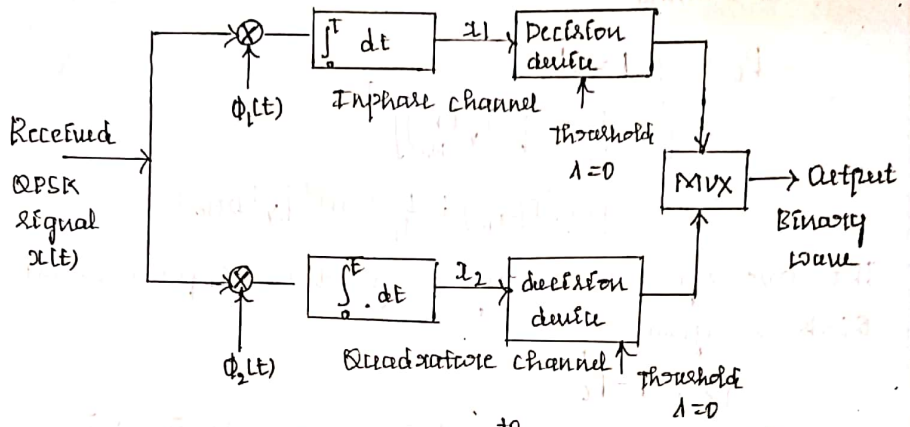

* A QPSK system is equivalent to two coherent binary PSK systems working in parallel and using carriers that are inphase and Quadrature.

* The inphase channel output x_1 and the Quadrature channel output x_2 may be viewed as the individual outputs of the two coherent binary PSK systems.

* In QPSK two bits are transmitted per symbol

$$E = 2E_b \qquad \sqrt{E_b} = \sqrt{E/2}$$

* The average probability of error in each channel of the coherent QPSK system is

$$P' = \frac{1}{2} \operatorname{erfc}\left(\sqrt{\frac{E_b}{N_0}}\right)$$

$$P^L = \frac{1}{2} \operatorname{erfc}\left(\sqrt{\frac{E}{2N_0}}\right)$$

Let P_c probability of correct decision is equal to the product of conditional probabilities in I-channel and Q channel

$$P_c = [1-p']^2$$

$$= \left[1 - \frac{1}{2}\operatorname{erfc}\left(\sqrt{\frac{E}{2N_0}}\right)\right]^2$$

$$= 1 - \operatorname{erfc}\left[\sqrt{E/2N_0}\right) + \frac{1}{4}\operatorname{erfc}^2\left[\sqrt{E/2N_0}\right)$$

The average probability of symbol error for coherent QPSK is given by

$$P_e = 1 - P_c$$

$$= 1 - \left[1 - \operatorname{erfc}\sqrt{E/2N_0} + \frac{1}{4}\operatorname{erfc}^2\left[\sqrt{E/2N_0}\right)\right]$$

$$= \operatorname{erfc}\sqrt{E/2N_0} - \frac{1}{4}\operatorname{erfc}^2\left[\sqrt{E/2N_0}\right)$$

* $\sqrt{E/2N_0} \gg 1$, hence we ignore the second term.

$$P_e \approx \operatorname{erfc}\left(\sqrt{E/2N_0}\right)$$

$$P_e \approx \operatorname{erfc}\left[\sqrt{2E_b/2N_0}\right) \qquad E = 2E_b$$

$$\left\langle P_e \approx \operatorname{erfc}\left[\sqrt{E_b/N_0}\right)\right\rangle$$

Non-coherent binary modulation techniques.

Non-coherent orthogonal modulation

* For binary signalling scheme that involves the use of two orthogonal signals with equal energy

$$S_1(t) \text{ & } S_2(t), \quad 0 \le t \le T$$

Let $g_1(t)$ & $g_2(t)$, $0 \le t \le T$

denote the phase shifted version of $S_1(t)$ & $S_2(t)$ respectively. after sent over an imperfect channel that shifts the carrier phase by an unknown amount.

These signals $g_1(t)$ & $g_2(t)$ are assumed that remain orthogonal and of equal energy. Such a signalling scheme is referred as 'Non-coherent orthogonal modulation'

* At the receiver, the received signal $x(t)$ can be expressed as

$$x(t) = \begin{cases} g_1(t) + w(t) & 0 \le t \le T \quad \{S_1(t)\} \\ g_2(t) + w(t) & 0 \le t \le T \quad \{S_2(t)\} \end{cases}$$

The receiver tries to descriminate between $S_1(t)$ and $S_2(t)$ regardless of the carrier phase. This goal can be achieved by the following receiver structure.

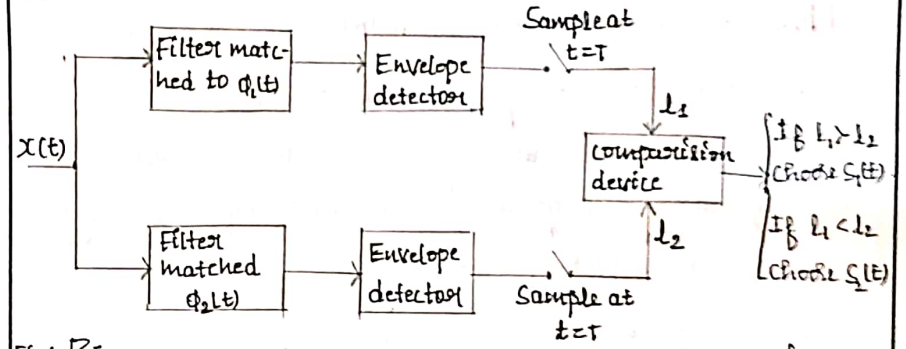

Fig: Binary receiver for non-coherent orthogonal modulation

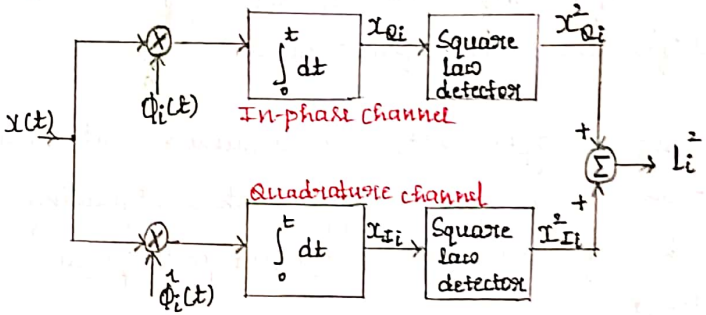

Fig: Quadrature receiver

A Non-coherent matched filter may be viewed as equivalent Quadrature receiver as shown in fig 2.

Let $\phi_1(t)$ and $\phi_2(t)$ be the orthonormal set of $S_1(t)$ & $S_2(t)$ respectively.

Let $\hat{\phi}_i(t)$ be the version of $\phi_i(t)$ that results from shifting the carrier phase by -90°

Where $\phi_i(t)$ and $\hat{\phi}_i(t)$ are orthogonal to each other.

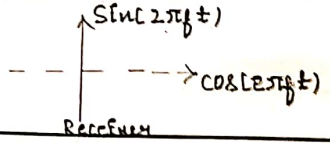

The average probability of error for the non-coherent receiver in Fig 1 or equivalently Fig 2 is given by

$$P_e = \frac{1}{2} \exp\left[\frac{-E}{2N_0}\right]$$

Where $E \rightarrow$ Signal energy per symbol

$N_0/2 \rightarrow$ Noise spectral density.

1. Non-coherent Binary FSK.

For the binary FSK, the transmitted signal is given by.

$$S_i(t) = \sqrt{\frac{2E_b}{T_b}} \cos(2\pi f_i t) \qquad 0 \le t \le T_b$$

Symbol '1' $\leftrightarrow$ $S_1(t)$ using frequency f_1

Symbol '0' $\leftrightarrow$ $S_2(t)$ using frequency f_2

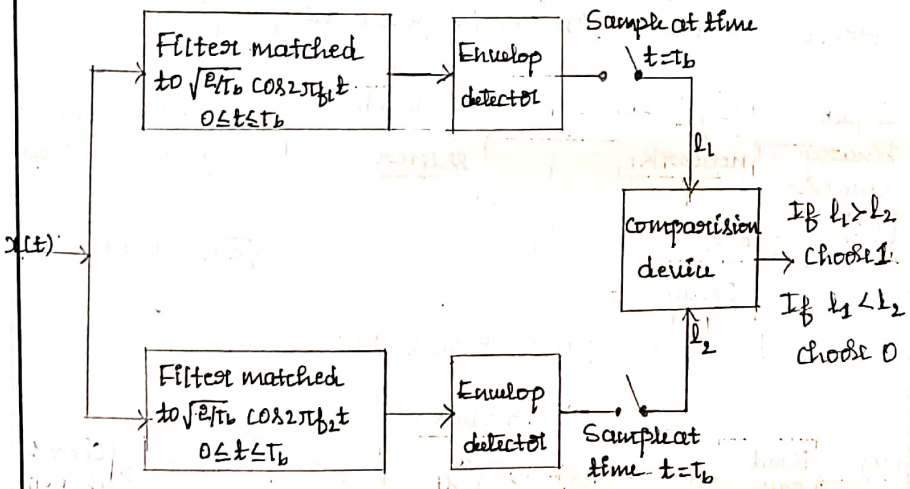

Noncoherent receiver for detection of binary FSK signals.

Thus the non-coherent binary FSK is a special case of non coherent orthogonal modulation with $T=T_b$ and $E=E_b$. Where T_b is the bit duration & E_b is the energy per bit.

The average probability of error for non-coherent BFSK is

$$\left\langle P_e = \frac{1}{2} Exp\left[\frac{-E_b}{2N_0}\right] = \frac{1}{2} e^{-E_b/2N_0} \right\rangle$$

2. Differential phase-shift keying [DPSK]

Differential phase shift keying is the non-coherent version of PSK.

DPSK performs

1) Differential encoding of the input binary wave.

2) Phase shift keying

Hence the name Differential phase shift keying.

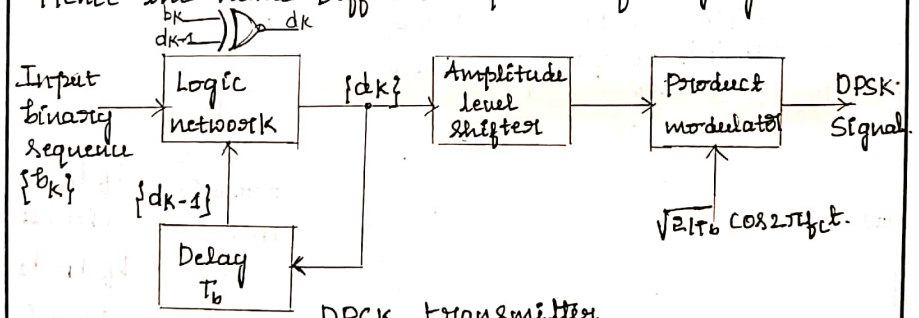

DPSK transmitter

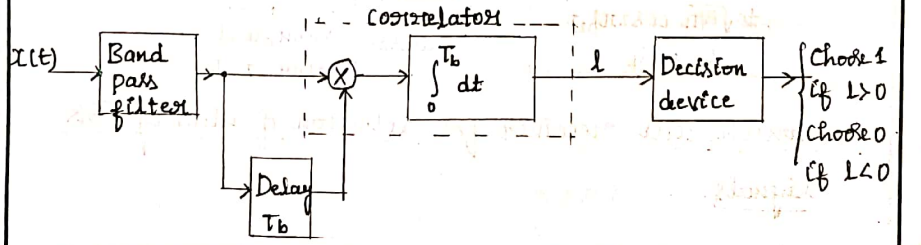

DPSK receiver

For symbol '1', a carrier with 0° phase shift is transmitted

For symbol '0', a carrier with 180° phase shift is transmitted.

* The differentially encoded bit d_{k-1} can be arbitrarily chosen to be either '0' or '1'.

* Input binary sequence $\{b_k\}$ is differentially encoded to get the sequence $\{d_k\}$

i.e $d_k = \overline{b_k \oplus d_{k-1}}$ ——— ⟨1⟩

where d_{k-1} → previous value of the differentially encoded bit.

$$d_k = b_k d_{k-1} + \bar{b}_k \bar{d}_{k-1} \quad \text{——— ⟨2⟩}$$

The amplitude level shifter produces amplitudes:

$+\sqrt{E_b}$ if $d_k = 1$

$-\sqrt{E_b}$ if $d_k = 0$

* The output of the product modulator is the required DPSK signal and it is given as

$\sqrt{\frac{2E_b}{T_b}} \cos 2\pi f_c t$ for $d_k = 1$

& $-\sqrt{\frac{2E_b}{T_b}} \cos 2\pi f_c t$ for $d_k = 0$

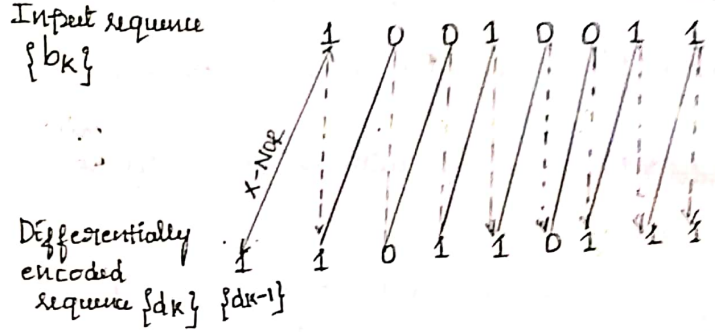

$$d_K = b_K d_{K-1} + \bar{b}_K \bar{d}_{K-1}$$

$$\langle d_K = \overline{b_K \oplus d_{K-1}} \rangle$$

* Transmitted phase:

If $d_K = 1$, Txed phase is '0' Radians

If $d_K = 0$, Txed phase is 'π' Radians.

* If $d_K = d_{K-1}$, then correlator o/p l is +ve

If $d_K \neq d_{K-1}$, then correlator o/p l is -ve

* If $l > 0$, then $\hat{b}_K = 1$

If $l < 0$, then $\hat{b}_K = 0$

* DPSK is a special case of Non-coherent orthogonal modulation with $T = 2T_b$ and $E = 2E_b$

* The average probability of error for DPSK is

$$\langle P_e = \frac{1}{2} \exp\left[\frac{-E_b}{N_0}\right] \rangle \quad \text{with } E = 2E_b$$

The probability of symbol error for QAM is given by

$$P_e = 1 - P_c$$
$$= 1 - (1 - P_e')^2$$
$$\simeq 2P_e'$$

$$\left\langle P_e \simeq 2\left[1 - \frac{1}{\sqrt{M}}\right] \operatorname{erfc}\left(\sqrt{\frac{E_0}{N_0}}\right) \right\rangle$$

M-ary QAM is two dimensional, we consider two signal constellations for M-ary QAM one vertically along the ϕ_2 axis [Quadratic] (a) and other horizontally along the ϕ_1 axis. [In-phase] (b)

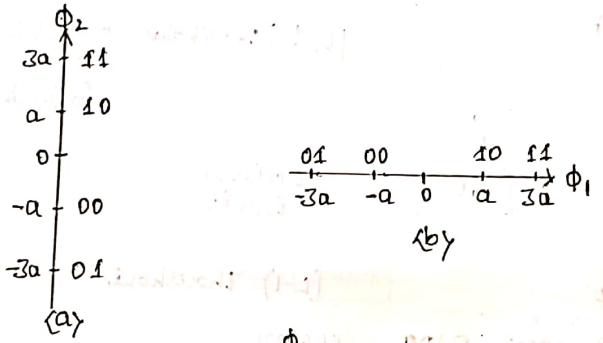

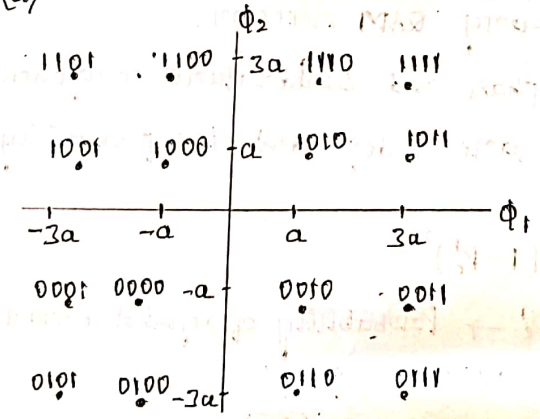

Signal space constellation for M-ary QAM for M=16.

of discrete amplitudes a_i and b_i. Hence the name Quadrature amplitude modulation.

The signal $s(t)$ expanded interms of pair of basis functions.

$$\phi_1(t) = \sqrt{\frac{2}{T}} \cos(2\pi f_c t) \qquad 0 \le t \le T$$

&

$$\phi_2(t) = \sqrt{\frac{2}{T}} \sin[2\pi f_c t] \qquad 0 \le t \le T$$

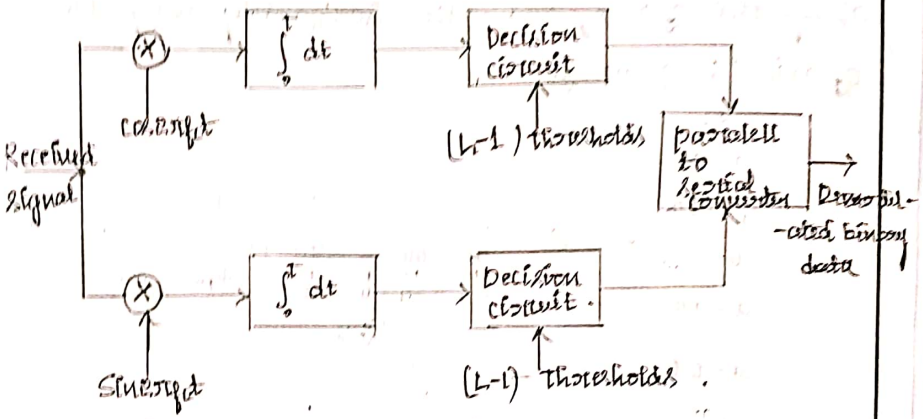

M-ary QAM receiver.

* The In-phase and Quadrature components of M-ary QAM are independent, the probability of correct detection is

$$P_c = (1 - P_e')^2$$

where P_e' → Probability of symbol error for either component.

$$P_e' = [1 - Y_L)\ \text{erfc}\left(\sqrt{\frac{E_0}{N_0}}\right)$$

where $L = \sqrt{M}$

M-ary QAM

* Quadrature amplitude modulation [QAM] is a hybrid form of modulation in which two carriers, are out of phase by 90° are modulated and the resultant output consists of both amplitude and phase variations.
* The carriers are known as Quadrature carriers.
* The modulated waves are summed at the output of transmitter, so the final waveform is combination of both ASK and PSK.

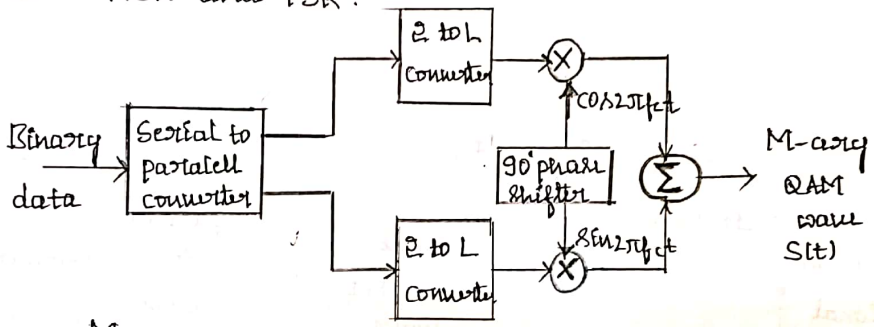

M-ary QAM transmitter

The general form of M-ary QAM wave is

$$S_i(t) = \sqrt{\frac{2E_0}{T}}\, a_i \cos[2\pi f_c t] + \sqrt{\frac{2E_0}{T}}\, b_i \sin[2\pi f_c t]$$

Where E_0 → Energy of the signal with lowest amplitude. $0 \le t \le T$

a_i and b_i → Pair of independent integers

$i = 0, \pm 1, \pm 2 \ldots$

The signal $S_i(t)$ involves two-phase quadrature carriers, each one of which is modulated by a set

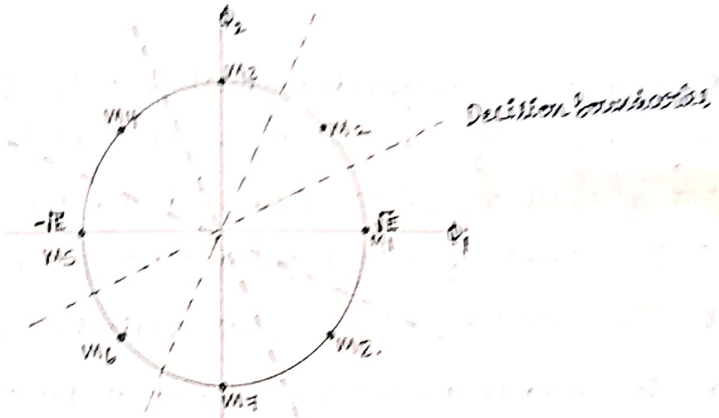

Signal constellation for Octonary-Shift-Keying (or M-PSK) with M=8

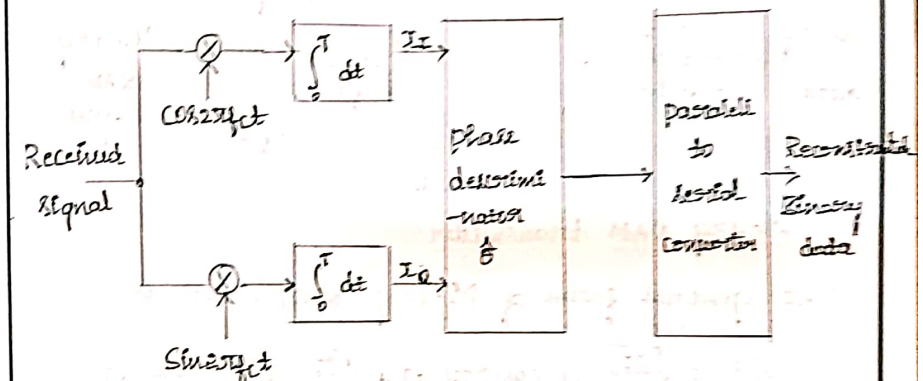

Receiver for coherent M-ary PSK.

Probability of symbol error

For M-ary PSK

$$P_e = erfc\left[\sqrt{\frac{E}{N_0}}\sin\left[\frac{\pi}{M}\right]\right] \qquad M \geq 4$$

For M-ary DPSK

$$P_e \leq erfc\left[\sqrt{\frac{2E}{N_0}}\sin\left(\frac{\pi}{\sqrt{2}M}\right)\right] \qquad M \geq 4$$

M-ary PSK.

The M-ary PSK modulated signal is represented as.

$$S_i(t) = \sqrt{\frac{2E}{T}} \cos[2\pi f_c t + \theta_i] \quad i = 0, 1, 2, \ldots M-1. \qquad \text{——— (1)}$$

Where $E \rightarrow$ Signal energy per symbol

$f_c \rightarrow$ carrier frequency, $f_c = n_c/T$

$\theta_i \rightarrow$ phase of the carrier takes one of M-possible values.

$$\theta_i = \frac{2\pi i}{M} \qquad i = 0, 1, 2, \ldots M-1.$$

$$S_i(t) = \sqrt{\frac{2E}{T}} \cos\left[2\pi f_c t + \frac{2\pi i}{M}\right] \qquad i = 0, 1, 2 \cdots M-1 \qquad \text{——— (2)}$$

By using trignometric relation

$\cos[A+B] = \cos A . \cos B - \sin A \sin B$

The equation (2) can be written as.

$$S_i(t) = \sqrt{\frac{2E}{T}} \cos(2\pi f_c t) \cdot \cos\frac{2\pi i}{M} - \sqrt{\frac{2E}{T}} \sin(2\pi f_c t) \cdot \sin\frac{2\pi i}{M}$$

$i = 0, 1, 2 \cdots M-1$ ——— (3)

$S_i(t)$ can be expanded interms of two basis functions

$$\phi_1(t) = \sqrt{\frac{2}{T}} \cos(2\pi f_c t) \qquad 0 \le t \le T$$

$$\phi_2(t) = \sqrt{\frac{2}{T}} \sin(2\pi f_c t) \qquad 0 \le t \le T$$

The signal constellation of M-ary PSK is two-dimensional. The M message points are equally spaced on a circle of radius $\sqrt{E}$ & center at the origin.

M-ary modulation techniques.

M-ary modulation: It is a digital modulation technique in which instead of transmitting one bit two or more bits are transmitted at a time.

* Single signal is used for multiple bit transmission so the channel bandwidth is reduced.

* In M-ary modulation scheme two or more bits are grouped together to form symbols & one of M possible signals, $S_1(t), S_2(t) \cdots S_M(t)$ is transmitted during each symbol duration T

* The number of possible signals is

$$M = 2^n$$

Where $n \rightarrow$ number of bits grouped

$$n = \log_2 M$$

Here we consider three differents M-ary signalling schemes. They are

1) M-ary PSK
2) M-ary QAM
3) M-ary FSK.

M-ary modulation techniques.

M-ary modulation: It is a digital modulation technique in which instead of transmitting one bit two or more bits are transmitted at a time.

* Single signal is used for multiple bit transmission so the channel bandwidth is reduced.

* In M-ary modulation scheme two or more bits are grouped together to form symbols & one of M possible signals, $S_1(t), S_2(t) \cdots S_M(t)$ is transmitted during each symbol duration T

* The number of possible signals is

$$M = 2^n$$

Where $n \rightarrow$ number of bits grouped

$$n = \log_2 M$$

Here we consider three differents M-ary signalling schemes. They are

1) M-ary PSK
2) M-ary QAM
3) M-ary FSK.

M-ary PSK.

The M-ary PSK modulated signal is represented as.

$$S_i(t) = \sqrt{\frac{2E}{T}} \cos[2\pi f_c t + \theta_i] \quad i = 0, 1, 2, \ldots M-1 \quad \text{——— (1)}$$

where $E \rightarrow$ Signal energy per symbol

$f_c \rightarrow$ carrier frequency, $f_c = n_c/T$

$\theta_i \rightarrow$ phase of the carrier takes one of M-possible values.

$$\theta_i = \frac{2\pi i}{M} \qquad i = 0, 1, 2, \ldots M-1.$$

$$S_i(t) = \sqrt{\frac{2E}{T}} \cos\left[2\pi f_c t + \frac{2\pi i}{M}\right] \quad i = 0, 1, 2 \ldots M-1 \quad \text{——— (2)}$$

By using trignometric relation

$\cos[A+B] = \cos A \cdot \cos B - \sin A \sin B$

The equation (2) can be written as.

$$S_i(t) = \sqrt{\frac{2E}{T}} \cos(2\pi f_c t) \cdot \cos\frac{2\pi i}{M} - \sqrt{\frac{2E}{T}} \sin(2\pi f_c t) \cdot \sin\frac{2\pi i}{M}$$

$i = 0, 1, 2 \ldots M-1 \quad \text{——— (3)}$

$S_i(t)$ can be expanded interms of two basis functions

$$\phi_1(t) = \sqrt{\frac{2}{T}} \cos(2\pi f_c t) \qquad 0 \le t \le T$$

$$\phi_2(t) = \sqrt{\frac{2}{T}} \sin(2\pi f_c t) \qquad 0 \le t \le T$$

The signal constellation of M-ary PSK is two-dimensional. The M message points are equally spaced on a circle of radius $\sqrt{E}$ & center at the origin.

M-ary QAM

* Quadrature amplitude modulation [QAM] is a hybrid form of modulation in which two carriers are out of phase by 90° are modulated and the resultant output consists of both amplitude and phase variations.

* The carriers are known as Quadrature carriers.

* The modulated waves are summed at the output of transmitter, so the final waveform is combination of both ASK and PSK.

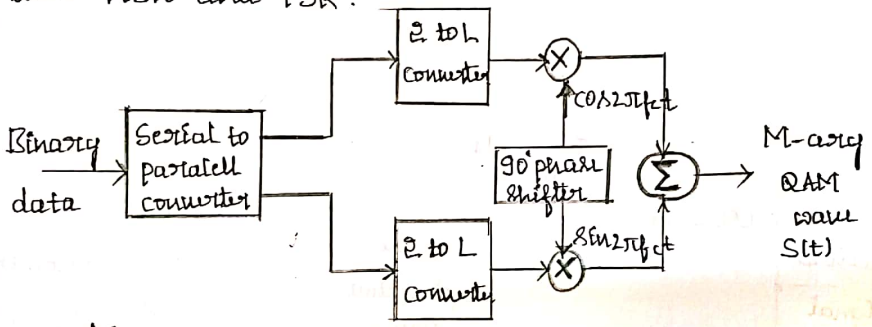

M-ary QAM transmitter

The general form of M-ary QAM wave is

$$S_i(t) = \sqrt{\frac{2E_0}{T}}\, a_i \cos[2\pi f_c t] + \sqrt{\frac{2E_0}{T}}\, b_i \sin[2\pi f_c t]$$

where E_0 → Energy of the signal with lowest amplitude. $0 \le t \le T$

a_i and b_i → pair of independent integers

$i = 0, \pm 1, \pm 2 \ldots$

The signal $S_i(t)$ involves two-phase quadrature carriers, each one of which is modulated by a bit

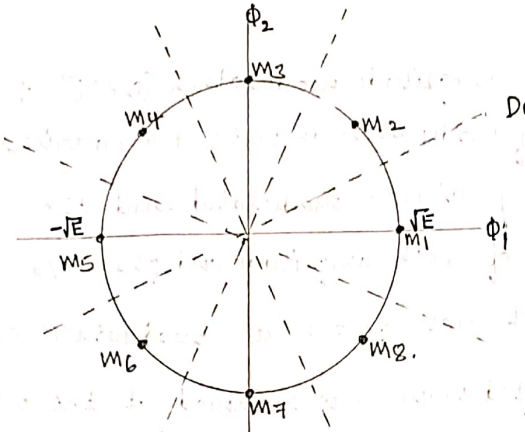

Signal constellation for octaphase-shift-keying (i.e M-PSK with M=8)

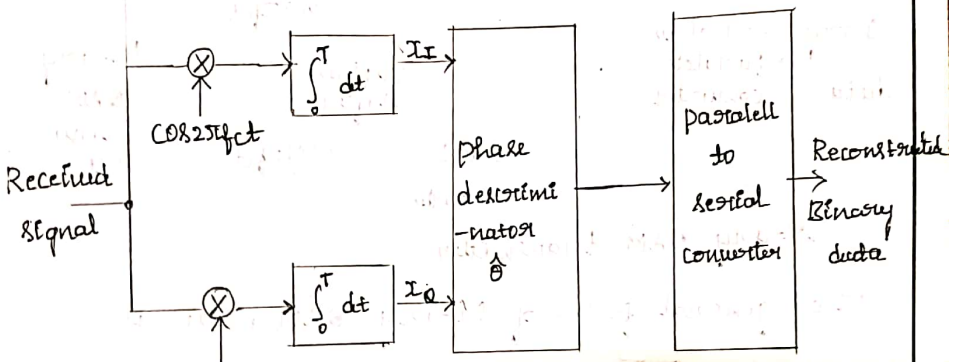

Receiver for coherent M-ary PSK.

Probability of symbol error

For M-ary PSK

$$P_e = \text{erfc}\left[\sqrt{\frac{E}{N_0}} \sin[\pi/M]\right] \qquad M \geq 4$$

For M-ary DPSK

$$P_e \leq \text{erfc}\left[\sqrt{\frac{2E}{N_0}} \sin\left(\frac{\pi}{2M}\right)\right] \qquad M \geq 4$$

The probability of symbol error for QAM is given by

$$P_e = 1 - P_c$$

$$= 1 - (1 - P_e')^2$$

$$\approx 2P_e'$$

$$\boxed{P_e \approx 2\left[1 - \frac{1}{\sqrt{M}}\right] \operatorname{erfc}\left(\sqrt{\frac{E_0}{N_0}}\right)}$$

M-ary QAM is two dimensional, we consider two signal constellations for M-ary QAM one vertically along the ϕ_2 axis (Quadrature) each other horizontally along the ϕ_1 axis. (In-phase)

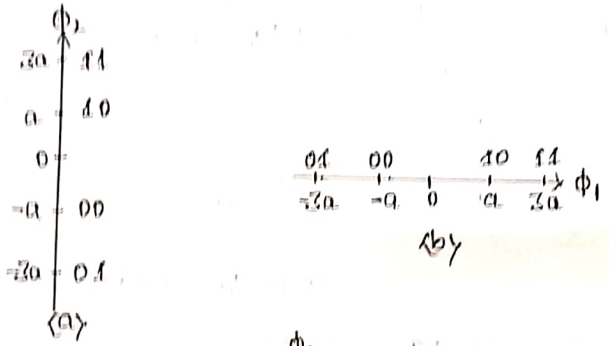

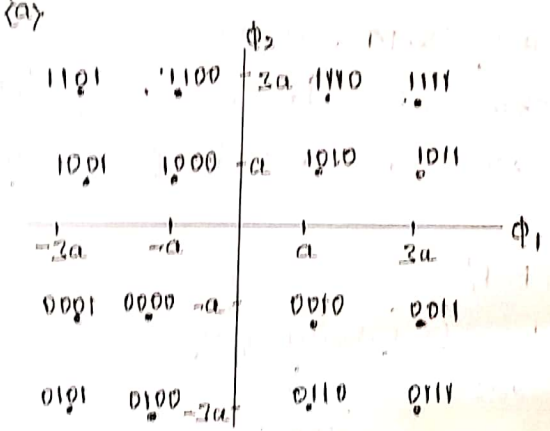

Signal space constellation for M-ary QAM for M=16.

of discrete amplitudes ai and bi. hence the name Quadrature amplitude amodullation.

The Signal Si(t) expanded interms of pair of basis functions.

$$\phi_1(t) = \sqrt{\frac{2}{T}} \cos(2\pi f_c t) \quad 0 \le t \le T$$

&

$$\phi_2(t) = \sqrt{\frac{2}{T}} \sin[2\pi f_c t] \quad 0 \le t \le T$$

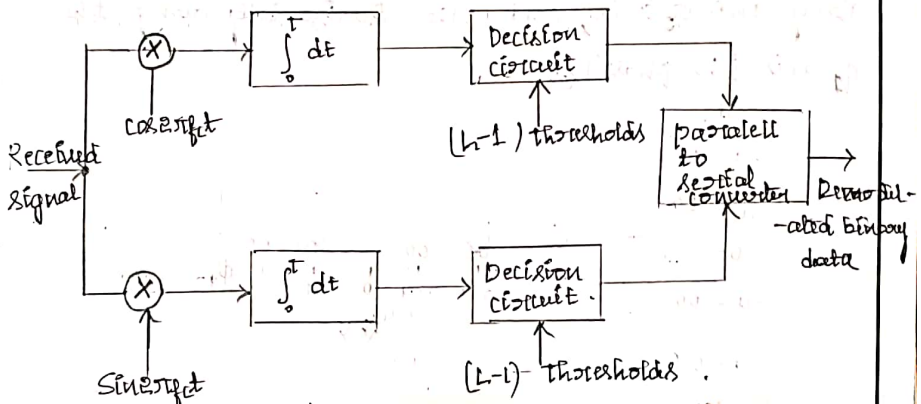

M-ary QAM receiver.

* the In-phase and Quadrature components of M-ary QAM are independent, the probability of correct detection is

$$P_c = (1 - P_e')^2$$

where P_e' → Probability of symbol error for either component.

$$P_e' = [1 - Y_L)\ \text{erfc}\left(\sqrt{\frac{E}{N_0}}\right)$$

where $L = \sqrt{M}$

Equalization

Introduction:

Equalization is the technique used to improve the received signal quality. Equalization compensates for inter symbol interference (ISI) created by multipath within time dispersive channels. **ISI –Inter symbol Interference**: if the modulation bandwidth exceeds the coherence bandwidth of the radio channel, ISI occurs and modulation pulses are spread in time**.**

Fundamentals of Equalization:

- Equalization is a technique used to combat inters symbol interference.
- In radio channels, a variety of adaptive equalizers can be used to cancel interference while providing diversity.
- Since the mobile fading channel is random and time varying equalizers must track the time varying characteristics of the mobile channel, and thus are called adaptive equalizers.
- In radio channels, a variety of adaptive equalizers can be used to cancel interference while providing diversity

Block Diagram:

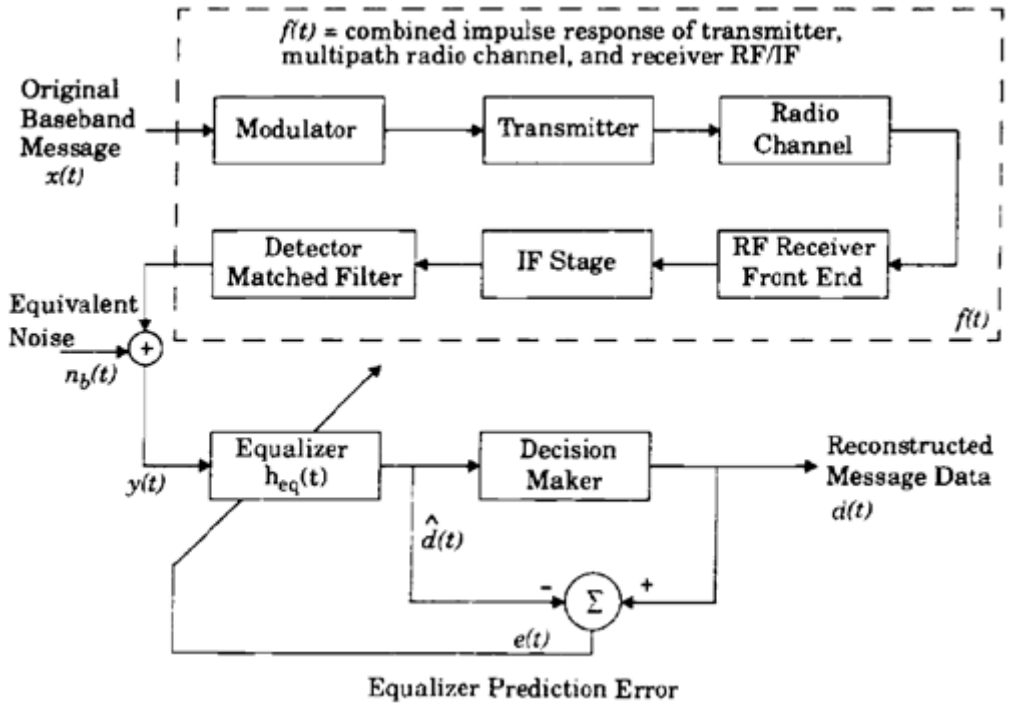

Figure 13.1 Block Diagram of equalizer

- If x (t) is the original information signal, and f(t) is the combined complex baseband impulse response of the transmitter, channel, and the RF/IF sections of the receiver, the signal received by the equalizer may be expressed as

$$y(t) = x(t) \otimes f^*(t) + n_b(t)$$

- where f* (t) is the complex conjugate off(t) , n_b(t) is the baseband noise at the input of the equalizer. If the impulse response of the equalizer is heq (t) , then the output of the equalizer is

$$\begin{aligned}\hat{d}(t) &= x(t) \otimes f^*(t) \otimes h_{eq}(t) + n_b(t) \otimes h_{eq}(t) \\ &= x(t) \otimes g(t) + n_b(t) \otimes h_{eq}(t)\end{aligned}$$

- where c_n is the complex filter coefficients of the equalizer

$$h_{eq}(t) = \sum_n c_n \delta(t - nT)$$

Equalization techniques can be subdivided into two general categories

1. Linear equalization.
2. Nonlinear equalization.

Types of Equalization Techniques: These categories are determined from how the output of an adaptive equalizer is used for subsequent control (feedback) of the equalizer.

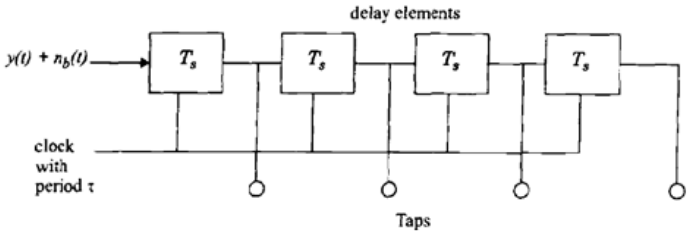

Figure 13.2

The decision maker determines the value of the digital data bit being received and applies a slicing or thresholding operation (a nonlinear operation) in order to determine the value of d(t).

1. **Linear Equalizer**: If d(t) is not used in the feedback path to adapt the equalizer, the equalization is linear.
2. **Non Linear Equalizer**: if d(t) is fed back to change the subsequent outputs of the equalizer, the equalization is nonlinear.

Linear transversal equalizer (LTE):

- The most common equalizer structure is a linear transversal equalizer (LTE).
- A linear transversal filter is made up of tapped delay lines, with the tappings spaced a symbol period (Ts).As shown in above fig13.2
- The simplest LTE uses only feedforward taps, and the transfer function of the equalizer filter is a polynomial in Z^{-1}. This filter has many zeroes but poles only at z = 0, and is called a **finite impulse response (FIR)** filter, or simply **a transversal filter.**
- If the equalizer has both feedforward and feedback taps, its transfer function is a rational function of Z^{-1} , and is called an **infinite impulse response (IIR) filter** with poles and zeros.
- Since IIR filters tend to be unstable when used in channels where the strongest pulse arrives after an echo pulse (i.e., leading echoes), they are rarely used.

Classification Of Equalization Technique (see figure 13.3)

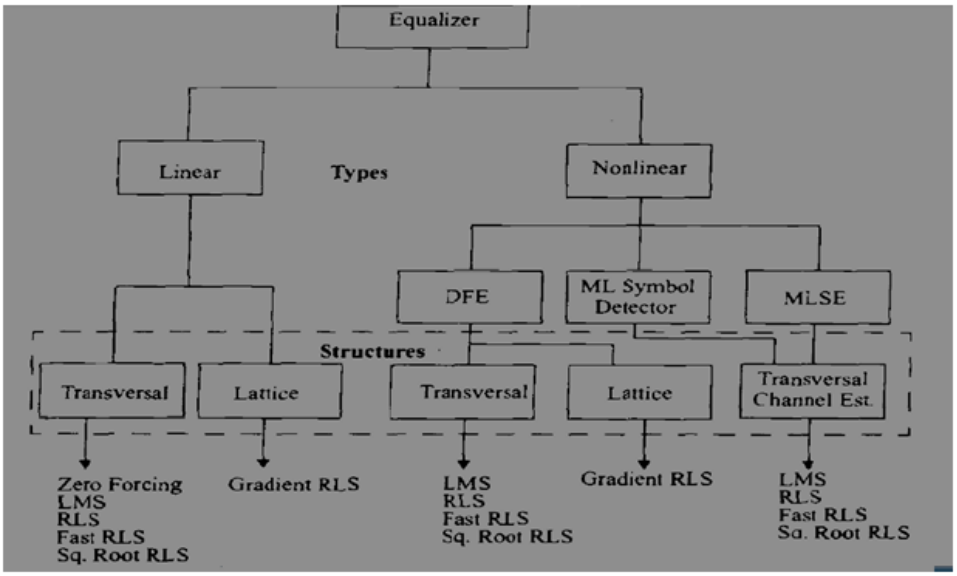

Figure 13.3

Linear Equalizer

Introduction:

A linear equalizer can be implemented as an FIR filter, otherwise known as the transversal filter.This type of equalizer is the simplest type available

Structure of a linear Equalizer:

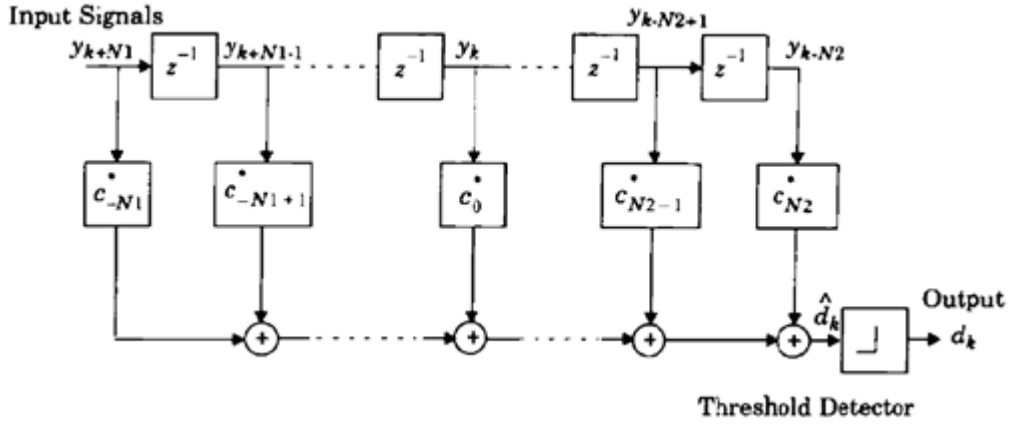

1. **linear transversal equalizer:** In such an equalizer, the current and past values of the received signal are linearly weighted by the filter coefficient and summed to produce the output, as shown in Figure 13.2

- The output of this transversal filter before decision making (threshold detection) is given

$$\hat{d}_k = \sum_{n=-N_1}^{N_2} (c_n^*) y_{k-n}$$

- C_n^* represents the complex filter coefficients or tap weights,
- d_k is the output at time index k,
- y_i is the input received signal at time t_0 iT,
- t_0 is the equalizer starting time ,N= N1 N2 1 is the number of taps
- ,N1&N2 denotes the number of taps in forward and reverse portion of the equalizer respectively.

The **minimum mean squared error** $E[|e(n)|^2]$ that a linear transversal equalizer can achieve is

$$E\left[|e(n)|^2\right] = \frac{T}{2\pi}\int_{-\pi/T}^{\pi/T}\frac{N_0}{\left|F\left(e^{j\omega T}\right)\right|^2 + N_0}d\omega$$

- where $|F(e^{jwt})|^2$ is the frequency response of the channel, and N0 is the noise spectral density.

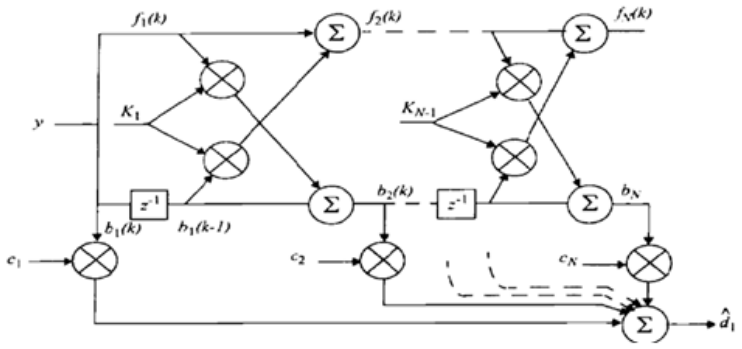

A lattice filter:The linear equalizer can also be implemented as a lattice filter.

- Each stage of the lattice is then characterized by the following recursive equations

$$f_1(k) = b_1(k) = y(k)$$

$$f_n(k) = y(k) - \sum_{i=1}^{n} K_i y(k-i) \models f_{n-1}(k) + K_{n-1}(k)\, b_{n-1}(k-1)$$

$$b_n(k) = y(k-n) - \sum_{i=1}^{n} K_i y(k-n+i)$$

$$= b_{n-1}(k-1) + K_{n-1}(k) f_{n-1}(k)$$

- Where Kn(k) is the reflection coefficient for the it th stage of the lattice
- Output of the equalizer is given by

$$\hat{d}_k = \sum_{n=1}^{N} c_n(k)\, b_n(k)$$

- Two main advantages of the lattice equalizer is its numerical stability and faster convergence.
- The unique structure of the lattice filter allows the dynamic assignment of the most effective length of the lattice equalizer.

Nonlinear Equalization

Nonlinear equalizers are used in applications where the channel distortion is too severe for a linear equalizer to handle**.**

Nonlinear Equalization Methods:

1. Decision Feedback Equalization (DFE)
2. Maximum Likelihood Symbol Detection
3. Maximum Likelihood Sequence Estimation (MLSE)

Decision Feedback Equalization (DFE): The basic idea behind decision feedback equalization is that once an informationsymbol has been detected and decided upon, the ISI that it induces on future symbols can be estimated and subtracted out before detection of subsequent symbols. It consists of a feed forward filter (FFF) and a feedback filter (FBF).

- The DFE can be realized in either the direct transversal form or as a lattice filter as shown in the fig 13.5.below
- The equalizer has N1 N2 1 taps in the feed forward filter and N3 taps in the feedback filter, and its output can be expressed as

$$\hat{d}_k = \sum_{n=-N_1}^{N_2} c_n^* y_{k-n} + \sum_{i=1}^{N_3} F_i d_k$$

- The minimum mean squared error a DFE can achieve is

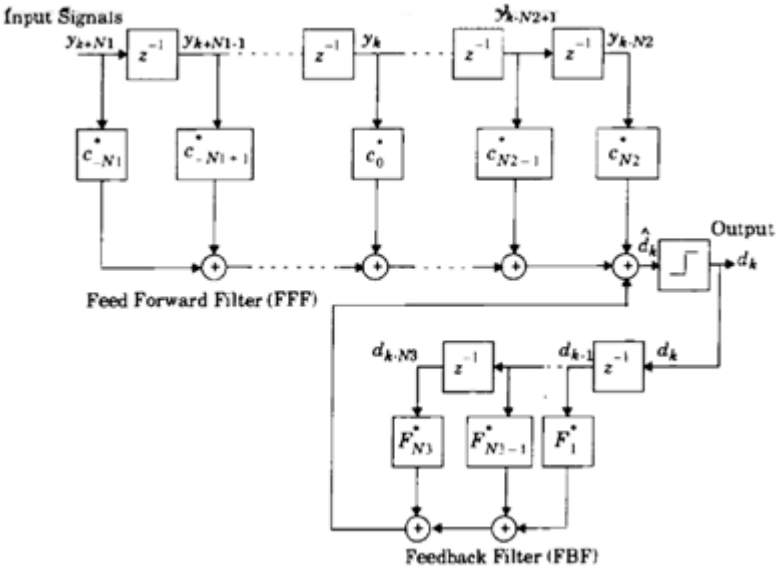

$$E\left[|e(n)|^2\right]_{min} = \exp\left\{\frac{T}{2\pi}\int_{-\pi/T}^{\pi/T} \ln\left[\frac{N_0}{|F(e^{j\omega T})|^2 + N_0}\right] d\omega\right\}$$

Advantages of DFE:

- DFE has significantly smaller minimum MSE than an LTE
- The mean squared error of a DFE is much better than a LTE.
- A DFE is more appropriate for severely distorted wireless channels

Predictive decision feedback equalizer

- It also consists of a feed forward filter (FFF) as in the conventional DFE.

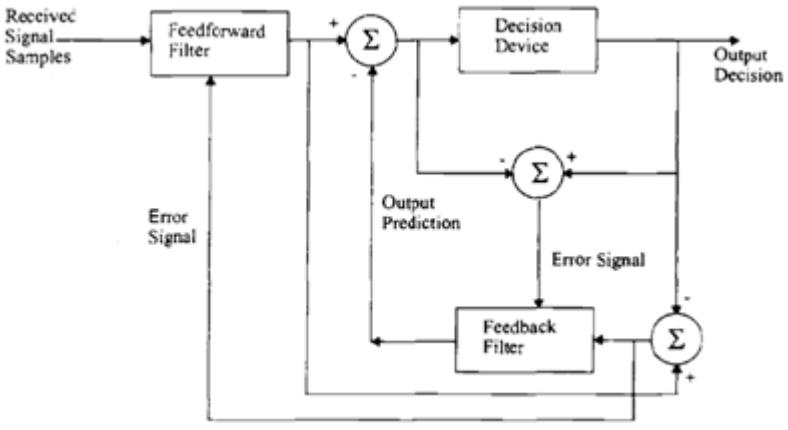

However, the feedback filter (FBF) is driven by an input sequence formed by the difference of the output of the detector and the output of the feed forward filter.

- Hence, the FBF here is called a noise predictor because it predicts the noise and the residual ISI contained in the signal at the FFF output and subtracts from it the detector output after some feedback delay.

Maximum Likelihood Sequence Estimation (MLSE) Equalizer :

The MSE-based linear equalizers described previously are optimum with respect to the criterion of minimum probability of symbol error when the channel does not introduce any amplitude distortion.

- Using a channel impulse response simulator within the algorithm, the MLSE tests all possible data sequences (rather than decoding each received symbol by itself), and chooses the data sequence with the maximum probability as the output**.**
- The MLSE is optimal in the sense that it minimizes the probability of a sequence error.
- The MLSE requires knowledge of the channel characteristics in order to compute the metrics for making decisions.
- The MLSE also requires knowledge of the statistical distribution of the noise corrupting the signal.

Adaptive Equalization

Adaptive equalizers compensate for signal distortion attributed to inter symbol interference (ISI), which is caused by multipath within time-dispersive channels. Typically employed in high-speed communication systems, which do not use differential modulation schemes or frequency division multiplexing. The equalizer is the most expensive component of a data demodulator and can consume over 80% of the total computations needed to demodulate a given signal

Adaptive Equalizer:

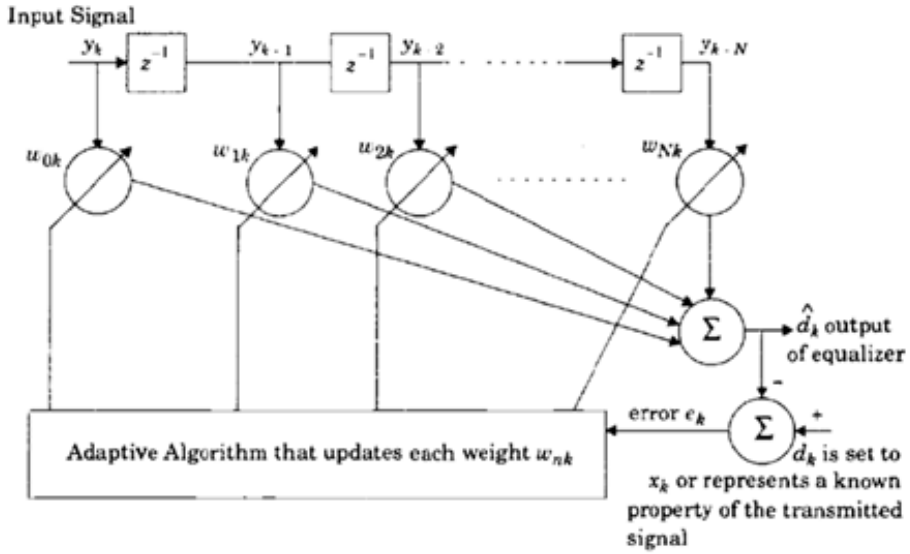

- The basic structure of an adaptive equalizer is shown in Figure 13.8, where the subscript k is used to denote a discrete time index
- Notice in Figure 13.8 that there is a single input y_k at any time instant. The value of $y_k$depends upon the instantaneous state of the radio channel and the specific value of the noise (see Figure 13.1).
- The adaptive equalizer structure shown above is called a transversal filter, and in this case has N delay elements, N I taps, and N I tunable complex multipliers, called weight
- The adaptive algorithm is controlled by the error signal ek. This error signal is derived by comparing the output of the equalizer, dk. The adaptive algorithm uses Ck to minimize a cost function and updates the equalizer weights in a manner that iteratively reduces the cost function

Algorithm:

- The input signal to the equalizer as

$$\mathbf{y}_k = \begin{bmatrix} y_k & y_{k-1} & y_{k-2} & \cdots & y_{k-N} \end{bmatrix}^T$$

- The output of the adaptive equalizer is a scalar given by

$$\hat{d}_k = \sum_{n=0}^{N} w_{nk} y_{k-n}$$

- Weight vector can be written as

$$\boldsymbol{w}_k = \begin{bmatrix} w_{0k} & w_{1k} & w_{2k} & \dots & w_{Nk} \end{bmatrix}^T$$

- Output in vector notation as

$$\hat{d}_k = \boldsymbol{y}_k^T \boldsymbol{w}_k = \boldsymbol{w}_k^T \boldsymbol{y}_k$$

- Error signal ek is given by

$$e_k = d_k - \hat{d}_k = x_k - \hat{d}_k$$

- Putting the value of $d_k$and d_k'the error signal is

$$e_k = x_k - \boldsymbol{y}_k^T \boldsymbol{w}_k = x_k - \boldsymbol{w}_k^T \boldsymbol{y}_k$$

Algorithms for Adaptive Equalization

Since an adaptive equalizer compensates for an unknown and time-varying channel, it requires a specific algorithm to update the equalizer coefficients and track the channel variations. A wide range of algorithms exist to adapt the filter coefficients.

The performance of an algorithm is determined by various factors which include:

- **Rate of convergence** This is defined as the number of iterations required for the algorithm, in response to stationary inputs, to converge close enough to the optimum solution. A fast rate of convergence allows the algorithm to adapt rapidly to a stationary environment of unknown statistics.
- **Misadjustment:** This parameter provides a quantitative measure of the amount by which the final value of the mean square error, averaged over an ensemble of adaptive filters, deviates from the optimal minimum mean square error.
- **Computational complexity:** This is the number of operations required to make one complete iteration of the algorithm

- **Numerical properties:** When an algorithm is implemented numerically, inaccuracies are produced due to round-oft' noise and representation errors in the computer. These kinds of errors influence the stability of the algorithm.

Three classic equalizer algorithms:

- Zero Forcing Algorithm
- Least mean squares (LMS) algorithm
- Recursive least squares (RLS) algorithm

Zero Forcing Algorithm:

- In a zero forcing equalizer, the equalizer coefficients Cn are chosen to force the samples of the combined channel and equalizer impulse response to zero at all but one of the NT spaced sample points in the tapped delay line filter.
- The zero forcing equalizer has the disadvantage that the inverse filter may excessively amplify noise at frequencies where the folded channel spectrum has high attenuation.
- The ZF equalizer thus neglects the effect of noise altogether, and is not often used for wireless links.

Least Mean Square Algorithm: Robust equalizer is the LMS equalizer

- The criterion used is the minimization of the mean square error (MSE) between the desired equalizer output and the actual equalizer output. .

$$\hat{d}_k(n) = \boldsymbol{w}_N^T(n)\boldsymbol{y}_N(n)$$

$$e_k(n) = x_k(n) - \hat{d}_k(n)$$

- $$\boldsymbol{w}_N(n+1) = \boldsymbol{w}_N(n) - \alpha e_k^*(n)\boldsymbol{y}_N(n)$$
- The LMS algorithm is the simplest equalization algorithm and requires only 2N 1 operations per iteration. Letting the variable n denote the sequence of iterations, LMS is computed iteratively by
- The convergence rate of the LMS algorithm is slow due to the fact that there is only one parameter, the step size a, that controls the adaptation rate.
- To prevent the adaptation from becoming unstable, the value of α is chosen from

$$0 < \alpha < 2 / \sum_{i=1}^{N} \lambda_i$$

- λ_i ith eigenvalue of the covariance matrix R_{NN}.

Recursive least squares (RLS):

- In order to achieve faster convergence, complex algorithms which involve additional parameters are used.
- A technique which significantly improves the convergence of adaptive equalizers is known as Recursive least squares (RLS).
- The least square error based on the time average is defined as

$$J(n) = \sum_{i=1}^{n} \lambda^{n-i} e^{*}(i,n)\, e(i,n$$

- λ is the weighting factor close to 1, but smaller than 1,e *(i, n) is the complex conjugate of e (i, n), and the error e (i, n) is given as

$$e(i,n) = x(i) - \boldsymbol{y}_N^T(i)\, \boldsymbol{w}_N(n) \qquad 0 \le i \le n$$

and

$$\boldsymbol{y}_N(i) = [y(i), y(i-1), \ldots\ldots, y(i-N+1)]^T$$

- $y_N(i)$ is the data input vector at time i

$$\sum_{i=1}^{N} \lambda_i = \boldsymbol{y}_N^T(n)\, \boldsymbol{y}_N(n)$$

Module-5

Nandini. S,
Assistant. Professor,
Dept. of ECE,
BVISIT.

Spread spectrum modulation

Spread spectrum modulation is a signalling technique used for transmitting a signal to provide a secure communi-cation.

The main advantage of spread spectrum communication technique is to prevent interference. The signals modulated with these techniques are hard to interfere and never allowed to crack signals with no official access.

Defnition of spread spectrum modulation.

* "The modulated signal occupies a much more bandwidth than the minimum required bandwidth"
* The spectrum spreading at the transmitter and despreading at the receiver is obtained by special code [chipping code] which is independent of data [message signal]

Advantages of spread spectrum

1) Cross talk elimination
2) Better output with data integrity
3) Reduced effect of multipath fading
4) Better security
5) Reduction in noise
6) co-existence with other systems
7) Longer operative distances.
8) Hard to detect

9) Not easy to demodulate/decode

10) Difficult to jam the signals.

Classification of spread spectrum systems.

Spread spectrum modulation techniques are classified as

1) Direct sequence spread spectrum [DSSS]

2) Frequency hopped spread spectrum [FHSS]

Direct sequence spread spectrum [DSSS]

The direct sequence spread spectrum uses two stages of modulation. In the first stage, each and every bit of the incoming data is multiplied by a secret code signal [PN signal]. This transforms the narrow band incoming signal into a wideband signal i.e the spectrum of the signal is spreaded.

In the second stage the wideband signal is modulated using Phase shift keying [PSK]

Frequency hopped spread spectrum.

In the frequency hopped spread spetrum the users are allowed to change the frequencies of usage, from one to another in a specified time interval. Hence the name frequency hopping.

The spectrum of the data modulated carrier is widened by changing the carrier frequency in pseudo random manner

For both direct sequence and frequency hopped spread spectrum modulation techniques, a noise like spreading code called Pseudo-noise [PN] sequence is used.

Model of spread spectrum digital communication system.

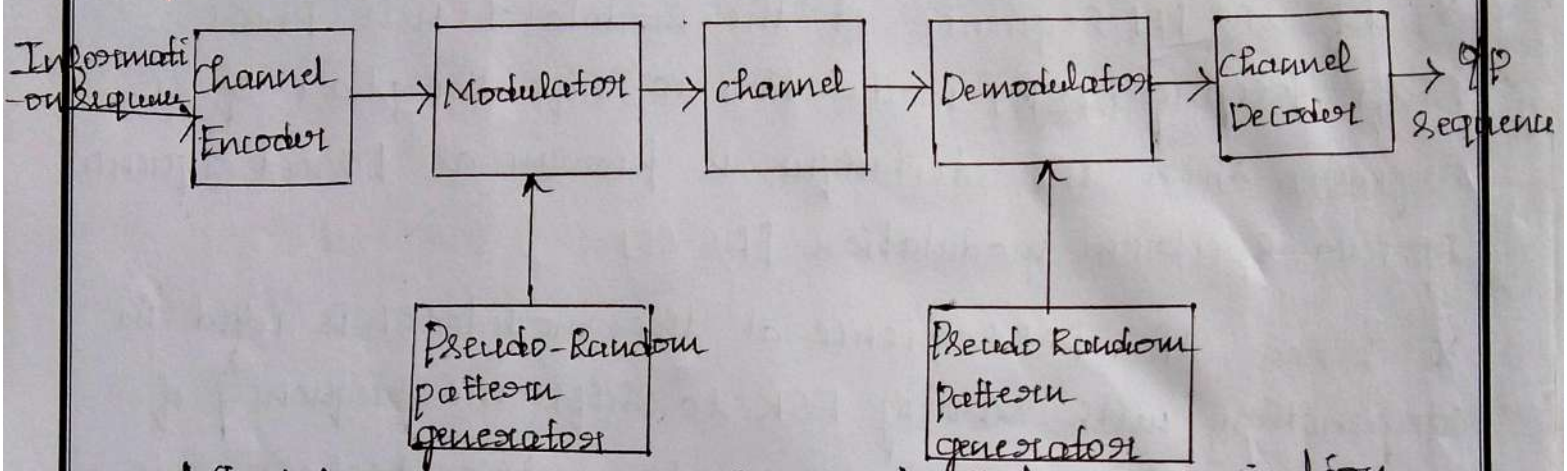

Model of spread spectrum digital communication system.

* The channel encoder encodes the binary information sequence
* The channel encoded sequence is then given to the modulator. The modulator gets pseudonoise [PN] sequence from the pseudo-random pattern generator.
* The PN sequence spreads the transmitted signal randomly over the wide frequency band. The signal at the output of the modulator is the spread spectrum modulated signal. This signal is transmitted over the channel.
* At the receiver, the demodulator recovers the encoded signal back from the spread spectrum signal

using the same PN sequence which was used at the transmitting end.

* Hence the pseudorandom pattern generators at the transmitter and receiver side operate in synchronisation with each other.
* The channel decoder decodes the binary information sequence back.
* If the PN sequence at the modulator uses phase shift keying [PSK] modulation to shift the phase of a signal, then this technique is known as Direct sequence spread spectrum modulation [DS-SS]
* When the PN sequence at the modulator is used in conjunction with M-ary FSK to shift the frequency of a signal pseudo randomly, then this technique is known as frequency hopped spread spectrum modulation [FH-SS]

PN [pseudonoise sequence]

A pseudo-noise [PN] sequence is defined as a coded sequence of 1s and 0s with certain autocorrelation properties.

Generation of pseudo-noise [PN] sequence

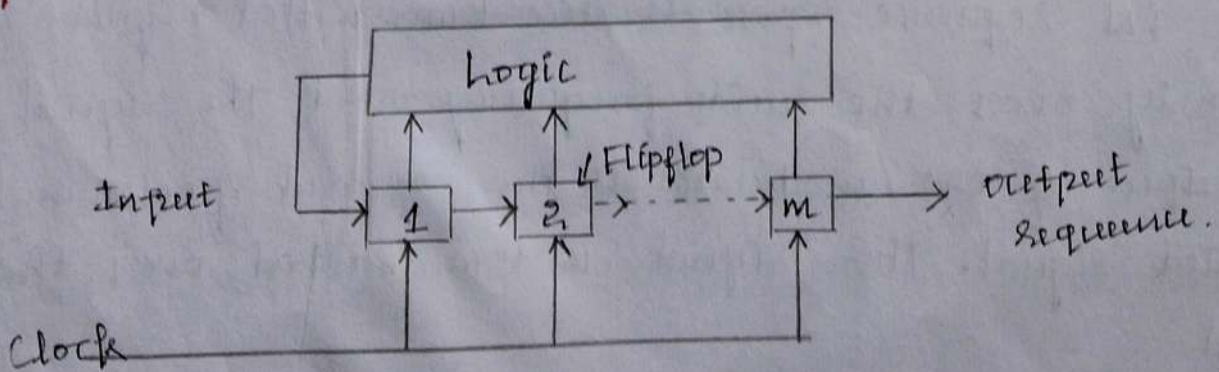

Feedback shift register to generate PN sequence

* A pseudo noise [pseudo-random] sequence is a noise like high frequency signal

* The PN sequence is generated by a feedback shift register and the combinational logic

* The feedback shift register consists of m flip-flops. The data of one flipflop is shifted to the next flipflop whenever the clock pulse is applied. At the same time the output of flipflop is given to the logic circuit.

* Depending upon the outputs of flipflops, the output of combinational circuit decided. The combination logic circuit output is given as input for the first flipflop of the shift register.

* The PN sequence generated at the output of the last flipflop in the shift register

* The generated PN sequence is periodic and it repeats after 2^m digits. This is because the m-stage shift register have 2^m states, hence the output sequence repeats after 2^m bits.

* The combinational logic circuit used is a mod-2 adder [XOR].

* If the shift registers enters a zero state [Eg: 000], it is not possible to come out of this state [i.e $0 \oplus 0 = 0$] and output sequence generated will be only zeros.

* To prevent this problem, the zero state is not allowed. Therefore the total number of states in m-stage

feedback shift register is reduced from 2^m to 2^{m-1}. The PN sequence generated have a period of $2^m - 1$ bits.

Maximum length sequences:

The pseudonoise [PN] sequence generated by a linear feedback shift register has the length $2^m - 1$, then the sequence is known as maximum length [ML] sequence.

Properties of maximum length sequences [ML]

1) Balance property: In each period of a maximum length sequence, the number of 1's is always greater by one number than the number of 0's. This property is called balance property.

For an ML-sequence generated by m-state shift register with linear feedback

i) Period = $2^m - 1$ bits.
ii) Number of 1's = 2^{m-1}.
iii) Number of 0's = $2^{m-1} - 1$.

2) Run property:

A Run is defined as a sequence of single type of binary [1's or 0's] digits.

* The appearance of an alternate digit in a sequence starts a new run.
* The length of the run is the number of digits in the run.
* Among the runs of 1's and 0's in each period of ML sequence, it is observed that one-half (1/2) the runs of each type [0's or 1's) are length 1.

one-fourth [Y_{14}] are of length 2, one-eighth are of length of 3 and so on.

* For a ML sequence generated by a m-stage linear feedback shift register,

The total number of runs $= \frac{L+1}{2}$ Where $L = 2^m - 1$

3. Autocorrelation property:

Let $\{C_0, C_1, C_2, \ldots\ldots C_{L-1}\}$ be a ML-sequence of period $L = 2^m - 1$, generated by a m-stage linear feedback register. The normalised circular autocorrelation function [ACR] of the sequence is given by

$$R(\tau) = \frac{1}{L} \sum_{i=0}^{L-1} C_i \, C_{(i \oplus \tau)_{mod\text{-}L}} \qquad \tau = 0, 1, 2, \ldots L-1.$$

Where τ is the shift.

* If The symbols 1 and 0 are represented by +1 volt and -1 volt respectively.

Autocorrelation function is defined as

$$R(\tau) = \begin{cases} 1 & \text{for } \tau = kL \quad k = 0, 1, 2 \ldots \\ -\frac{1}{L} & \text{for } \tau \neq kL \quad k = 0, 1, 2 \ldots \end{cases}$$

Direct sequence spread-spectrum system with BPSK [OR] DS-SS BPSK.

Consider the transmission of binary information sequence modulated by binary phase shift keying [BPSK] The information rate is R bits/sec, channel bandwidth is B_c Hz, where $B_c >> R$. At the modulator, the bandwidth of the information signal is expanded to $W = B_c$ Hz by using pseudo-noise [PN] sequence.

Generation of DS-SS signal [OR] DS-SS BPSK transmitter.

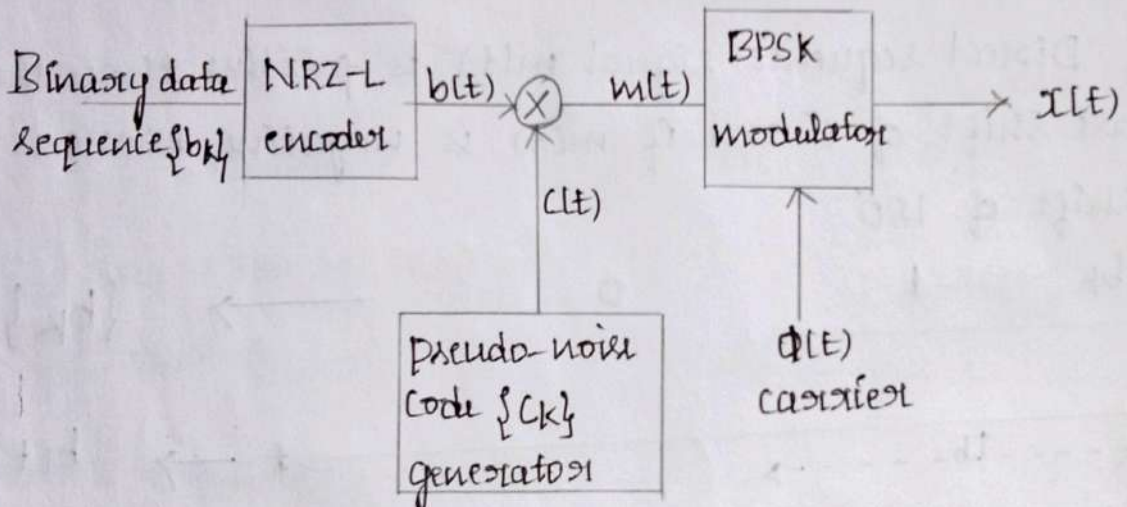

DS-SS BPSK transmitter.

* Let the data sequence be represented $\{b_k\}$. this data sequence is converted to polar NRZ waveform b(t).

i.e when $b_k = 1$, $b(t) = +1$

when $b_k = 0$, $b(t) = -1$

* Let $\{c_k\}$ denote the PN sequence and c(t) denotes the polar NRZ signal generated by c_k.

i.e when $c_k = 1$, $c(t) = +1$

when $c_k = 0$, $c(t) = -1$

* The multiplier multiplies two signals b(t) & c(t) outputs direct sequence spread spectrum signal m(t).
* This signal is given as modulating signal to BPSK transmitter.
* The Direct sequence BPSK signal is generated at the output [x(t)].
* Let $\phi(t)$ be the carrier

$$\phi(t) = \sqrt{2/T}\ \sin 2\pi f_c t.$$

* then transmitted signal x(t) is

$$\boxed{x(t) = \sqrt{2/T}.\ m(t).\sin 2\pi f_c t.}$$ where $m(t) = b(t).c(t)$

* When Direct sequence signal m(t) is positive then there is a phase shift of 0° and if m(t) is negative, there is a phase shift of 180°

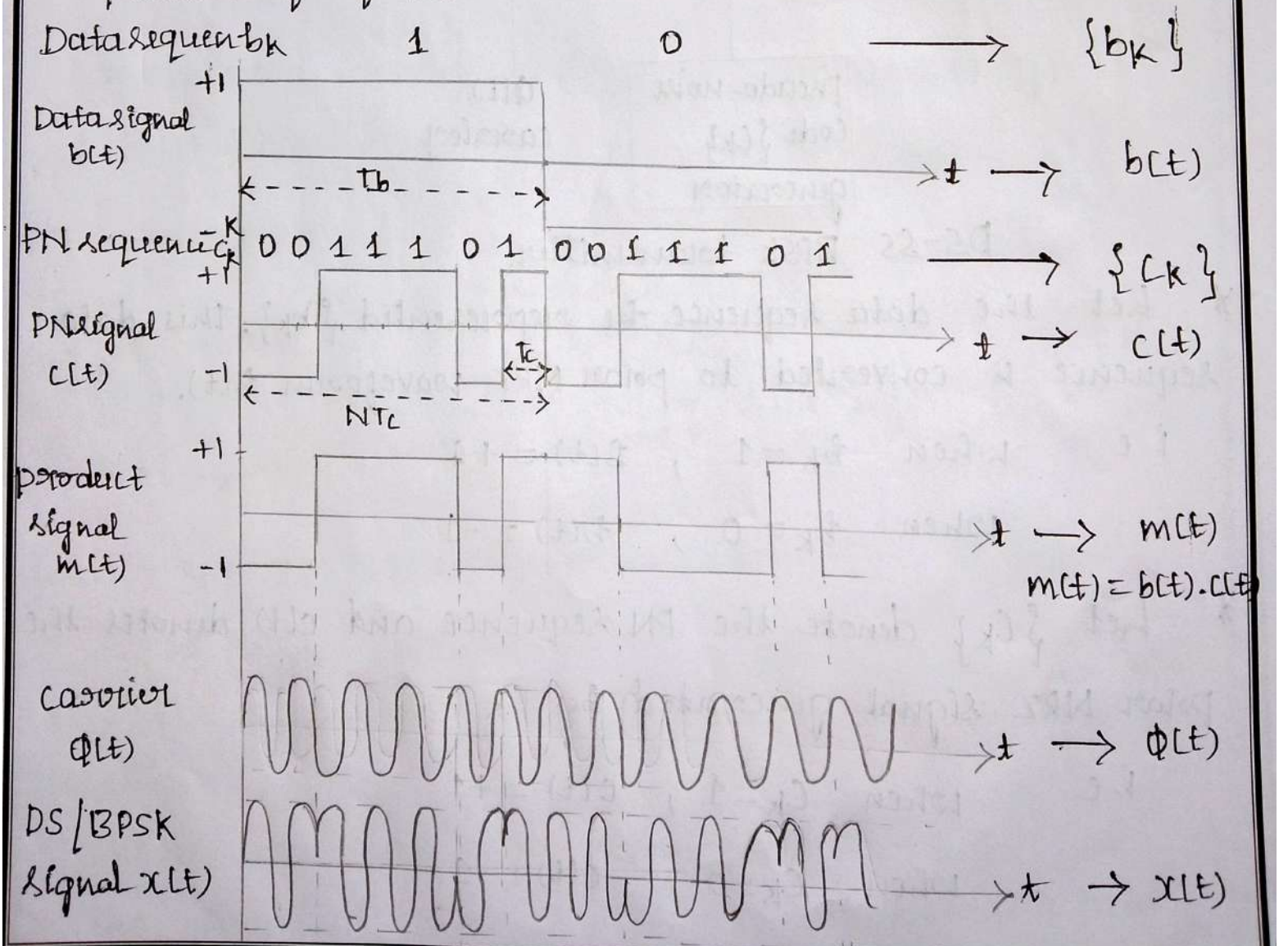

Spectrum spreading using simple rectangular spectra.

(a) Spectrum of data signal b(t)

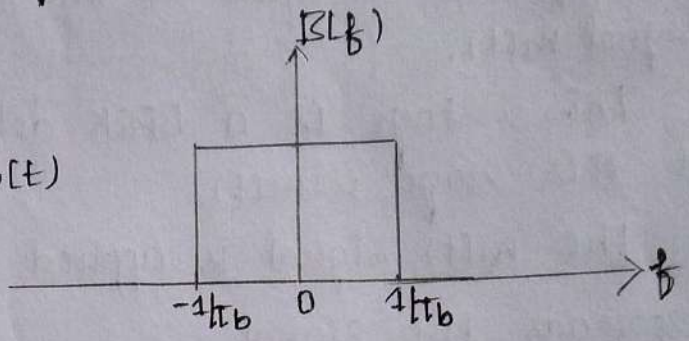

(b) Spectrum of carrier (PN) signal c(t)

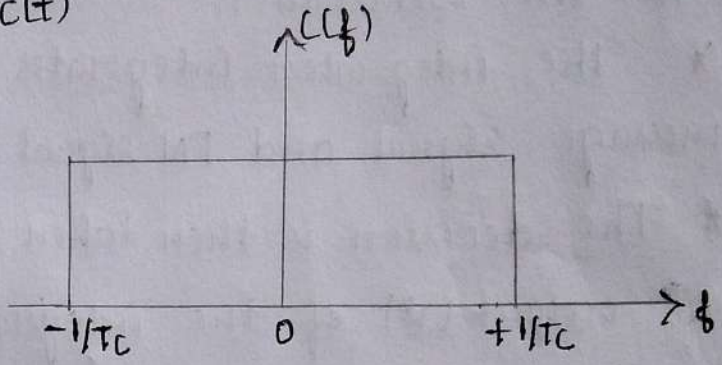

(c) convolution of spectra of b(t) & c(t)

$m(t) = b(t) * c(t)$

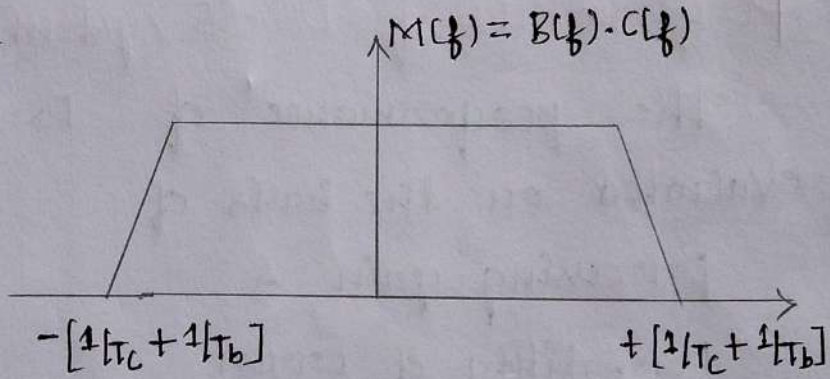

Convolution of the spectra of data signal with PN code signal.

Direct sequence spread spectrum BPSK receiver OR

DS-SS BPSK Receiver

* Fig shows the block diagram of DS-SS BPSK receiver
* there are two stages of demodulation
  1) the received signal y(t) is multiplied with locally generated coherent carrier.

* The multiplied signal is passed through LPF. The Bandwidth of LPF is equal to the bandwidth of modulating signal m(t).
* This stage is a BPSK detector. The signal obtained at this stage is m(t).
(i) The m(t) signal is applied to second demodulator which despreads the signal
* The local PN signal is exact replica of that used at the transmitter.
* The integrator integrates the product of detected message signal and PN signal over one bit period Tb.
* The decision is then taken depending on the polarity of output (V) of the integrator.

Performance of DS-SS system

The performance of DS-SS system can be evaluated on the basis of
processing gain &
Probability of error.

▷ **Processing gain [PG]:** Processing gain is defined as the ratio of the bandwidth of spreaded message signal to the bandwidth of the unspreaded message signal.

$$PG = \frac{\text{BW of spread signal}}{\text{BW of unspreaded signal.}}$$

Bandwidth of unspreaded msg signal, $R_b = \frac{1}{T_b}$.

Bandwidth of spreaded msg signal, $W_c = \frac{1}{T_c}$

Then $PG = \frac{1/T_c}{1/T_b}$ $T_b \rightarrow$ bit period

$$\boxed{PG = \frac{T_b}{T_c}} \longrightarrow (1)$$ $T_c \rightarrow$ chip period

We know that one bit period T_b of message signal is equal to 'N' bits periods of PN code signal.

i.e $$\boxed{T_b = NT_c} \longrightarrow (2)$$

By substituting eqn (2) in eqn (1)

$$PG = \frac{NT_c}{T_c}$$

$$\boxed{PG = N}$$

2) Probability of error

The probability of error for DS-BPSK system is

$$P_e = \frac{1}{2} erfc\left(\sqrt{E_b/JT_c}\right) \longrightarrow (1)$$

where $J \rightarrow$ average interference noise power.

W.K.T for coherent PSK.

$$P_e = \frac{1}{2} erfc\left(\sqrt{E_b/N_0}\right) \longrightarrow (2)$$

In DS - BPSK, the Interference may be treated as wideband noise power density $N_0/2$ defined as.

From eqn (1) and (2).

$$\frac{N_0}{2} = \frac{JT_c}{2}$$

$$N_0 = JT_c$$

* The bit energy $E_b = PT_b$

Where $P \rightarrow$ average signal power.

* The bit energy to noise density ratio is defined as

$$\frac{E_b}{N_0} = \frac{PT_b}{JT_c}$$

$$\frac{E_b}{N_0} = \frac{T_b}{T_c} \cdot \frac{P}{J}$$

$$\frac{E_b}{N_0} = PG_1 \cdot \frac{P}{J}$$

$$\boxed{\frac{J}{P} = \frac{PG_1}{E_b/N_0}}$$

The ratio of J/P is termed as Jamming margin

$$(\text{Jamming margin})_{dB} = 10 \log_{10}\left(\frac{PG_1}{E_b/N_0}\right)$$

$$= 10\log_{10}(PG_1) - 10\log_{10}(E_b/N_0)_{min}$$

$$\left[\begin{matrix}\text{Jamming} \\ \text{margin}\end{matrix}\right]_{dB} = (PG_1)_{dB} - 10\log_{10}(E_b/N_0)_{min}$$

Effect of despreading on a Narrowband Interference

If the data sequence $b(t)$ is narrowband & PN sequence $c(t)$ is wideband.

Transmitted signal / spreaded signal $m(t) = c(t) \cdot b(t)$

Received signal $y(t) = m(t) + i(t)$

$$y(t) = c(t) \cdot b(t) + i(t)$$

where $i(t) \rightarrow$ interference signal.

* The received signal is demodulated by using a locally generated PN sequence ($c(t)$).

Demodulated signal is

$$z(t) = c(t) \cdot y(t) = c(t) [\, c(t) \cdot b(t) + i(t)\,]$$

$$z(t) = b(t)\, c^2(t) + i(t) \cdot c(t)$$

* As $c(t)$ alternates between -1 & $+1$, when it is squared $c^2(t) = 1$ for all t.

$$z(t) = \underbrace{b(t)}_{\text{Narrow band signal}} + \underbrace{c(t)\, i(t)}_{\rightarrow \text{spreading code affects only it}}$$

* The term $i(t) \cdot c(t)$ results in wideband interference with power spectral density $I_0 = P_x / W$
* The desired signal $b(t)$ is demodulated by passing $z(t)$ through matched filter that has a bandwidth R.
* The total power in the interference at the output of demodulator is

$$I_0 R = \frac{P_x}{W} \cdot R = \frac{P_x}{W/R} = \frac{P_x}{T_b/T_c} = \frac{P_x}{L_c}$$

* The power in the interfering signal is reduced by an amount equal to the bandwidth expansion factor W/R.

* The Reduction in the interference power is the basic reason for using spread-spectrum signals to transmit digital information over interfering channels.

Frequency hop spread spectrum [FH-SS]

The spread spectrum in which the carrier hops randomly from one frequency to another is called frequency hop spread spectrum technique. The modulation used is MFSK [M-ary FSK]

The FH-SS are of two types.

1) Slow FH-SS
2) Fast FH-SS.

In Slow FH-SS, the symbol rate 'R_s' of the MFSK signal is an integer multiple of the hop rate 'R_h'

i.e Several symbols are transmitted in each frequency hop.

hop rate $R_h < R_s$

In Fast FH-SS, the hop rate R_h is an integer multiple of the MFSK symbol rate 'R_s'. i.e carrier frequency will change or hop several times during the transmission of one symbol. $R_h > R_s$

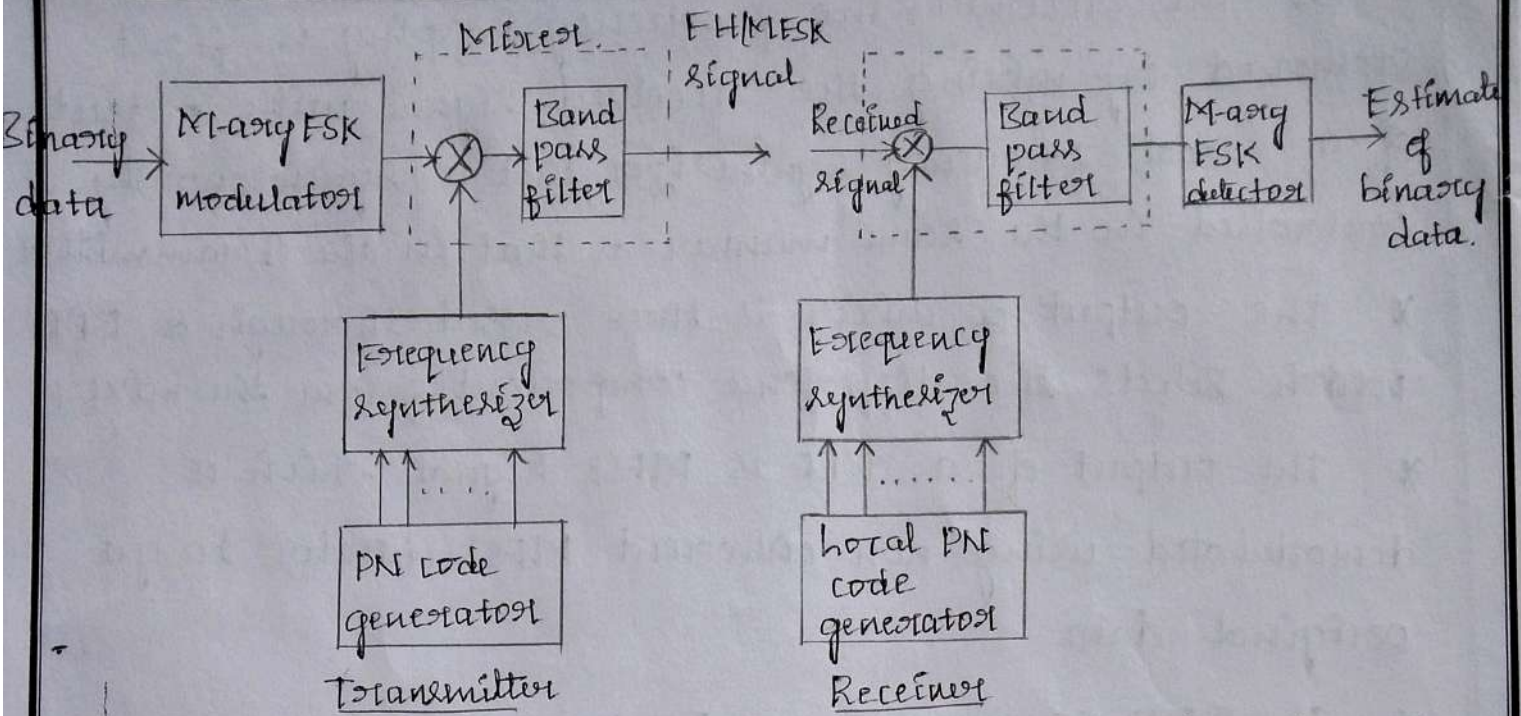

Fig shows the block diagram of a FH/MFSK transmitter and receiver

* the FH/MFSK transmitter involves frequency shift keying followed by mixer.
* the incoming data is applied to M-ary FSK system. The resulting modulated wave & output from a digital frequency synthesizer are then applied to a mixer that consists of a multiplier followed by a filter.
* The BPF is designed to select sum frequency component resulting from multiplication process.
* PN sequence will drive the frequency synthesizer, which enables carrier frequency over 2^k distinct values.
* on single hop, bandwidth of the transmitted signal is same as that resulting from the use of conventional MFSK format.
* For complete range of 2^k frequency hops, FH/MFSK signal occupies a much larger bandwidth.
* The Non coherent MFSK detector is used.

* At the receiver, the frequency hopping is first removed by mixing the received signal with output of a local frequency synthesizer that is synchronously controlled in the same manner as that in the transmitter.
* the output of mixer is then passed through a BPF which selects the difference component from the mixer.
* The output of a BPF is MFSK signal which is demodulated using non-coherent MFSK detector to get original data.
* In FH SS system, an FH tone of shortest duration is called 'chip'

the chip rate R_c,

$$\underline{R_c = \max(R_h, R_s)}$$

$R_h \rightarrow$ hop rate

$R_s \rightarrow$ Symbol rate

* For slow FH-SS system

$$R_c = R_s$$

$$\therefore R_c = R_s = \frac{R_b}{k} \geq R_h \quad \text{where } k = \log_2 M$$

* For Fast FH-SS system

$$R_c = R_h$$

* Processing gain

$$PG = \frac{\text{BW of spreaded signal}}{\text{BW of unspreaded signal}} = \frac{\text{BW of FH-signal}}{\text{BW of Baseband signal}}$$

Let f_s be the symbol frequency. Out there are 2^k frequency hops generated from k-bits of PN sequence.

∴ BW of the FH-signal is $2^k f_s$ f

BW of the unspreaded signal is f_s

$$P_{PJ} = \frac{2^k f_s}{f_s}$$

$$\boxed{P_{PJ} = 2^k}$$

Applications of Direct sequence spread spectrum [DS-SS] systems.

1> Low detectability signal transmission.
OR
Low probability Intercept.

For this application, the signal spectral density is intensionally kept small with respect to channel noise and receiver noise so that the presence of the signal is not detected easily.

Consider the average received signal power at the intended receiver is Pav and the noise power is Nav. Then the signal is transmitted at low power levels. Such that $\frac{P_{av}}{N_{av}} << 1$. Hence the receivers which are in the vicinity of the intended receiver cannot detect the presence of the signal.

The intended receiver recovers the message signal with the help of processing gain and coding gain. Other receivers who doesn't know the PN sequence hence they can not receive the information signal with the help of processing gain and coding gain This is called as the signal has low probability of being intercepted. [LPI]

2) Code-division multiple Access with DS-SS [CDMA]

Many users transmit their signals on the same channel bandwidth. Each transmitter and receiver pair has a distinct PN sequence. Thus signals of particular transmitter are received by its intended receiver only. Even if many users are transmitting at the same time the signals from other users appear as additive interference which are rejected by the spread decoder. The level of interference depends on the number of users transmitting at a time.

The main advantage of CDMA is that the number of users sharing a same channel can be increased or decreased very easily.

Large number of users can transmit on the same channel if their messages are for short periods of time.

3) Wireless LAN

Spread spectrum signals have been used in the IEEE wireless LAN standards 802.11 and 802.11b which operate in the 2.4GHz frequency band.

The available channel bandwidth is subdivided into 14 overlapping 22MHz channels, although not all channels are used in all countries.

In the 802.11 standard, an 11-chip Barker sequence is modulated and transmitted at a rate of 11MHz. The 11 chip Barker sequence is { 1, -1, 1, 1, -1, 1, 1, 1, -1, -1, -1 }

The Barker sequence is modulated either with BPSK or QPSK. When BPSK is used with 11 chips per bit a data rate of 1 Mbps is achieved. When QPSK is used with 11-chips per symbol [2-bits] - a data rate of 2Mbps. is achieved.

In the 802.11b standard 11 MHz chip rate is maintained but the Barker sequence is replaced by a set of 8-chip waveform sequences called complementary code shift keying [CCK]. The use of CCK modulation results in a data rate of 1 Mbps.

CDMA System based on IS-95

In this system, several users transmit messages simultaneously over the same channel. Each user is allocated a particular code [PN sequence] for transmitting over the common channel.

* CDMA [1st generation digital cellular communication system) was developed by Qualcomm, and it has been standardized and designated as IS-95 [Interim-standard] by Telecommunication Industry Association [TIA] for use in the 800MHz and 1800 MHz frequency bands.
* CDMA system based IS-95 is widely used in North America and some eastern countries.
* A major advantage of CDMA is that a large number of users can be accomodated., if each user transmits messages for a short period of time.

* Advantage of CDMA over other multiple access methods [TDMA & FDMA] is that the entire frequency band is available at each base station.

* The nominal bandwidth used for transmission from a base station to the mobile receivers [forward link] is 1.25 MHz. A separate channel (1.25 MHz bandwidth) is used for signal transmission from mobile receiver to base station [reverse link].

Forward link:

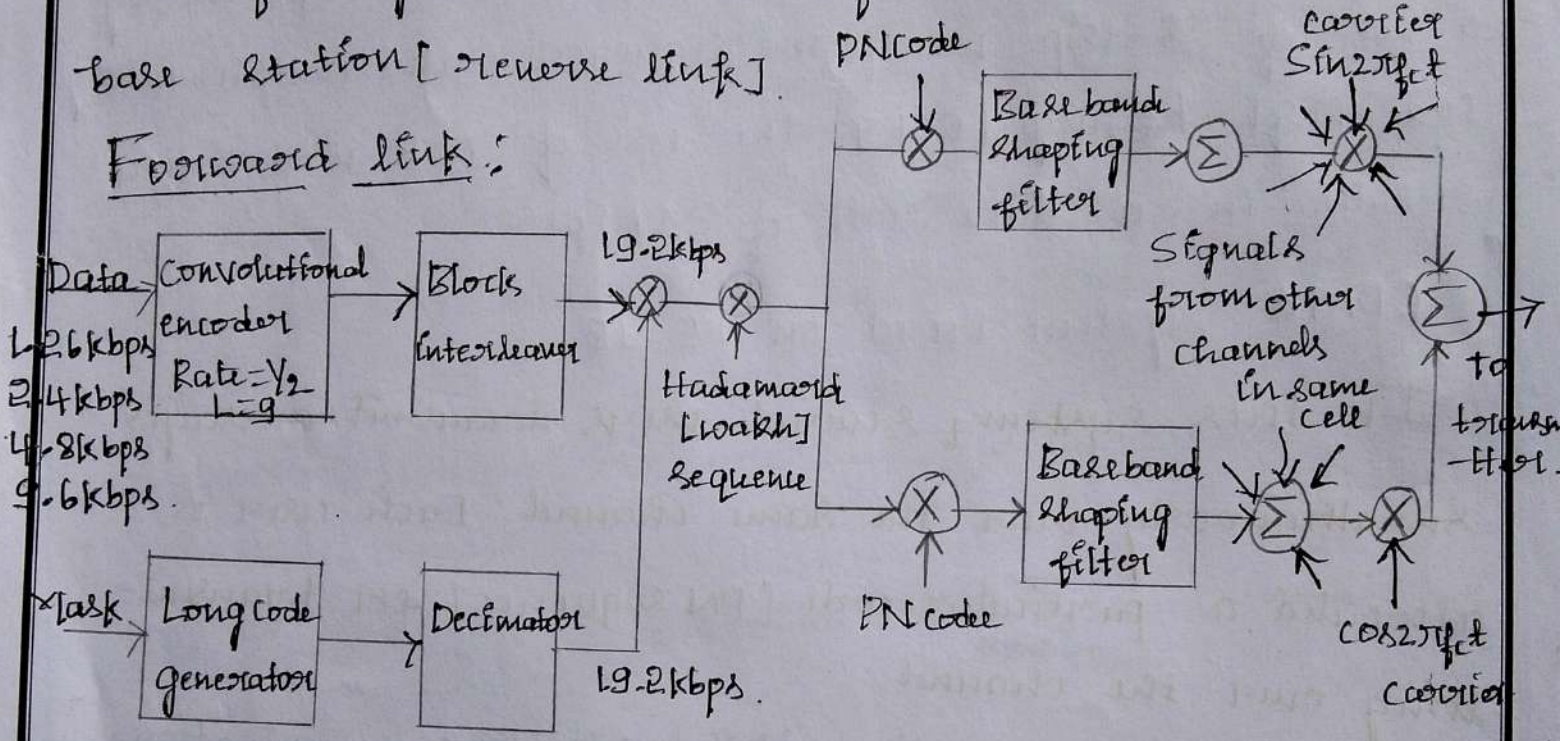

* The data from the speech coder is encoded by a rate 1/2, constraint length L=9, convolutional code. the speech coder generates data at the variable rates of 9.6 kbps, 4.8 kbps, 2.4 kbps & 1.2 kbps.

* The encoded bit for each frame are passed through a block interleaver, which overcomes the effect of burst errors that may occur in transmission through the channel.

* The data bits from the block interleaver are scrambled by multiplication with the output of a long code generator running at chip rate of 1.2288×10^6 chips/sec, but whose output is decimated by a factor of 64 to 19.2 k chip/sec.

* Each channel user is assigned Hadamard [walsh] sequence of length 64.
* Each user, using the assigned Hadamard sequence, multiplies the data sequence by the assigned Hadamard sequence. Thus each encoded data bit is multiplies the Hadamard sequence of length 64
* The resulting binary sequence is spread by multiplication with two PN sequences of length $N = 2^{15}$, this creates inphase & Quadrature phase signal components. Thus the binary data signal is converted to a four-phase and both I & Q components are filtered by baseband spectral shaping filter.
* Different base stations are identified by different offset of these PN sequences.
* The signals for all 64 channels are transmitted synchronously.

Reverse link

* Reverse link uses a rate $1/3$, $K=9$ convolution coder. This code has essentially the same coding gain in an AWGN channel.
* For each 20ms frame, the 576 encoded bits are block interleaved and passed to the modulator. The data is modulated using $M=64$ orthogonal signal set of Hadamard sequences each of length 64. Thus a 6-bit block of data is mapped into one of the 64 Hadamard sequences. The result is a chip rate of 307.2 kbps at the output of the modulator.

* To reduce interference to other users, the time positions of the transmitted code symbol repetitions are randomised. Randomised signal is spreaded by the output of long code generator. Hence there are only four PN chips for every bit of the Hadamard sequence for the modulation.

* the resulting binary sequence create I & Q signal [QPSK] that are filtered by baseband shaping filter and then passed to Quadrature mixers.

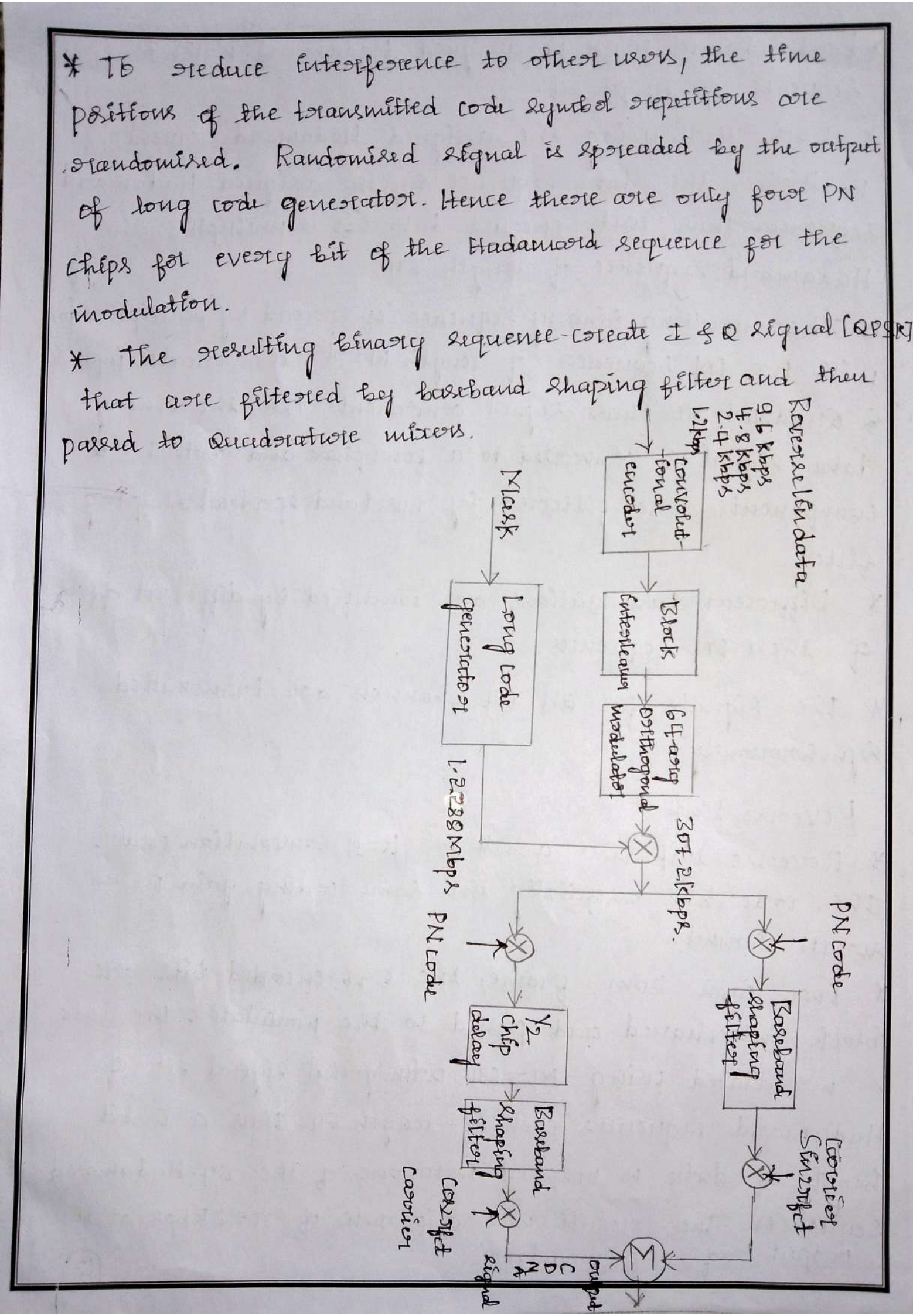

13

Fading Channels I: Characterization and Signaling

The previous chapters have described the design and performance of digital communication systems for transmission on either the classical AWGN channel or a linear filter channel with AWGN. We observed that the distortion inherent in linear filter channels requires special signal design techniques and rather sophisticated adaptive equalization algorithms in order to achieve good performance.

In this chapter, we consider the signal design, receiver structure, and receiver performance for more complex channels, namely, channels having randomly time variant impulse responses. This characterization serves as a model for signal transmission over many radio channels such as shortwave ionospheric radio communication in the 3–30 MHz frequency band (HF), tropsopheric scatter (beyond-the-horizon) radio communications in the 300–3000 MHz frequency band (UHF), and 3000–30,000 MHz frequency band (SHF), and ionospheric forward scatter in the 30–300 MHz frequency band (VHF). The time-variant impulse responses of these channels are a consequence of the constantly changing physical characteristics of the media. For example, the ions in the ionospheric layers that reflect the signals transmitted in the HF band are always in motion. To the user of the channel, the motion of the ions appears to be random. Consequently, if the same signal is transmitted at HF in two widely separated time intervals, the two received signals will be different. The time-varying responses that occur are treated in statistical terms.

We shall begin our treatment of digital signaling over fading multipath channels by first developing a statistical characterization of the channel. Then we shall evaluate the performance of several basic digital signaling techniques for communication over such channels. The performance results will demonstrate the severe penalty in SNR that must be paid as a consequence of the fading characteristics of the received signal. We shall then show that the penalty in SNR can be dramatically reduced by means of efficient modulation/coding and demodulation/decoding techniques.

13.1
CHARACTERIZATION OF FADING MULTIPATH CHANNELS

If we transmit an extremely short pulse, ideally an impulse, over a time-varying multipath channel, the received signal might appear as a train of pulses, as shown in Figure 13.1–1. Hence, one characteristic of a multipath medium is the time spread introduced in the signal that is transmitted through the channel.

A second characteristic is due to the time variations in the structure of the medium. As a result of such time variations, the nature of the multipath varies with time. That is, if we repeat the pulse-sounding experiment over and over, we shall observe changes in the received pulse train, which will include changes in the sizes of the individual pulses, changes in the relative delays among the pulses, and, quite often, changes in the number of pulses observed in the received pulse train as shown in Figure 13.1–1. Moreover, the time variations appear to be unpredictable to the user of the channel. Therefore, it is reasonable to characterize the time-variant multipath channel statistically. Toward this end, let us examine the effects of the channel on a transmitted signal that is represented in general as

$$s(t) = \text{Re}\left[s_l(t)e^{j2\pi f_c t}\right] \tag{13.1–1}$$

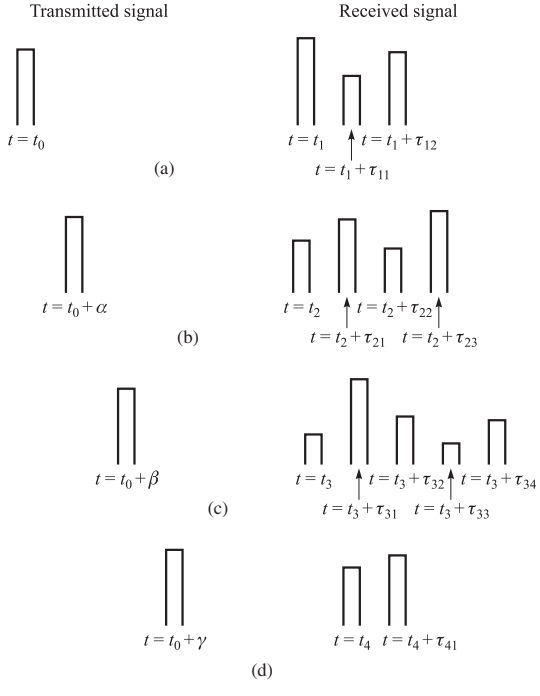

FIGURE 13.1–1
Example of the response of a time-variant multipath channel to a very narrow pulse.

We assume that there are multiple propagation paths. Associated with each path is a propagation delay and an attenuation factor. Both the propagation delays and the attenuation factors are time-variant as a result of changes in the structure of the medium. Thus, the received bandpass signal may be expressed in the form

$$x(t) = \sum_n \alpha_n(t) s[t - \tau_n(t)] \tag{13.1–2}$$

where $\alpha_n(t)$ is the attenuation factor for the signal received on the nth path and $\tau_n(t)$ is the propagation delay for the nth path. Substitution for $s(t)$ from Equation 14.1–1 into Equation 13.1–2 yields the result

$$x(t) = \text{Re}\left(\left\{ \sum_n \alpha_n(t) e^{-j2\pi f_c \tau_n(t)} s_l[t - \tau_n(t)] \right\} e^{j2\pi f_c t} \right) \tag{13.1–3}$$

It is apparent from Equation 13.1–3 that in the absence of noise the equivalent lowpass received signal is

$$r_l(t) = \sum_n \alpha_n(t) e^{-j2\pi f_c \tau_n(t)} s_l[t - \tau_n(t)] \tag{13.1–4}$$

Since $r_l(t)$ is the response of an equivalent lowpass channel to the equivalent lowpass signal $s_l(t)$, it follows that the equivalent lowpass channel is described by the time-variant impulse response

$$c(\tau; t) = \sum_n \alpha_n(t) e^{-j2\pi f_c \tau_n(t)} \delta[\tau - \tau_n(t)] \tag{13.1–5}$$

For some channels, such as the tropospheric scatter channel, it is more appropriate to view the received signal as consisting of a continuum of multipath components. In such a case, the received signal $x(t)$ is expressed in the integral form

$$x(t) = \int_{-\infty}^{\infty} \alpha(\tau; t) s(t - \tau) d\tau \tag{13.1–6}$$

where $\alpha(\tau; t)$ denotes the attenuation of the signal components at delay τ and at time instant t. Now substitution for $s(t)$ from Equation 13.1–1 into Equation 13.1–6 yields

$$x(t) = \text{Re}\left\{ \left[\int_{-\infty}^{\infty} \alpha(\tau; t) e^{-j2\pi f_c \tau} s_l(t - \tau)\, d\tau \right] e^{j2\pi f_c t} \right\} \tag{13.1–7}$$

Since the integral in Equation 13.1–7 represents the convolution of $s_l(t)$ with an equivalent lowpass time-variant impulse response $c(\tau; t)$, it follows that

$$c(\tau; t) = \alpha(\tau; t) e^{-j2\pi f_c \tau} \tag{13.1–8}$$

where $c(\tau; t)$ represents the response of the channel at time t due to an impulse applied at time $t - \tau$. Thus Equation 13.1–8 is the appropriate definition of the equivalent lowpass impulse response when the channel results in continuous multipath and Equation 13.1–5 is appropriate for a channel that contains discrete multipath components.

Now let us consider the transmission of an unmodulated carrier at frequency f_c. Then $s_l(t) = 1$ for all t, and, hence, the received signal for the case of discrete multipath,

given by Equation 13.1–4, reduces to

$$\begin{aligned} r_l(t) &= \sum_n \alpha_n(t) e^{-j2\pi f_c \tau_n(t)} \\ &= \sum_n \alpha_n(t) e^{j\theta_n(t)} \end{aligned} \tag{13.1–9}$$

where $\theta_n(t) = -2\pi f_c \tau_n(t)$. Thus, the received signal consists of the sum of a number of time-variant vectors (phasors) having amplitudes $\alpha_n(t)$ and phases $\theta_n(t)$. Note that large dynamic changes in the medium are required for $\alpha_n(t)$ to change sufficiently to cause a significant change in the received signal. On the other hand, $\theta_n(t)$ will change by 2π rad whenever τ_n changes by $1/f_c$. But $1/f_c$ is a small number and, hence, θ_n can change by 2π rad with relatively small motions of the medium. We also expect the delays $\tau_n(t)$ associated with the different signal paths to change at different rates and in an unpredictable (random) manner. This implies that the received signal $r_l(t)$ in Equation 13.1–9 can be modeled as a random process. When there are a large number of paths, the central limit theorem can be applied. That is, $r_l(t)$ may be modeled as a complex-valued Gaussian random process. This means that the time-variant impulse response $c(\tau; t)$ is a complex-valued Gaussian random process in the t variable.

The multipath propagation model for the channel embodied in the received signal $r_l(t)$, given in Equation 13.1–9, results in signal fading. The fading phenomenon is primarily a result of the time variations in the phases $\{\theta_n(t)\}$. That is, the randomly time variant phases $\{\theta_n(t)\}$ associated with the vectors $\{\alpha_n e^{j\theta_n}\}$ at times result in the vectors adding destructively. When that occurs, the resultant received signal $r_l(t)$ is very small or practically zero. At other times, the vectors $\{\alpha_n e^{j\theta_n}\}$ add constructively, so that the received signal is large. Thus, the amplitude variations in the received signal, termed *signal fading*, are due to the time-variant multipath characteristics of the channel.

When the impulse response $c(\tau; t)$ is modeled as a zero-mean complex-valued Gaussian process, the envelope $|c(\tau; t)|$ at any instant t is Rayleigh-distributed. In this case the channel is said to be a *Rayleigh fading channel*. In the event that there are fixed scatterers or signal reflectors in the medium, in addition to randomly moving scatterers, $c(\tau; t)$ can no longer be modeled as having zero-mean. In this case, the envelope $|c(\tau; t)|$ has a Rice distribution and the channel is said to be a *Ricean fading channel*. Another probability distribution function that has been used to model the envelope of fading signals is the Nakagami-*m* distribution. These fading channel models are considered in Section 13.1–2.

13.1–1 Channel Correlation Functions and Power Spectra

We shall now develop a number of useful correlation functions and power spectral density functions that define the characteristics of a fading multipath channel. Our starting point is the equivalent lowpass impulse response $c(\tau; t)$, which is characterized as a complex-valued random process in the t variable. We assume that $c(\tau; t)$ is wide-sense-stationary. Then we define the autocorrelation function of $c(\tau; t)$ as

$$R_c(\tau_2, \tau_1; \Delta t) = E\left[c^*(\tau_1; t) c(\tau_2; t + \Delta t)\right] \tag{13.1–10}$$

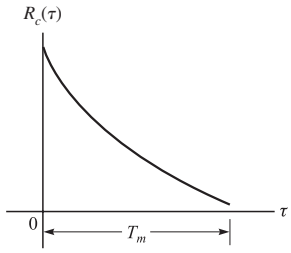

FIGURE 13.1–2
Multipath intensity profile.

In most radio transmission media, the attentuation and phase shift of the channel associated with path delay τ_1 is uncorrelated with the attenuation and phase shift associated with path delay τ_2. This is usually called *uncorrelated scattering*. We make the assumption that the scattering at two different delays is uncorrelated and incorporate it into Equation 13.1–10 to obtain

$$E\left[c^*(\tau_1; t)c(\tau_2; t + \Delta t)\right] = R_c(\tau_1; \Delta t)\delta(\tau_2 - \tau_1) \tag{13.1–11}$$

If we let $\Delta t = 0$, the resulting autocorrelation function $R_c(\tau; 0) \equiv R_c(\tau)$ is simply the average power output of the channel as a function of the time delay τ. For this reason, $R_c(\tau)$ is called the *multipath intensity profile* or the *delay power spectrum* of the channel. In general, $R_c(\tau; \Delta t)$ gives the average power output as a function of the time delay τ and the difference Δt in observation time.

In practice, the function $R_c(\tau; \Delta t)$ is measured by transmitting very narrow pulses or, equivalently, a wideband signal and cross-correlating the received signal with a delayed version of itself. Typically, the measured function $R_c(\tau)$ may appear as shown in Figure 13.1–2. The range of values of τ over which $R_c(\tau)$ is essentially nonzero is called the *multipath spread of the channel* and is denoted by T_m.

A completely analogous characterization of the time-variant multipath channel begins in the frequency domain. By taking the Fourier transform of $c(\tau; t)$, we obtain the time-variant transfer function $C(f; t)$, where f is the frequency variable. Thus,

$$C(f; t) = \int_{-\infty}^{\infty} c(\tau; t)e^{-j2\pi f\tau}\, d\tau \tag{13.1–12}$$

If $c(\tau; t)$ is modeled as a complex-valued zero-mean Gaussian random process in the t variable, it follows that $C(f; t)$ also has the same statistics. Under the assumption that the channel is wide-sense-stationary, we define the autocorrelation function

$$R_C(f_2, f_1; \Delta t) = E\left[C^*(f_1; t)C(f_2; t + \Delta t)\right] \tag{13.1–13}$$

Since $C(f; t)$ is the Fourier transform of $c(\tau; t)$, it is not surprising to find that $R_C(f_2, f_1; \Delta t)$ is related to $R_c(\tau; \Delta t)$ by the Fourier transform. The relationship is

easily established by substituting Equation 13.1–12 into Equation 13.1–13. Thus,

$$\begin{aligned} R_C(f_2, f_1; \Delta t) &= \int_{-\infty}^{\infty}\int_{-\infty}^{\infty} E\left[c^*(\tau_1; t)c(\tau_2; t+\Delta t)\right] e^{j2\pi(f_1\tau_1 - f_2\tau_2)} d\tau_1 d\tau_2 \\ &= \int_{-\infty}^{\infty}\int_{-\infty}^{\infty} R_c(\tau_1; \Delta t)\delta(\tau_2 - \tau_1) e^{j2\pi(f_1\tau_1 - f_2\tau_2)} d\tau_1 d\tau_2 \\ &= \int_{-\infty}^{\infty} R_c(\tau_1; \Delta t) e^{j2\pi(f_1 - f_2)\tau_1} d\tau_1 \\ &= \int_{-\infty}^{\infty} R_c(\tau_1; \Delta t) e^{-j2\pi\Delta f\,\tau_1} d\tau_1 \equiv R_C(\Delta f; \Delta t) \end{aligned} \tag{13.1–14}$$

where $\Delta f = f_2 - f_1$. From Equation 13.1–14, we observe that $R_C(\Delta f; \Delta t)$ is the Fourier transform of the multipath intensity profile. Furthermore, the assumption of uncorrelated scattering implies that the autocorrelation function of $C(f; t)$ in frequency is a function of only the frequency difference $\Delta f = f_2 - f_1$. Therefore, it is appropriate to call $R_C(\Delta f; \Delta t)$ the *spaced-frequency, spaced time correlation function of the channel*. It can be measured in practice by transmitting a pair of sinusoids separated by Δf and cross-correlating the two separately received signals with a relative delay Δt.

Suppose we set $\Delta t = 0$ in Equation 13.1–14. Then, with $R_C(\Delta f; 0) \equiv R_C(\Delta f)$ and $R_c(\tau; 0) \equiv R_c(\tau)$, the transform relationship is simply

$$R_C(\Delta f) = \int_{-\infty}^{\infty} R_c(\tau) e^{-j2\pi\Delta f\,\tau} d\tau \tag{13.1–15}$$

The relationship is depicted graphically in Figure 13.1–3. Since $R_C(\Delta f)$ is an autocorrelation function in the frequency variable, it provides us with a measure of the frequency coherence of the channel. As a result of the Fourier transform relationship between $R_C(\Delta f)$ and $R_c(\tau)$, the reciprocal of the multipath spread is a measure of the *coherence bandwidth of the channel*. That is,

$$(\Delta f)_c \approx \frac{1}{T_m} \tag{13.1–16}$$

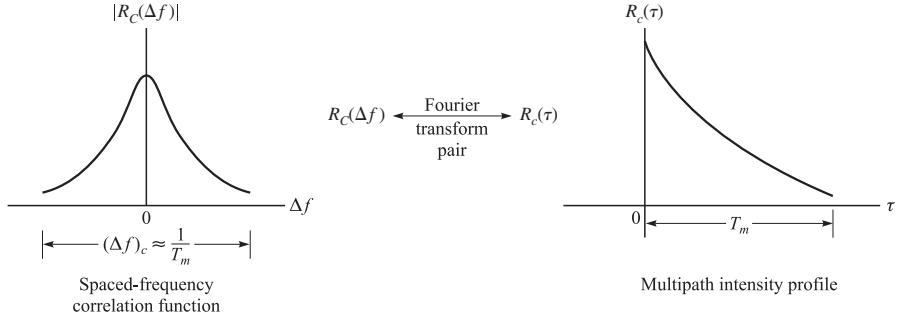

FIGURE 13.1–3
Relationship between $R_C(\Delta f)$ and $R_c(\tau)$.

where $(\Delta f)_c$ denotes the coherence bandwidth. Thus, two sinusoids with frequency separation greater than $(\Delta f)_c$ are affected differently by the channel. When an information-bearing signal is transmitted through the channel, if $(\Delta f)_c$ is small in comparison to the bandwidth of the transmitted signal, the channel is said to be *frequency-selective*. In this case, the signal is severely distorted by the channel. On the other hand, if $(\Delta f)_c$ is large in comparison with the bandwidth of the transmitted signal, the channel is said to be *frequency-nonselective*.

We now focus our attention on the time variations of the channel as measured by the parameter Δt in $R_C(\Delta f; \Delta t)$. The time variations in the channel are evidenced as a Doppler broadening and, perhaps, in addition as a Doppler shift of a spectral line. In order to relate the Doppler effects to the time variations of the channel, we define the Fourier transform of $R_C(\Delta f; \Delta t)$ with respect to the variable Δt to be the function $\mathcal{S}_C(\Delta f; \lambda)$. That is,

$$\mathcal{S}_C(\Delta f; \lambda) = \int_{-\infty}^{\infty} R_C(\Delta f; \Delta t) e^{-j2\pi\lambda\,\Delta t} d\,\Delta t \tag{13.1–17}$$

With Δf set to zero and $\mathcal{S}_C(0; \lambda) \equiv \mathcal{S}_C(\lambda)$, the relation in Equation 14.1–17 becomes

$$\mathcal{S}_C(\lambda) = \int_{-\infty}^{\infty} R_C(0; \Delta t) e^{-j2\pi\lambda\,\Delta t} d\,\Delta t \tag{13.1–18}$$

The function $\mathcal{S}_C(\lambda)$ is a power spectrum that gives the signal intensity as a function of the Doppler frequency λ. Hence, we call $\mathcal{S}_C(\lambda)$ the *Doppler power spectrum of the channel*.

From Equation 13.1–18, we observe that if the channel is time-invariant, $R_C(\Delta t) = 1$ and $\mathcal{S}_C(\lambda)$ becomes equal to the delta function $\delta(\lambda)$. Therefore, when there are no time variations in the channel, there is no spectral broadening observed in the transmission of a pure frequency tone.

The range of values of λ over which $\mathcal{S}_C(\lambda)$ is essentially nonzero is called the *Doppler spread* B_d *of the channel*. Since $\mathcal{S}_C(\lambda)$ is related to $R_C(\Delta t)$ by the Fourier transform, the reciprocal of B_d is a measure of the coherence time of the channel. That is,

$$(\Delta t)_c \approx \frac{1}{B_d} \tag{13.1–19}$$

where $(\Delta t)_c$ denotes the *coherence time*. Clearly, a slowly changing channel has a large coherence time or, equivalently, a small Doppler spread. Figure 13.1–4 illustrates the relationship between $R_C(\Delta t)$ and $\mathcal{S}_C(\lambda)$.

We have now established a Fourier transform relationship between $R_C(\Delta f; \Delta t)$ and $R_c(\tau; \Delta t)$ involving the variables $(\tau, \Delta f)$, and a Fourier transform relationship between $R_C(\Delta f; \Delta t)$ and $\mathcal{S}_C(\Delta f; \lambda)$ involving the variables $(\Delta t, \lambda)$. There are two additional Fourier transform relationships that we can define, which serve to relate $R_c(\tau; \Delta t)$ to $\mathcal{S}_C(\Delta f; \lambda)$ and, thus, close the loop. The desired relationship is obtained by defining a new function, denoted by $\mathcal{S}(\tau; \lambda)$, to be the Fourier transform of $R_c(\tau; \Delta t)$

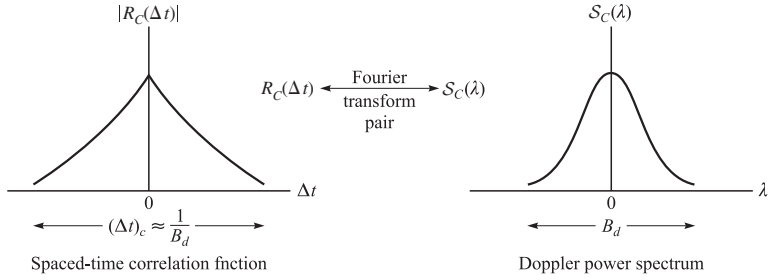

FIGURE 13.1–4
Relationship between $R_C(\Delta t)$ and $\mathcal{S}_C(\lambda)$.

in the Δt variable. That is,

$$\mathcal{S}(\tau; \lambda) = \int_{-\infty}^{\infty} R_c(\tau; \Delta t) e^{-j2\pi\lambda\,\Delta t} d\Delta t \tag{13.1–20}$$

It follows that $\mathcal{S}(\tau; \lambda)$ and $\mathcal{S}_C(\Delta f; \lambda)$ are a Fourier transform pair. That is,

$$\mathcal{S}(\tau; \lambda) = \int_{-\infty}^{\infty} \mathcal{S}_C(\Delta f; \lambda) e^{j2\pi\tau\,\Delta f} d\Delta f \tag{13.1–21}$$

Furthermore, $\mathcal{S}(\tau; \lambda)$ and $R_C(\Delta f; \Delta t)$ are related by the double Fourier transform

$$\mathcal{S}(\tau; \lambda) = \int_{-\infty}^{\infty} \int_{-\infty}^{\infty} R_C(\Delta f; \Delta t) e^{-j2\pi\lambda\,\Delta t} e^{j2\pi\tau\,\Delta f}\, d\Delta t\, d\Delta f \tag{13.1–22}$$

This new function $\mathcal{S}(\tau; \lambda)$ is called the *scattering function of the channel*. It provides us with a measure of the average power output of the channel as a function of the time delay τ and the Doppler frequency λ.

The relationships among the four functions $R_C(\Delta f; \Delta t)$, $R_c(\tau; \Delta t)$, $\mathcal{S}_C(\Delta f; \lambda)$, and $\mathcal{S}(\tau; \lambda)$ are summarized in Figure 13.1–5.

EXAMPLE 13.1–1. SCATTERING FUNCTION OF A TROPOSPHERIC SCATTER CHANNEL. The scattering function $\mathcal{S}(\tau; \lambda)$ measured on a 150-mi tropospheric scatter link is shown in Figure 13.1–6. The signal used to probe the channel had a time resolution of 0.1 μs. Hence, the time-delay axis is quantized in increments of 0.1 μs. From the graph, we observe that the multipath spread $T_m = 0.7\,\mu$s. On the other hand, the Doppler spread, which may be defined as the 3-dB bandwidth of the power spectrum for each signal path, appears to vary with each signal path. For example, in one path it is less than 1 Hz, while in some other paths it is several hertz. For our purposes, we shall take the largest of these 3-dB bandwidths of the various paths and call that the *Doppler spread*.

EXAMPLE 13.1–2. MULTIPATH INTENSITY PROFILE OF MOBILE RADIO CHANNELS. The multipath intensity profile of a mobile radio channel depends critically on the type of terrain. Numerous measurements have been made under various conditions in many parts of the world. In urban and suburban areas, typical values of multipath spreads

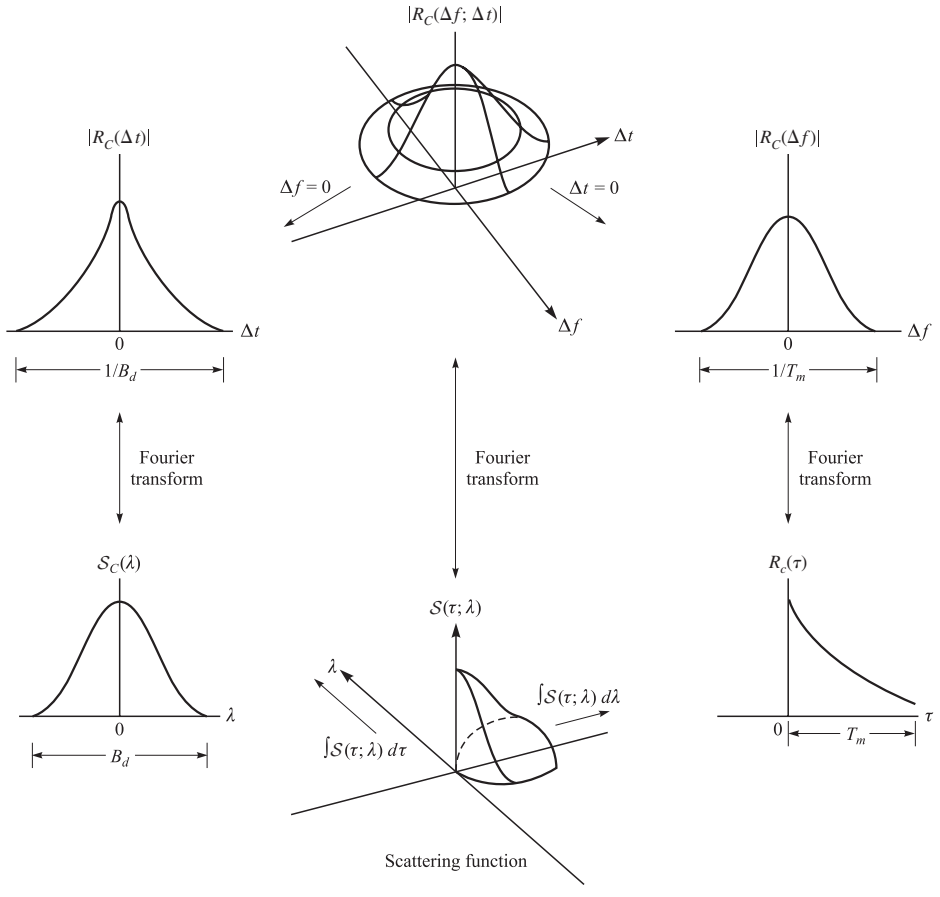

FIGURE 13.1–5
Relationships among the channel correlation functions and power spectra. [*From Green (1962), with permission.*]

range from 1 to 10 μs. In rural mountainous areas, the multipath spreads are much greater, with typical values in the range of 10 to 30 μs. Two models for the multipath intensity profile that are widely used in evaluating system performance for these two types of terrain are illustrated in Figure 13.1–7.

EXAMPLE 13.1–3. DOPPLER POWER SPECTRUM OF MOBILE RADIO CHANNELS. A widely used model for the Doppler power spectrum of a mobile radio channel is the so-called Jakes' model (Jakes, 1974). In this model, the autocorrelation of the time-variant transfer function $C(f; t)$ is given as

$$\begin{aligned} R_C(\Delta t) &= E[C^*(f; t)C(f; t + \Delta t)] \\ &= J_0(2\pi f_m \Delta t) \end{aligned}$$

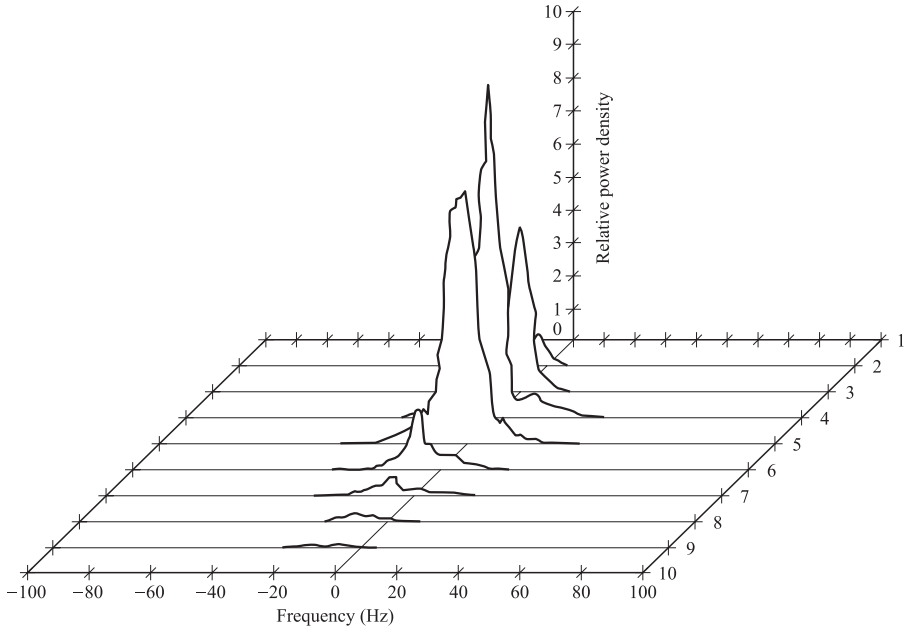

FIGURE 13.1–6
Scattering function of a medium-range tropospheric scatter channel. The taps delay increment is 0.1 μs.

where $J_0(\cdot)$ is the zero-order Bessel function of the first kind and $f_m = vf_0/c$ is the maximum Doppler frequency, where v is the vehicle speed in meters per second (m/s), f_0 is the carrier frequency, and c is the speed of light (3×10^8 m/s). The Fourier transform of this autocorrelation function yields the Doppler power spectrum. That is

$$\begin{aligned}\mathcal{S}_C(\lambda) &= \int_{-\infty}^{\infty} R_C(\Delta t) e^{-j2\pi\lambda\,\Delta t}\, d\Delta t \\ &= \int_{-\infty}^{\infty} J_0(2\pi f_m\,\Delta t) e^{-j2\pi\lambda\,\Delta t}\, d\Delta t \\ &= \begin{cases} \dfrac{1}{\pi f_m} \dfrac{1}{\sqrt{1-(f/f_m)^2}} & |f| \le f_m \\ 0 & |f| > f_m \end{cases}\end{aligned}$$

The graph of $\mathcal{S}_C(\lambda)$ is shown in Figure 13.1–8.

13.1–2 Statistical Models for Fading Channels

There are several probability distributions that can be considered in attempting to model the statistical characteristics of the fading channel. When there are a large number of scatterers in the channel that contribute to the signal at the receiver, as is the case in

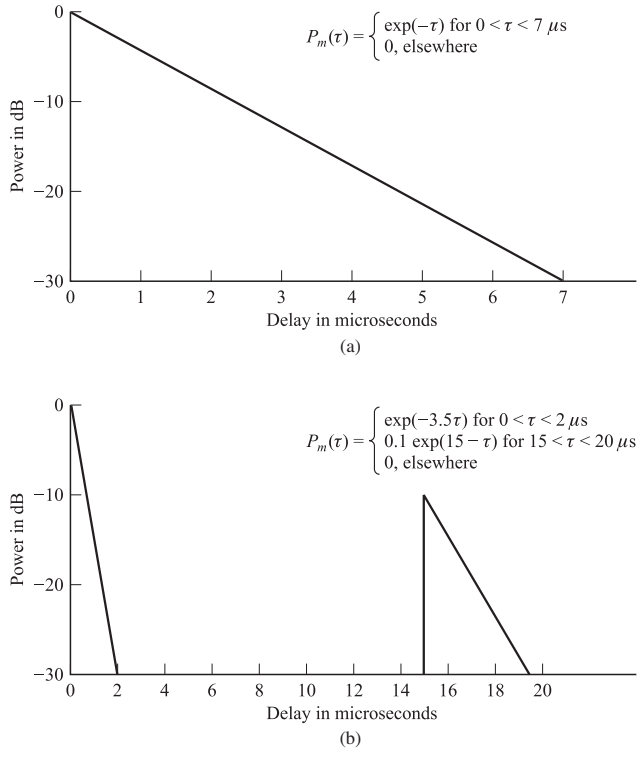

FIGURE 13.1–7
Cost 207 average power delay profiles: (a) typical delay profile for suburban and urban areas; (b) typical "bad"-case delay profile for hilly terrain. [*From Cost 207 Document 207 TD (86)51 rev 3*.]

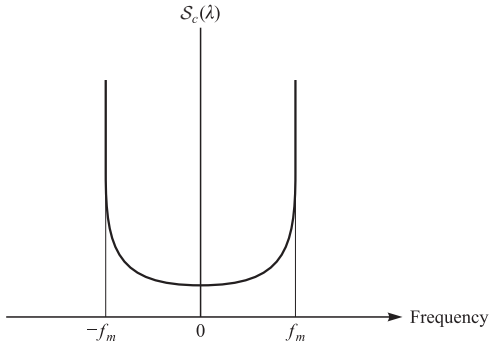

FIGURE 13.1–8
Model of Doppler spectrum for a mobile radio channel.

ionospheric or tropospheric signal propagation, application of the central limit theorem leads to a Gaussian process model for the channel impulse response. If the process is zero-mean, then the envelope of the channel response at any time instant has a Rayleigh probability distribution and the phase is uniformly distributed in the interval $(0, 2\pi)$.

That is

$$p_R(r) = \frac{2r}{\Omega} e^{-r^2/\Omega}, \qquad r \geq 0 \tag{13.1–23}$$

where

$$\Omega = E(R^2) \tag{13.1–24}$$

We observe that the Rayleigh distribution is characterized by the single parameter $E(R^2)$.

An alternative statistical model for the envelope of the channel response is the Nakagami-*m* distribution given by the PDF in Equation 2.3–67. In contrast to the Rayleigh distribution, which has a single parameter that can be used to match the fading channel statistics, the Nakagami-*m* is a two-parameter distribution, involving the parameter m and the second moment $\Omega = E(R^2)$. As a consequence, this distribution provides more flexibility and accuracy in matching the observed signal statistics. The Nakagami-*m* distribution can be used to model fading channel conditions that are either more or less severe than the Rayleigh distribution, and it includes the Rayleigh distribution as a special case ($m = 1$). For example, Turin et al. (1972) and Suzuki (1977) have shown that the Nakagami-*m* distribution provides the best fit for data signals received in urban radio multipath channels.

The Rice distribution is also a two-parameter distribution. It may be expressed by the PDF given in Equation 2.3–56, where the parameters are s and σ^2, where s^2 is called the *noncentrality parameter* in the equivalent chi-square distribution. It represents the power in the nonfading signal components, sometimes called *specular components*, of the received signal.

There are many radio channels in which fading is encountered that are basically line-of-sight (LOS) communication links with multipath components arising from secondary reflections, or signal paths, from surrounding terrain. In such channels, the number of multipath components is small, and, hence, the channel may be modeled in a somewhat simpler form. We cite two channel models as examples.

As the first example, let us consider an airplane to ground communication link in which there is the direct path and a single multipath component at a delay t_0 relative to the direct path. The impulse response of such a channel may be modeled as

$$c(\tau; t) = \alpha\delta(\tau) + \beta(t)\delta[\tau - \tau_0(t)] \tag{13.1–25}$$

where α is the attenuation factor of the direct path and $\beta(t)$ represents the time-variant multipath signal component resulting from terrain reflections. Often, $\beta(t)$ can be characterized as a zero-mean Gaussian random process. The transfer function for this channel model may be expressed as

$$C(f; t) = \alpha + \beta(t)e^{-j2\pi f \tau_0(t)} \tag{13.1–26}$$

This channel fits the Ricean fading model defined previously. The direct path with attenuation α represents the specular component and $\beta(t)$ represents the Rayleigh fading component.

A similar model has been found to hold for microwave LOS radio channels used for long-distance voice and video transmission by telephone companies throughout the

world. For such channels, Rummler (1979) has developed a three-path model based on channel measurements performed on typical LOS links in the 6-GHz frequency band. The differential delay on the two multipath components is relatively small, and, hence, the model developed by Rummler is one that has a channel transfer function

$$C(f) = \alpha[1 - \beta e^{-j2\pi(f-f_0)\tau_0}] \tag{13.1–27}$$

where α is the overall attenuation parameter, β is called a shape parameter which is due to the multipath components, f_0 is the frequency of the fade minimum, and τ_0 is the relative time delay between the direct and the multipath components. This simplified model was used to fit data derived from channel measurements.

Rummler found that the parameters α and β may be characterized as random variables that, for practical purposes, are nearly statistically independent. From the channel measurements, he found that the distribution of β has the form $(1 - \beta)^{2.3}$. The distribution of α is well modeled by the lognormal distribution, i.e., $-\log\alpha$ is Gaussian. For $\beta > 0.5$, the mean of $-20\log\alpha$ was found to be 25 dB and the standard deviation was 5 dB. For smaller values of β, the mean decreases to 15 dB. The delay parameter determined from the measurements was $\tau_0 = 6.3$ ns. The magnitude-square response of $C(f)$ is

$$|C(f)|^2 = \alpha^2[1 + \beta^2 - 2\beta\cos 2\pi(f - f_0)\tau_0] \tag{13.1–28}$$

$|C(f)|$ is plotted in Figure 13.1–9 as a function of the frequency $f - f_0$ for $\tau_0 = 6.3$ ns. Note that the effect of the multipath component is to create a deep attenuation at $f = f_0$ and at multiples of $1/\tau_0 \approx 159$ MHz. By comparison, the typical channel bandwidth is 30 MHz. This model was used by Lundgren and Rummler (1979) to determine the error rate performance of digital radio systems.

Propagation models for mobile radio channels In the link budget calculations that were described in Section 4.10–2, we had characterized the path loss of radio waves propagating through free space as being inversely proportional to d^2, where d is the distance between the transmitter and the receiver. However, in a mobile radio

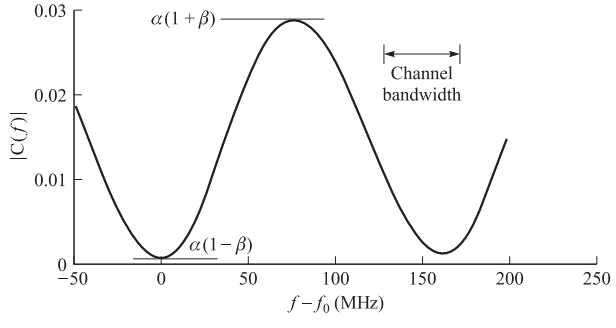

FIGURE 13.1–9
Magnitude frequency response of LOS channel model.

channel, propagation is generally neither free space nor line of sight. The mean path loss encountered in mobile radio channels may be characterized as being inversely proportional to d^p, where $2 \leq p \leq 4$, with d^4 being a worst-case model. Consequently, the path loss is usually much more severe compared to that of free space.

There are a number of factors affecting the path loss in mobile radio communications. Among these factors are base station antenna height, mobile antenna height, operating frequency, atmospheric conditions, and presence or absence of buildings and trees. Various mean path loss models have been developed that incorporate such factors. For example, a model for a large city in an urban area is the Hata model, in which the mean path loss is expressed as

$$\begin{aligned}\text{Loss in dB} = {} & 69.55 + 26.16 \log_{10} f - 13.82 \log_{10} h_t - a(h_r) \\ & + (44.9 - 6.55 \log_{10} h_t) \log_{10} d\end{aligned} \tag{13.1–29}$$

where f is the operating frequency in MHz ($150 < f < 1500$), h_t is the transmitter antenna height in meters ($30 < h_t < 200$), h_r is the receiver antenna height in meters ($1 < h_r < 10$), d is the distance between transmitter and receiver in km ($1 < d < 20$), and

$$a(h_r) = 3.2(\log_{10} 11.75 h_r)^2 - 4.97, \qquad f \geq 400\,\text{MHz} \tag{13.1–30}$$

Another problem with mobile radio propagation is the effect of shadowing of the signal due to large obstructions, such as large buildings, trees, and hilly terrain between the transmitter and the receiver. Shadowing is usually modeled as a multiplicative and, generally, slowly time varying random process. That is, the received signal may be characterized mathematically as

$$r(t) = A_0 g(t) s(t) \tag{13.1–31}$$

where A_0 represents the mean path loss, $s(t)$ is the transmitted signal, and $g(t)$ is a random process that represents the shadowing effect. At any time instant, the shadowing process is modeled statistically as lognormally distributed. The probability density function for the lognormal distribution is

$$p(g) = \begin{cases} \dfrac{1}{\sqrt{2\pi\sigma^2}\, g} e^{-(\ln g - \mu)^2/2\sigma^2} & (g \geq 0) \\ 0 & (g < 0) \end{cases} \tag{13.1–32}$$

If we define a new random variable X as $X = \ln g$, then

$$p(x) = \frac{1}{\sqrt{2\pi\sigma^2}} e^{-(x-\mu)^2/2\sigma^2}, \qquad -\infty < x < \infty \tag{13.1–33}$$

The random variable X represents the path loss measured in dB, μ is the mean path loss in dB, and σ is the standard deviation of the path loss in dB. For typical cellular and microcellular environments, σ is in the range of 5–12 dB.

13.2 THE EFFECT OF SIGNAL CHARACTERISTICS ON THE CHOICE OF A CHANNEL MODEL

Having discussed the statistical characterization of time-variant multipath channels generally in terms of the correlation functions describe in Section 13.1, we now consider the effect of signal characteristics on the selection of a channel model that is appropriate for the specified signal. Thus, let $s_l(t)$ be the equivalent lowpass signal transmitted over the channel and let $S_l(f)$ denote its frequency content. Then the equivalent lowpass received signal, exclusive of additive noise, may be expressed either in terms of the time-domain variables $c(\tau; t)$ and $s_l(t)$ as

$$r_l(t) = \int_{-\infty}^{\infty} c(\tau; t) s_l(t - \tau)\, d\tau \tag{13.2–1}$$

or in terms of the frequency functions $C(f; t)$ and $S_l(f)$ as

$$r_l(t) = \int_{-\infty}^{\infty} C(f; t) S_l(f) e^{j2\pi f t}\, df \tag{13.2–2}$$

Suppose we are transmitting digital information over the channel by modulating (either in amplitude, or in phase, or both) the basic pulse $s_l(t)$ at a rate $1/T$, where T is the signaling interval. It is apparent from Equation 13.2–2 that the time-variant channel characterized by the transfer function $C(f; t)$ distorts the signal $S_l(f)$. If $S_l(f)$ has a bandwidth W greater than the coherence bandwidth $(\Delta f)_c$ of the channel, $S_l(f)$ is subjected to different gains and phase shifts across the band. In such a case, the channel is said to be *frequency-selective*. Additional distortion is caused by the time variations in $C(f; t)$. This type of distortion is evidenced as a variation in the received signal strength, and has been termed *fading*. It should be emphasized that the frequency selectivity and fading are viewed as two different types of distortion. The former depends on the multipath spread or, equivalently, on the coherence bandwidth of the channel relative to the transmitted signal bandwidth W. The latter depends on the time variations of the channel, which are grossly characterized by the coherence time $(\Delta t)_c$ or, equivalently, by the Doppler spread B_d.

The effect of the channel on the transmitted signal $s_l(t)$ is a function of our choice of signal bandwidth and signal duration. For example, if we select the signaling interval T to satisfy the condition $T \gg T_m$, the channel introduces a negligible amount of intersymbol interference. If the bandwidth of the signal pulse $s_l(t)$ is $W \approx 1/T$, the condition $T \gg T_m$ implies that

$$W \ll \frac{1}{T_m} \approx (\Delta f)_c \tag{13.2–3}$$

That is, the signal bandwidth W is much smaller than the coherence bandwidth of the channel. Hence, the channel is *frequency-nonselective*. In other words, all the frequency components in $S_l(f)$ undergo the same attenuation and phase shift in transmission through the channel. But this implies that, within the bandwidth occupied by $S_l(f)$, the time-variant transfer function $C(f; t)$ of the channel is a complex-valued constant

in the frequency variable. Since $S_l(f)$ has its frequency content concentrated in the vicinity of $f = 0$, $C(f; t) = C(0; t)$. Consequently, Equation 13.2–2 reduces to

$$\begin{aligned} r_l(t) &= C(0; t) \int_{-\infty}^{\infty} S_l(f) e^{j2\pi f t}\, df \\ &= C(0; t) s_l(t) \end{aligned} \tag{13.2–4}$$

Thus, when the signal bandwidth W is much smaller than the coherence bandwidth $(\Delta f)_c$ of the channel, the received signal is simply the transmitted signal multiplied by a complex-valued random process $C(0; t)$, which represents the time-variant characteristics of the channel. In this case, we say that the multipath components in the received are not resolvable because $W \ll (\Delta f)_c$.

The transfer function $C(0; t)$ for a frequency-nonselective channel may be expressed in the form

$$C(0; t) = \alpha(t) e^{j\phi(t)} \tag{13.2–5}$$

where $\alpha(t)$ represents the envelope and $\phi(t)$ represents the phase of the equivalent lowpass channel. When $C(0; t)$ is modeled as a zero-mean complex-valued Gaussian random process, the envelope $\alpha(t)$ is Rayleigh-distributed for any fixed value of t and $\phi(t)$ is uniformly distributed over the interval $(-\pi, \pi)$. The rapidity of the fading on the frequency-nonselective channel is determined either from the correlation function $R_C(\Delta t)$ or from the Doppler power spectrum $\mathcal{S}_C(\lambda)$. Alternatively, either of the channel parameters $(\Delta t)_c$ or B_d can be used to characterize the rapidity of the fading.

For example, suppose it is possible to select the signal bandwidth W to satisfy the condition $W \ll (\Delta f)_c$ and the signaling interval T to satisfy the condition $T \ll (\Delta t)_c$. Since T is smaller than the coherence time of the channel, the channel attenuation and phase shift are essentially fixed for the duration of at least one signaling interval. When this condition holds, we call the channel a *slowly fading channel*. Furthermore, when $W \approx 1/T$, the conditions that the channel be frequency-nonselective and slowly fading imply that the product of T_m and B_d must satisfy the condition $T_m B_d < 1$.

The product $T_m B_d$ is called the *spread factor* of the channel. If $T_m B_d < 1$, the channel is said to be *underspread*; otherwise, it is *overspread*. The multipath spread, the Doppler spread, and the spread factor are listed in Table 13.2–1 for several channels.

TABLE 13.2–1
Multipath Spread, Doppler Spread, and Spread Factor for Several Time-Variant Multipath Channels

Type of channel	Multipath duration, s	Doppler spread, Hz	Spread factor
Shortwave ionospheric propagation (HF)	10^{-3}–10^{-2}	10^{-1}–1	10^{-4}–10^{-2}
Ionospheric propagation under distributed auroral conditions (HF)	10^{-3}–10^{-2}	10–100	10^{-2}–1
Ionospheric forward scatter (VHF)	10^{-4}	10	10^{-3}
Tropospheric scatter (SHF)	10^{-6}	10	10^{-5}
Orbital scatter (X band)	10^{-4}	10^{3}	10^{-1}
Moon at max. libration ($f_0 = 0.4$ kmc)	10^{-2}	10	10^{-1}

We observe from this table that several radio channels, including the moon when used as a passive reflector, are underspread. Consequently, it is possible to select the signal $s_l(t)$ such that these channels are frequency-nonselective and slowly fading. The slow-fading condition implies that the channel characteristics vary sufficiently slowly that they can be measured.

In Section 13.3, we shall determine the error rate performance for binary signaling over a frequency-nonselective slowly fading channel. This channel model is, by far, the simplest to analyze. More importantly, it yields insight into the performance characteristics for digital signaling on a fading channel and serves to suggest the type of signal waveforms that are effective in overcoming the fading caused by the channel.

Since the multipath components in the received signal are not resolvable when the signal bandwidth W is less than the coherence bandwidth $(\Delta f)_c$ of the channel, the received signal appears to arrive at the receiver via a single fading path. On the other hand, we may choose $W \gg (\Delta f)_c$, so that the channel becomes frequency-selective. We shall show later that, under this condition, the multipath components in the received signal are resolvable with a resolution in time delay of $1/W$. Thus, we shall illustrate that the frequency-selective channel can be modeled as a tapped delay line (transversal) filter with time-variant tap coefficients. We shall then derive the performance of binary signaling over such a frequency-selective channel model.

13.3
FREQUENCY-NONSELECTIVE, SLOWLY FADING CHANNEL

In this section, we derive the error rate performance of binary PSK and binary FSK when these signals are transmitted over a frequency-nonselective, slowly fading channel. As described in Section 13.2, the frequency-nonselective channel results in multiplicative distortion of the transmitted signal $s_l(t)$. Furthermore, the condition that the channel fades slowly implies that the multiplicative process may be regarded as a constant during at least one signaling interval. Consequently, if the transmitted signal is $s_l(t)$, the received equivalent lowpass signal in one signaling interval is

$$r_l(t) = \alpha e^{j\phi} s_l(t) + z(t), \qquad 0 \le t \le T \tag{13.3–1}$$

where $z(t)$ represents the complex-valued white Gaussian noise process corrupting the signal.

Let us assume that the channel fading is sufficiently slow that the phase shift ϕ can be estimated from the received signal without error. In that case, we can achieve ideal coherent detection of the received signal. Thus, the received signal can be processed by passing it through a matched filter in the case of binary PSK or through a pair of matched filters in the case of binary FSK. One method that we can use to determine the performance of the binary communication systems is to evaluate the decision variables and from these determine the probability of error. However, we have already done this for a fixed (time-invariant) channel. That is, for a fixed attenuation α, we know the probability of error for binary PSK and binary FSK. From Equation 4.3–13, the

expression for the error rate of binary PSK as a function of the received SNR γ_b is

$$P_b(\gamma_b) = Q\left(\sqrt{2\gamma_b}\right) \tag{13.3–2}$$

where $\gamma_b = \alpha^2 \mathcal{E}_b / N_0$. The expression for the error rate of binary FSK, detected coherently, is given by Equation 4.2–32 as

$$P_b(\gamma_b) = Q\left(\sqrt{\gamma_b}\right) \tag{13.3–3}$$

We view Equations 13.3–2 and 13.3–3 as conditional error probabilities, where the condition is that α is fixed. To obtain the error probabilities when α is random, we must average $P_b(\gamma_b)$, given in Equations 13.3–2 and 13.3–3, over the probability density function of γ_b. That is, we must evaluate the integral

$$P_b = \int_0^\infty P_b(\gamma_b) p(\gamma_b)\, d\gamma_b \tag{13.3–4}$$

where $p(\gamma_b)$ is the probability density function of γ_b when α is random.

Rayleigh fading When α is Rayleigh-distributed, α^2 has a chi-square probability distribution with two degrees of freedom. Consequently, γ_b also is chi-square-distributed. It is easily shown that

$$p(\gamma_b) = \frac{1}{\bar{\gamma}_b} e^{-\gamma_b/\bar{\gamma}_b}, \qquad \gamma_b \geq 0 \tag{13.3–5}$$

where $\overline{\gamma}_b$ is the average signal-to-noise ratio, defined as

$$\overline{\gamma}_b = \frac{\mathcal{E}_b}{N_0} E(\alpha^2) \tag{13.3–6}$$

The term $E(\alpha^2)$ is simply the average value of α^2.

Now we can substitute Equation 13.3–5 into Equation 13.3–4 and carry out the integration for $P_b(\gamma_b)$ as given by Equations 13.3–2 and 13.3–3. The result of this integration for binary PSK is (see Problems 4.44 and 4.50)

$$P_b = \frac{1}{2}\left(1 - \sqrt{\frac{\overline{\gamma}_b}{1 + \bar{\gamma}_b}}\right) \tag{13.3–7}$$

If we repeat the integration with $P_b(\gamma_b)$ given by Equation 13.3–3, we obtain the probability of error for binary FSK, detected coherently, in the form

$$P_b = \frac{1}{2}\left(1 - \sqrt{\frac{\overline{\gamma}_b}{2 + \bar{\gamma}_b}}\right) \tag{13.3–8}$$

In arriving at the error rate results in Equations 13.3–7 and 13.3–8, we have assumed that the estimate of the channel phase shift, obtained in the presence of slow fading, is noiseless. Such an ideal condition may not hold in practice. In such a case, the expressions in Equations 13.3–7 and 13.3–8 should be viewed as representing the best achievable performance in the presence of Rayleigh fading. In Appendix C we consider

the problem of estimating the phase in the presence of noise and we evaluate the error rate performance of binary and multiphase PSK.

On channels for which the fading is sufficiently rapid to preclude the estimation of a stable phase reference by averaging the received signal phase over many signaling intervals, DPSK, is an alternative signaling method. Since DPSK requires phase stability over only two consecutive signaling intervals, this modulation technique is quite robust in the presence of signal fading. In deriving the performance of binary DPSK for a fading channel, we begin again with the error probability for a nonfading channel, which is

$$P_b(\gamma_b) = \tfrac{1}{2}e^{-\gamma_b} \tag{13.3–9}$$

This expression is substituted into the integral in Equation 13.3–4 along with $p(\gamma_b)$ obtained from Equation 13.3–5. Evaluation of the resulting integral yields the probability of error for binary DPSK, in the form

$$P_b = \frac{1}{2(1+\overline{\gamma}_b)} \tag{13.3–10}$$

If we choose not to estimate the channel phase shift at all, but instead employ a noncoherent (envelope or square-law) detector with binary, orthogonal FSK signals, the error probability for a nonfading channel is

$$P_b(\gamma_b) = \tfrac{1}{2}e^{-\gamma_b/2} \tag{13.3–11}$$

When we average $P_b(\gamma_b)$ over the Rayleigh fading channel attenuation, the resulting error probability is

$$P_b = \frac{1}{2+\overline{\gamma}_b} \tag{13.3–12}$$

The error probabilities in Equations 13.3–7, 13.3–8, 13.3–10, and 13.3–12 are illustrated in Figure 13.3–1. In comparing the performance of the four binary signaling systems, we focus our attention on the probabilities of error for large SNR, i.e., $\overline{\gamma}_b \gg 1$. Under this condition, the error rates in Equations 13.3–7, 13.3–8, 13.3–10, and 13.3–12 simplify to

$$P_b \approx \begin{cases} 1/4\overline{\gamma}_b & \text{for coherent PSK} \\ 1/2\overline{\gamma}_b & \text{for coherent, orthogonal FSK} \\ 1/2\overline{\gamma}_b & \text{for DPSK} \\ 1/\overline{\gamma}_b & \text{for noncoherent, orthogonal FSK} \end{cases} \tag{13.3–13}$$

From Equation 13.3–13, we observe that coherent PSK is 3 dB better than DPSK and 6 dB better than noncoherent FSK. More striking, however, is the observtion that the error rates decrease only inversely with SNR. In contrast, the decrease in error rate on a nonfading channel is exponential with SNR. This means that, on a fading channel, the transmitter must transmit a large amount of power in order to obtain a low probability of error. In many cases, a large amount of power is not possible, technically and/or economically. An alternative solution to the problem of obtaining acceptable

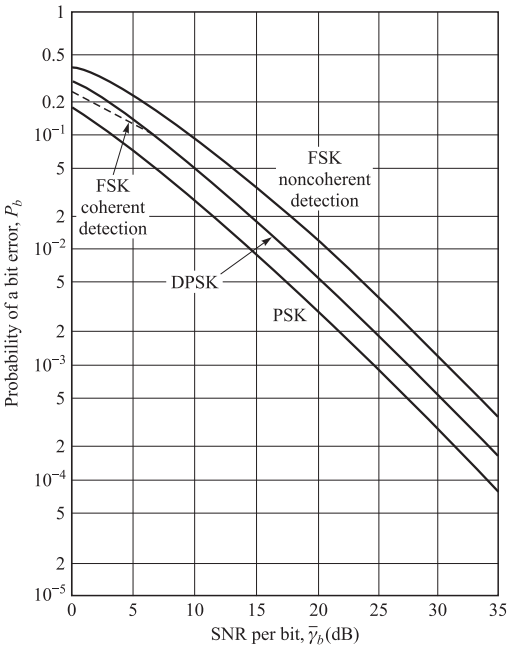

FIGURE 13.3–1
Performance of binary signaling on a Rayleigh fading channel.

performance on a fading channel is the use of redundancy, which can be obtained by means of diversity techniques, as discussed in Section 13.4.

Nakagami fading If α is characterized statistically by the Nakagami-m distribution, the random variable $\gamma = \alpha^2 \mathcal{E}_b / N_0$ has the PDF (see Problem 13.14)

$$p(\gamma) = \frac{m^m}{\Gamma(m)\overline{\gamma}^m} \gamma^{m-1} e^{-m\gamma/\overline{\gamma}} \tag{13.3–14}$$

where $\overline{\gamma} = E(\alpha^2)\mathcal{E}/N_0$.

The average probability of error for any of the modulation methods is simply obtained by averaging the appropriate error probability for a nonfading channel over the fading signal statistics.

As an example of the performance obtained with Nakagami-m fading statistics, Figure 13.3–2 illustrates the probability of error of binary PSK with m as a parameter. We recall that $m = 1$ corresponds to Rayleigh fading. We observe that the performance improves as m is increased above $m = 1$, which is indicative of the fact that the fading is less severe. On the other hand, when $m < 1$, the performance is worse than Rayleigh fading.

Other fading signal statistics Following the procedure describe above, one can determine the performance of the various modulation methods for other types of fading signal statistics, such as Ricean Fading.

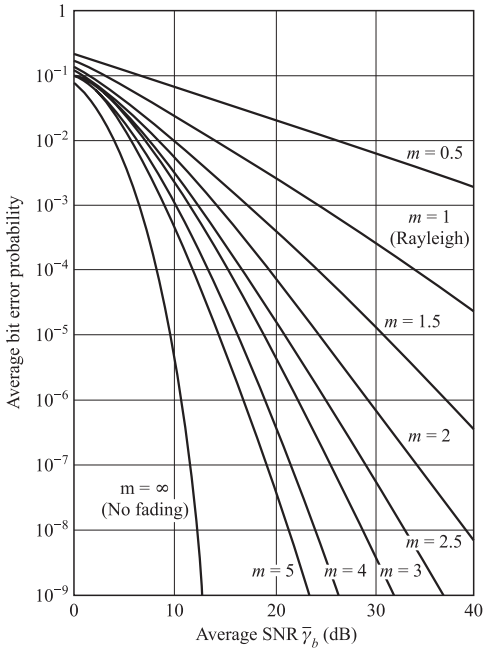

FIGURE 13.3–2
Average error probability for two-phase PSK with Nakagami fading.

Error probability results for Rice-distributed fading statistics can be found in the paper by Lindsey (1964), while for Nakagami-*m* fading statistics, the reader may refer to the papers by Esposito (1967), Miyagaki et al. (1978), Charash (1979), Al-Hussaini et al. (1985), and Beaulieu and Abu-Dayya (1991).

13.4
DIVERSITY TECHNIQUES FOR FADING MULTIPATH CHANNELS

Diversity techniques are based on the notion that errors occur in reception when the channel attenuation is large, i.e., when the channel is in a deep fade. If we can supply to the receiver several replicas of the same information signal transmitted over independently fading channels, the probability that all the signal components will fade simultaneously is reduced considerably. That is, if p is the probability that any one signal will fade below some critical value, then p^L is the probability that all L independently fading replicas of the same signal will fade below the critical value. There are several ways in which we can provide the receiver with L independently fading replicas of the same information-bearing signal.

One method is to employ *frequency diversity*. That is, the same information-bearing signal is transmitted on L carriers, where the separation between successive carriers equals or exceeds the coherence bandwidth $(\Delta f)_c$ of the channel.

A second method for achieving L independently fading versions of the same information-bearing signal is to transmit the signal in L different time slots, where

the separation between successive time slots equals or exceeds the coherence time $(\Delta t)_c$ of the channel. This method is called *time diversity*.

Note that the fading channel fits the model of a bursty error channel. Furthermore, we may view the transmission of the same information either at different frequencies or in difference time slots (or both) as a simple form of repetition coding. The separation of the diversity transmissions in time by $(\Delta t)_c$ or in frequency by $(\Delta f)_c$ is basically a form of block-interleaving the bits in the repetition code in an attempt to break up the error bursts and, thus, to obtain independent errors. Later in the chapter, we shall demonstrate that, in general, repetition coding is wasteful of bandwidth when compared with nontrivial coding.

Another commonly used method for achieving diversity employs multiple antennas. For example, we may employ a single transmitting antenna and multiple receiving antennas. The latter must be spaced sufficiently far apart that the multipath components in the signal have significantly different propagation delays at the antennas. Usually a separation of a few wavelengths is required between two antennas in order to obtain signals that fade independently.

A more sophisticated method for obtaining diversity is based on the use of a signal having a bandwidth much greater than the coherence bandwidth $(\Delta f)_c$ of the channel. Such a signal with bandwidth W will resolve the multipath components and, thus, provide the receiver with several independently fading signal paths. The time resolution is $1/W$. Consequently, with a multipath spread of T_m seconds, there are $T_m W$ resolvable signal components. Since $T_m \approx 1/(\Delta f)_c$, the number of resolvable signal components may also be expressed as $W/(\Delta f)_c$. Thus, the use of a wideband signal may be viewed as just another method for obtaining frequency diversity of order $L \approx W/(\Delta f)_c$. The optimum demodulator for processing the wideband signal will be derived in Section 13.5. It is called a *RAKE correlator* or a *RAKE matched filter* and was invented by Price and Green (1958).

There are other diversity techniques that have received some consideration in practice, such as angle-of-arrival diversity and polarization diversity. However, these have not been as widely used as those described above.

13.4–1 Binary Signals

We shall now determine the error rate performance for a binary digital communication system with diversity. We begin by describing the mathematical model for the communication system with diversity. First of all, we assume that there are L diversity channels, carrying the same information-bearing signal. Each channel is assumed to be frequency-nonselective and slowly fading with Rayleigh-distributed envelope statistics. The fading processes among the L diversity channels are assumed to be mutually statistically independent. The signal in each channel is corrupted by an additive zero-mean white Gaussian noise process. The noise processes in the L channels are assumed to be mutually statistically independent, with identical autocorrelation functions. Thus, the equivalent low-pass received signals for the L channels can be expressed in the form

$$r_{lk}(t) = \alpha_k e^{j\phi_k} s_{km}(t) + z_k(t), \qquad k = 1, 2, \ldots, L, \qquad m = 1, 2 \qquad (13.4\text{–}1)$$

where $\{\alpha_k e^{j\phi_k}\}$ represent the attenuation factors and phase shifts for the L channels, $s_{km}(t)$ denotes the mth signal transmitted on the kth channel, and $z_k(t)$ denotes the additive white Gaussian noise on the kth channel. All signals in the set $\{s_{km}(t)\}$ have the same energy.

The optimum demodulator for the signal received from the kth channel consists of two matched filters, one having the impulse response

$$b_{k1}(t) = s_{k1}^*(T - t) \tag{13.4–2}$$

and the other having the impulse response

$$b_{k2}(t) = s_{k2}^*(T - t) \tag{13.4–3}$$

Of course, if binary PSK is the modulation method used to transmit the information, then $s_{k1}(t) = -s_{k2}(t)$. Consequently, only a single matched filter is required for binary PSK. Following the matched filters is a combiner that forms the two decision variables. The combiner that achieves the best performance is one in which each matched filter output is multiplied by the corresponding complex-valued (conjugate) channel gain $\alpha_k e^{-j\phi_k}$. The effect of this multiplication is to compensate for the phase shift in the channel and to weight the signal by a factor that is proportional to the signal strength. Thus, a strong signal carries a larger weight than a weak signal. After the complex-valued weighting operation is performed, two sums are formed. One consists of the real parts of the weighted outputs from the matched filters corresponding to a transmitted 0. The second consists of the real part of the outputs from the matched filters corresponding to a transmitted 1. This optimum combiner is called a *maximal ratio combiner* by Brennan (1959). Of course, the realization of this optimum combiner is based on the assumption that the channel attenuations $\{\alpha_k\}$ and the phase shifts $\{\phi_k\}$ are known perfectly. That is, the estimates of the parameters $\{\alpha_k\}$ and $\{\phi_k\}$ contain no noise. (The effect of noisy estimates on the error rate performance of multiphase PSK is considered in Appendix C.)

A block diagram illustrating the model for the binary digital communication system described above is shown in Figure 13.4–1.

Let us first consider the performance of binary PSK with Lth-order diversity. The output of the maximal ratio combiner can be expressed as a single decision variable in the form

$$\begin{aligned} U &= \text{Re}\left(2\mathcal{E}\sum_{k=1}^{L}\alpha_k^2 + \sum_{k=1}^{L}\alpha_k N_k\right) \\ &= 2\mathcal{E}\sum_{k=1}^{L}\alpha_k^2 + \sum_{k=1}^{L}\alpha_k N_{kr} \end{aligned} \tag{13.4–4}$$

where N_{kr} denotes the real part of the complex-valued Gaussian noise variable

$$N_k = e^{-j\phi_k}\int_0^T z_k(t)s_k^*(t)\,dt \tag{13.4–5}$$

We follow the approach used in Section 13.3 in deriving the probability of error. That is, the probability of error conditioned on a fixed set of attenuation factors $\{\alpha_k\}$ is obtained

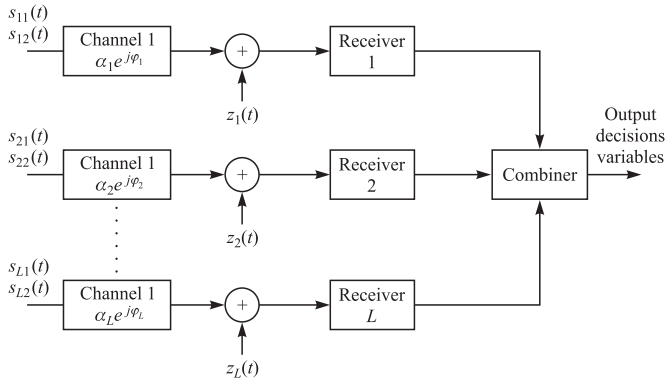

FIGURE 13.4–1
Model of binary digital communication system with diversity.

first. Then the conditional probability of error is averaged over the probability density function of the $\{\alpha_k\}$.

Rayleigh fading For a fixed set of $\{\alpha_k\}$ the decision variable U is Gaussian with mean

$$E(U) = 2\mathcal{E}\sum_{k=1}^{L}\alpha_k^2 \tag{13.4–6}$$

and variance

$$\sigma_U^2 = 2\mathcal{E}N_0\sum_{k=1}^{L}\alpha_k^2 \tag{13.4–7}$$

For these values of the mean and variance, the probability that U is less than zero is simply

$$P_b(\gamma_b) = Q\left(\sqrt{2\gamma_b}\right) \tag{13.4–8}$$

where the SNR per bit, γ_b, is given as

$$\begin{aligned}\gamma_b &= \frac{\mathcal{E}}{N_0}\sum_{k=1}^{L}\alpha_k^2 \\ &= \sum_{k=1}^{L}\gamma_k\end{aligned} \tag{13.4–9}$$

where $\gamma_k = \mathcal{E}\alpha_k^2/N_0$ is the instantaneous SNR on the kth channel. Now we must determine the probability density function $p(\gamma_b)$. This function is most easily determined via the characteristic function of γ_b. First of all, we note that for $L = 1$, $\gamma_b \equiv \gamma_1$ has a chi-square probability density function given in Equation 13.3–5. The characteristic

function of γ_1 is easily shown to be

$$\begin{aligned}\Phi_{\gamma_1}(v) &= E(e^{jv\gamma_1}) \\ &= \frac{1}{1 - jv\overline{\gamma}_c}\end{aligned} \tag{13.4–10}$$

where $\overline{\gamma}_c$ is the average SNR per channel, which is assumed to be identical for all channels. That is,

$$\overline{\gamma}_c = \frac{\mathcal{E}}{N_0} E(\alpha_k^2) \tag{13.4–11}$$

independent of k. This assumption applies for the results throughout this section. Since the fading on the L channels is mutually statistically independent, the $\{\gamma_k\}$ are statistically independent, and, hence, the characteristic function for the sum γ_b is simply the result in Equation 13.4–10 raised to the Lth power, i.e.,

$$\Phi_{\gamma_b}(v) = \frac{1}{(1 - jv\overline{\gamma}_c)^L} \tag{13.4–12}$$

But this is the characteristic function of a chi-square-distributed random variable with $2L$ degrees of freedom. It follows from Equation 2.3–21 that the probability density function $p(\gamma_b)$ is

$$p(\gamma_b) = \frac{1}{(L-1)!\overline{\gamma}_c^L} \gamma_b^{L-1} e^{-\gamma_b/\overline{\gamma}_c} \tag{13.4–13}$$

The final step in this derivation is to average the conditional error probability given in Equation 13.4–8 over the fading channel statistics. Thus, we evaluate the integral

$$P_b = \int_0^\infty P_2(\gamma_b) p(\gamma_b)\, d\gamma_b \tag{13.4–14}$$

There is a closed-form solution for Equation 13.4–14, which can be expressed as

$$P_b = \left[\tfrac{1}{2}(1-\mu)\right]^L \sum_{k=0}^{L-1} \binom{L-1+k}{k} \left[\tfrac{1}{2}(1+\mu)\right]^k \tag{13.4–15}$$

where, by definition

$$\mu = \sqrt{\frac{\overline{\gamma}_c}{1+\overline{\gamma}_c}} \tag{13.4–16}$$

When the average SNR per channel, $\overline{\gamma}_c$, satisfies the condition $\overline{\gamma}_c \gg 1$, the term $\frac{1}{2}(1+\mu) \approx 1$ and the term $\frac{1}{2}(1-\mu) \approx 1/4\overline{\gamma}_c$. Furthermore,

$$\sum_{k=0}^{L-1} \binom{L-1+k}{k} = \binom{2L-1}{L} \tag{13.4–17}$$

Therefore, when $\overline{\gamma}_c$ is sufficiently large (greater than 10 dB), the probability of error in Equation 13.4–15 can be approximated as

$$P_b \approx \left(\frac{1}{4\overline{\gamma}_c}\right)^L \binom{2L-1}{L} \tag{13.4–18}$$

We observe from Equation 13.4–18 that the probability of error varies as $1/\overline{\gamma}_c$ raised to the Lth power. Thus, with diversity, the error rate decreases inversely with the Lth power of the SNR.

Having obtained the performance of binary PSK with diversity, we now turn our attention to binary, orthogonal FSK that is detected coherently. In this case, the two decision variables at the output of the maximal ratio combiner may be expressed as

$$\begin{aligned} U_1 &= \text{Re}\left(2\mathcal{E}\sum_{k=1}^{L}\alpha_k^2 + \sum_{k=1}^{L}\alpha_k N_{k1}\right) \\ U_2 &= \text{Re}\left(\sum_{k=1}^{L}\alpha_k N_{k2}\right) \end{aligned} \tag{13.4–19}$$

where we have assumed that signal $s_{k1}(t)$ was transmitted and where $\{N_{k1}\}$ and $\{N_{k2}\}$ are the two sets of noise components at the output of the matched filters. The probability of error is simply the probability that $U_2 > U_1$. This computation is similar to the one performed for PSK, except that we now have twice the noise power. Consequently, when the $\{\alpha_k\}$ are fixed, the conditional probability of error is

$$P_b(\gamma_b) = Q\left(\sqrt{\gamma_b}\right) \tag{13.4–20}$$

We use Equation 13.4–13 to average $P_b(\gamma_b)$ over the fading. It is not surprising to find that the result given in Equation 13.4–15 still applies, with $\overline{\gamma}_c$ replaced by $\frac{1}{2}\overline{\gamma}_c$. That is, Equation 13.4–15 is the probability of error for binary, orthogonal FSK with coherent detection, where the parameter μ is defined as

$$\mu = \sqrt{\frac{\overline{\gamma}_c}{2+\overline{\gamma}_c}} \tag{13.4–21}$$

Furthermore, for large values of $\overline{\gamma}_c$, the performance P_b can be approximated as

$$P_b \approx \left(\frac{1}{2\overline{\gamma}_c}\right)^L \binom{2L-1}{L} \tag{13.4–22}$$

In comparing Equation 13.4–22 with Equation 13.4–18, we observe that the 3-dB difference in performance between PSK and orthogonal FSK with coherent detection, which exists in a nonfading, nondispersive channel, is the same also in a fading channel.

In the above discussion of binary PSK and FSK, detected coherently, we assumed that noiseless estimates of the complex-valued channel parameters $\{\alpha_k e^{j\phi_k}\}$ were used at the receiver. Since the channel is time-variant, the parameters $\{\alpha_k e^{j\phi_k}\}$ cannot be estimated perfectly. In fact, on some channels, the time variations may be sufficiently fast to preclude the implementation of coherent detection. In such a case, we should consider using either DPSK or FSK with noncoherent detection.

Let us consider DPSK first. In order for DPSK to be a viable digital signaling method, the channel variations must be sufficiently slow so that the channel phase shifts $\{\phi_k\}$ do not change appreciably over two consecutive signaling intervals. In our analysis, we assume that the channel parameters $\{\alpha_k e^{j\phi_k}\}$ remain constant over two successive signaling intervals. Thus the combiner for binary DPSK will yield as an output the decision variable

$$U = \text{Re}\left[\sum_{k=1}^{L} \left(2\mathcal{E}\alpha_k e^{j\phi_k} + N_{k2}\right)\left(2\mathcal{E}\alpha_k e^{-j\phi_k} + N_{k1}^*\right)\right] \tag{13.4–23}$$

where $\{N_{k1}\}$ and $\{N_{k2}\}$ denote the received noise components at the output of the matched filters in the two consecutive signaling intervals. The probability of error is simply the probability that $U < 0$. Since U is a special case of the general quadratic form in complex-valued Gaussian random variables treated in Appendix B, the probability of error can be obtained directly from the results given in that appendix. Alternatively, we may use the error probability given in Equation 11.1–13, which applies to binary DPSK transmitted over L time-invariant channels, and average it over the Rayleigh fading channel statistics. Thus, we have the conditional error probability

$$P_b(\gamma_b) = (\tfrac{1}{2})^{2L-1} e^{-\gamma_b} \sum_{k=0}^{L-1} b_k \gamma_b^k \tag{13.4–24}$$

where γ_b is given by Equation 13.4–9 and

$$b_k = \frac{1}{k!} \sum_{n=0}^{L-1-k} \binom{2L-1}{n} \tag{13.4–25}$$

The average of $P_b(\gamma_b)$ over the fading channel statistics given by $p(\gamma_b)$ in Equation 13.4–13 is easily shown to be

$$P_b = \frac{1}{2^{2L-1}(L-1)!(1+\overline{\gamma}_c)^L} \sum_{k=0}^{L-1} b_k (L-1+k)! \left(\frac{\overline{\gamma}_c}{1+\overline{\gamma}_c}\right)^k \tag{13.4–26}$$

We indicate that the result in Equation 13.4–26 can be manipulated into the form given in Equation 13.4–15, which applies also to coherent PSK and FSK. For binary DPSK, the parameter μ in Equation 13.4–15 is defined as (see Appendix C)

$$\mu = \frac{\overline{\gamma}_c}{1+\overline{\gamma}_c} \tag{13.4–27}$$

For $\overline{\gamma}_c \gg 1$, the error probability in Equation 13.4–26 can be approximated by the expression

$$P_b \approx \left(\frac{1}{2\overline{\gamma}_c}\right)^L \binom{2L-1}{L} \tag{13.4–28}$$

Orthogonal FSK with noncoherent detection is the final signaling technique that we consider in this section. It is appropriate for both slow and fast fading. However, the analysis of the performance presented below is based on the assumption that the fading is sufficiently slow so that the channel parameters $\{\alpha_k e^{j\phi_k}\}$ remain constant for

the duration of the signaling interval. The combiner for the multichannel signals is a square-law combiner. Its output consists of the two decision variables

$$\begin{aligned} U_1 &= \sum_{k=1}^{L} |2\mathcal{E}\alpha_k e^{j\phi_k} + N_{k1}|^2 \\ U_2 &= \sum_{k=1}^{L} |N_{k2}|^2 \end{aligned} \tag{13.4–29}$$

where U_1 is assumed to contain the signal. Consequently the probability of error is the probability that $U_2 > U_1$.

As in DPSK, we have a choice of two approaches in deriving the performance of FSK with square-law combining. In Section 11.1, we indicated that the expression for the error probability for square-law-combined FSK is the same as that for DPSK with γ_b replaced by $\frac{1}{2}\gamma_b$. That is, the FSK system requires 3 dB of additional SNR to achieve the same performance on a time-invariant channel. Consequently, the conditional error probability for DPSK given in Equation 13.4–24 applies to square-law-combined FSK when γ_b is replaced by $\frac{1}{2}\gamma_b$. Furthermore, the result obtained by averaging Equation 13.4–24 over the fading, which is given by Equation 13.4–26, must also apply to FSK with $\overline{\gamma}_c$ replaced by $\frac{1}{2}\overline{\gamma}_c$. But we also stated previously that Equations 13.4–26 and 13.4–15 are equivalent. Therefore, the error probability given in Equation 13.4–15 also applies to square-law-combined FSK with the parameter μ defined as

$$\mu = \frac{\overline{\gamma}_c}{2 + \overline{\gamma}_c} \tag{13.4–30}$$

An alternative derivation used by Pierce (1958) to obtain the probability that the decision variable $U_2 > U_1$ is just as easy as the method described above. It begins with the probability density functions $p(u_1)$ and $p(u_2)$. Since the complex-valued random variables $\{\alpha_k e^{j\phi_k}\}$, $\{N_{k1}\}$, and $\{N_{k2}\}$ are zero-mean Gaussian-distributed, the decision variables U_1 and U_2 are distributed according to a chi-square probability distribution with $2L$ degrees of freedom. That is,

$$p(u_1) = \frac{1}{(2\sigma_1^2)^L (L-1)!} u_1^{L-1} \exp\left(-\frac{u_1}{2\sigma_1^2}\right) \tag{13.4–31}$$

where

$$\begin{aligned} \sigma_1^2 &= \tfrac{1}{2} E\left(|2\mathcal{E}\alpha_k e^{-j\phi_k} + N_{k1}|^2\right) \\ &= 2\mathcal{E}N_0(1 + \overline{\gamma}_c) \end{aligned}$$

Similarly,

$$p(u_2) = \frac{1}{\left(2\sigma_2^2\right)(L-1)!} u_2^{L-1} \exp\left(-\frac{u_2}{2\sigma_2^2}\right) \tag{13.4–32}$$

where

$$\sigma_2^2 = 2\mathcal{E}N_0$$

The probability of error is just the probability that $U_2 > U_1$. It is left as an exercise for the reader to show that this probability is given by Equation 13.4–15, where μ is defined by Equation 13.4–30.

When $\overline{\gamma}_c \gg 1$, the performance of square-law-detected FSK can be simplified as we have done for the other binary multichannel systems. In this case, the error rate is well approximated by the expression

$$P_b \approx \left(\frac{1}{\overline{\gamma}_c}\right)^L \binom{2L-1}{L} \tag{13.4–33}$$

The error rate performance of PSK, DPSK, and square-law-detected orthogonal FSK is illustrated in Figure 13.4–2 for $L = 1$, 2, and 4. The performance is plotted as a function of the average SNR per bit, $\overline{\gamma}_b$, which is related to the average SNR per channel, $\overline{\gamma}_c$, by the formula

$$\overline{\gamma}_b = L\overline{\gamma}_c \tag{13.4–34}$$

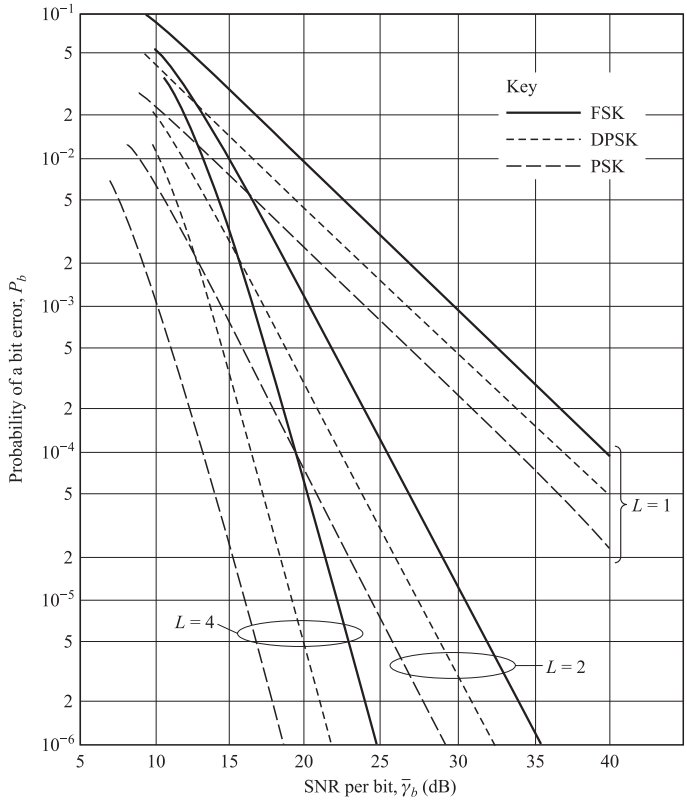

FIGURE 13.4–2
Performance of binary signals with diversity.

The results in Figure 13.4–2 clearly illustrate the advantage of diversity as a means for overcoming the severe penalty in SNR caused by fading.

Nakagami fading It is a simple matter to extend the results of this section to other fading models. We shall briefly consider Nakagami fading. Let us compare the Nakagami PDF for the single-channel SNR parameter $\gamma_b = \alpha^2 \mathcal{E}_b / N_0$, previously given by Equation 13.3–14 as

$$p(\gamma_b) = \frac{1}{\Gamma(m)(\overline{\gamma}_b/m)^m} \gamma_b^{m-1} e^{-\gamma_b/(\overline{\gamma}_b/m)} \tag{13.4–35}$$

with the PDF $p(\gamma_b)$ obtained for the L-channel SNR with Rayleigh fading, given by Equation 13.4–13 as

$$p(\gamma_b) = \frac{1}{(L-1)!\overline{\gamma}_c^L} \gamma_b^{L-1} e^{-\gamma_b/\overline{\gamma}_c} \tag{13.4–36}$$

By noting that $\overline{\gamma}_c = \overline{\gamma}_b/L$ in the case of an Lth order diversity system, it is clear that the two PDFs are identical for $L = m =$ integer. When $L = m = 1$, the two PDFs correspond to a single channel Rayleigh fading system. For the case in which the Nakagami parameter $m = 2$, the performance of the single-channel system is identical to the performance obtained in a Rayleigh fading channel with dual ($L = 2$) diversity. More generally, any single-channel system with Nakagami fading in which the parameter m is an integer, is equivalent to an L-channel diversity system for a Rayleigh fading channel. In view of this equivalence, the characteristic function of a Nakagami-m random variable must be of the form

$$\Phi_{\gamma_b}(v) = \frac{1}{(1 - jv\overline{\gamma}_b/m)^m} \tag{13.4–37}$$

which is consistent with the result given in Equation 13.4–12 for the characteristic function of the combined signal in a system with Lth-order diversity in a Rayleigh fading channel. Consequently, it follows that a K-channel system transmitting in a Nakagami fading channel with independent fading is equivalent to an $L = Km$ channel diversity in a Rayleigh fading channel.

13.4–2 Multiphase Signals

Multiphase signaling over a Rayleigh fading channel is the topic presented in some detail in Appendix C. Our main purpose in this section is to cite the general result for the probability of a symbol error in M-ary PSK and DPSK systems and the probability of a bit error in four-phase PSK and DPSK.

The general result for the probability of a symbol error in M-ary PSK and DPSK is

$$P_e = \frac{(-1)^{L-1}(1-\mu^2)^L}{\pi(L-1)!}\left(\frac{\partial^{L-1}}{\partial b^{L-1}}\left\{\frac{1}{b-\mu^2}\left[\frac{\pi}{M}(M-1) - \frac{\mu\sin(\pi/M)}{\sqrt{b-\mu^2\cos^2(\pi/M)}}\cot^{-1}\frac{-\mu\cos(\pi/M)}{\sqrt{b-\mu^2\cos^2(\pi/M)}}\right]\right\}\right)_{b=1} \tag{13.4–38}$$

where

$$\mu = \sqrt{\frac{\overline{\gamma}_c}{1+\overline{\gamma}_c}} \tag{13.4–39}$$

for coherent PSK and

$$\mu = \frac{\overline{\gamma}_c}{1+\overline{\gamma}_c} \tag{13.4–40}$$

for DPSK. Again $\overline{\gamma}_c$ is the average received SNR per channel. The SNR per bit is $\overline{\gamma}_b = L\overline{\gamma}_c/k$, where $k = \log_2 M$.

The bit error rate for four-phase PSK and DPSK is derived on the basis that the pair of information bits is mapped into the four phases according to a Gray code. The expression for the bit error rate derived in Appendix C is

$$P_b = \frac{1}{2}\left[1 - \frac{\mu}{\sqrt{2-\mu^2}}\sum_{k=0}^{L-1}\binom{2k}{k}\left(\frac{1-\mu^2}{4-2\mu^2}\right)^k\right] \tag{13.4–41}$$

where μ is again given by Equations 13.4–39 and 13.4–40 for PSK and DPSK, respectively.

Figure 13.4–3 illustrates the probability of a symbol error of DPSK and coherent PSK for $M = 2$, 4, and 8 with $L = 1$. Note that the difference in performance between DPSK and coherent PSK is approximately 3 dB for all three values of M. In fact, when $\overline{\gamma}_b \gg 1$ and $L = 1$, Equation 13.4–38 is well approximated as

$$P_e \approx \frac{M-1}{(M\log_2 M)[\sin^2(\pi/M)]\overline{\gamma}_b} \tag{13.4–42}$$

for DPSK and as

$$P_e \approx \frac{M-1}{(M\log_2 M)[\sin^2(\pi/M)]2\overline{\gamma}_b} \tag{13.4–43}$$

for PSK. Hence, at high SNR, coherent PSK is 3 dB better than DPSK on a Rayleigh fading channel. This difference also holds as L is increased.

Bit error probabilities are depicted in Figure 13.4–4 for two-phase, four-phase, and eight-phase DPSK signaling with $L = 1$, 2, and 4. The expression for the bit error probability of eight-phase DPSK with Gray encoding is not given here, but it is available in the paper by Proakis (1968). In this case, we observe that the performances for two- and four-phase DPSK are (approximately) the same, while that for eight-phase DPSK is about 3 dB poorer. Although we have not shown the bit error probability for

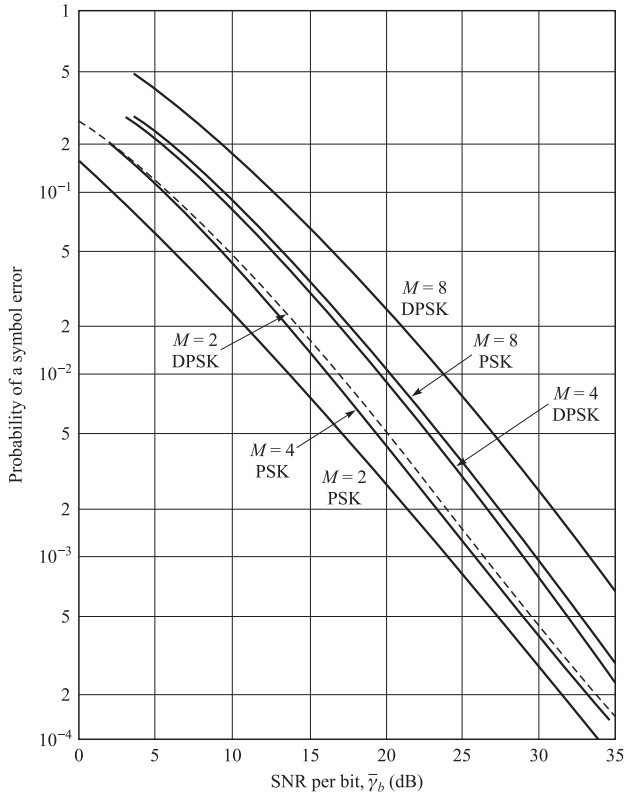

FIGURE 13.4–3
Probability of symbol error for PSK and DPSK for Rayleigh fading.

coherent PSK, it can be demonstrated that two- and four-phase coherent PSK also yield approximately the same performance.

13.4–3 M-ary Orthogonal Signals

In this subsection, we determine the performance of M-ary orthogonal signals transmitted over a Rayleigh fading channel and we assess the advantages of higher-order signal alphabets relative to a binary alphabet. The orthogonal signals may be viewed as M-ary FSK with a minimum frequency separation of an integer multiple of $1/T$, where T is the signaling interval. The same information-bearing signal is transmitted on L diversity channels. Each diversity channel is assumed to be frequency-nonselective and slowly fading, and the fading processes on the L channels are assumed to be mutually statistically independent. An additive white Gaussian noise process corrupts the signal on each diversity channel. We assume that the additive noise processes are mutually statistically independent.

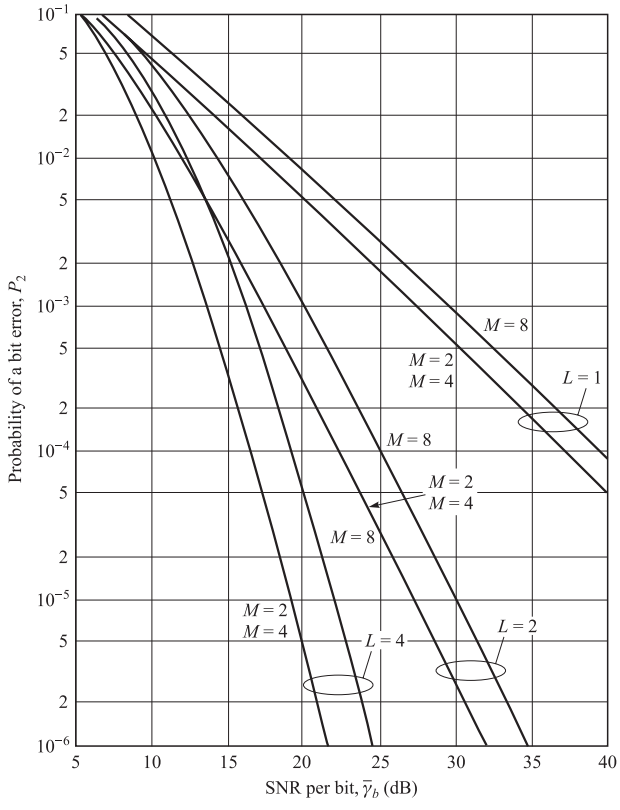

FIGURE 13.4–4
Probability of a bit error for DPSK with diversity for Rayleigh fading.

Although it is relatively easy to formulate the structure and analyze the performance of a maximal ratio combiner for the diversity channels in the M-ary communication system, it is more likely that a practical system would employ noncoherent detection. Consequently, we confine our attention to square-law combining of the diversity signals. The output of the combiner containing the signal is

$$U_1 = \sum_{k=1}^{L} |2\mathcal{E}\alpha_k e^{j\phi_k} + N_{k1}|^2 \tag{13.4–44}$$

while the outputs of the remaining $M - 1$ combiners are

$$U_m = \sum_{k=1}^{L} |N_{km}|^2, \qquad m = 2, 3, 4, \ldots, M \tag{13.4–45}$$

The probability of error is simply 1 minus the probability that $U_1 > U_m$ for $m = 2, 3, \ldots, M$. Since the signals are orthogonal and the additive noise processes are mutually statistically independent, the random variables $U_1, U_2, \ldots, U_M$ are also mutually

statistically independent. The probability density function of U_1 was given in Equation 13.4–31. On the other hand, $U_2, \ldots, U_M$ are identically distributed and described by the marginal probability density function in Equation 13.4–32. With U_1 fixed, the joint probability $P(U_2 < U_1, U_3 < U_1, \ldots, U_m < U_1)$ is equal to $P(U_2 < U_1)$ raised to the $M - 1$ power. Now,

$$\begin{aligned} P(U_2 < U_1 \mid U_1 = u_1) &= \int_0^{u_1} p(u_2)\, du_2 \\ &= 1 - \exp\left(-\frac{u_1}{2\sigma_2^2}\right) \sum_{k=0}^{L-1} \frac{1}{k!} \left(\frac{u_1}{2\sigma_2^2}\right)^k \end{aligned} \tag{13.4–46}$$

where $\sigma_2^2 = 2\mathcal{E}N_0$. The $M - 1$ power of this probability is then averaged over the probability density function of U_1 to yield the probability of a correct decision. If we subtract this result from unity, we obtain the probability of error in the form given by Hahn (1962)

$$\begin{aligned} P_e &= 1 - \int_0^{\infty} \frac{1}{\left(2\sigma_1^2\right)^L (L-1)!} u_1^{L-1} \exp\left(-\frac{u_1}{2\sigma_1^2}\right) \\ &\quad \times \left[1 - \exp\left(-\frac{u_1}{2\sigma_2^2}\right) \sum_{k=0}^{L-1} \frac{1}{k!} \left(\frac{u_1}{2\sigma_2^2}\right)^k\right]^{M-1} du_1 \\ &= 1 - \int_0^{\infty} \frac{1}{(1+\overline{\gamma}_c)^L (L-1)!} u_1^{L-1} \exp\left(-\frac{u_1}{1+\overline{\gamma}_c}\right) \\ &\quad \times \left(1 - e^{-u_1} \sum_{k=0}^{L-1} \frac{u_1^k}{k!}\right)^{M-1} du_1 \end{aligned} \tag{13.4–47}$$

where $\overline{\gamma}_c$ is the average SNR per diversity channel. The average SNR per bit is $\overline{\gamma}_b = L\overline{\gamma}_c / \log_2 M = L\overline{\gamma}_c / k$.

The integral in Equation 13.4–47 can be expressed in closed form as a double summation. This can be seen if we write

$$\left(\sum_{k=0}^{L-1} \frac{u_1^k}{k!}\right)^m = \sum_{k=0}^{m(L-1)} \beta_{km} u_1^k \tag{13.4–48}$$

where β_{km} is the set of coefficients in the above expansion. Then it follows that Equation 13.4–47 reduces to

$$\begin{aligned} P_e &= \frac{1}{(L-1)!} \sum_{m=1}^{M-1} \frac{(-1)^{m+1} \binom{M-1}{m}}{(1+m+m\overline{\gamma}_c)^L} \\ &\quad \times \sum_{k=0}^{m(L-1)} \beta_{km} (L-1+k)! \left(\frac{1+\overline{\gamma}_c}{1+m+m\overline{\gamma}_c}\right)^k \end{aligned} \tag{13.4–49}$$

When there is no diversity ($L = 1$), the error probability in Equation 13.4–49 reduces to the simple form

$$P_e = \sum_{m=1}^{M-1} \frac{(-1)^{m+1} \binom{M-1}{m}}{1 + m + m\overline{\gamma}_c} \tag{13.4–50}$$

The symbol error rate P_e may be converted to an equivalent bit error rate by multiplying P_e with $2^{k-1}/(2^k - 1)$.

Although the expression for P_e given in Equation 13.4–49 is in closed form, it is computationally cumbersome to evaluate for large values of M and L. An alternative is to evaluate P_M by numerical integration using the expression in Equation 13.4–47. The results illustrated in the following graphs were generated from Equation 13.4–47.

First of all, let us observe the error rate performance of M-ary orthogonal signaling with square-law combining as a function of the order of diversity. Figures 13.4–5 and 13.4–6 illustrate the characteristics of P_e for $M = 2$ and 4 as a function of L when the total SNR, defined as $\overline{\gamma}_t = L\overline{\gamma}_c$, remains fixed. These results indicate that there is an optimum order of diversity for each $\overline{\gamma}_t$. That is, for any $\overline{\gamma}_t$, there is a value of L for which P_e is a minimum. A careful observation of these graphs reveals that the minimum

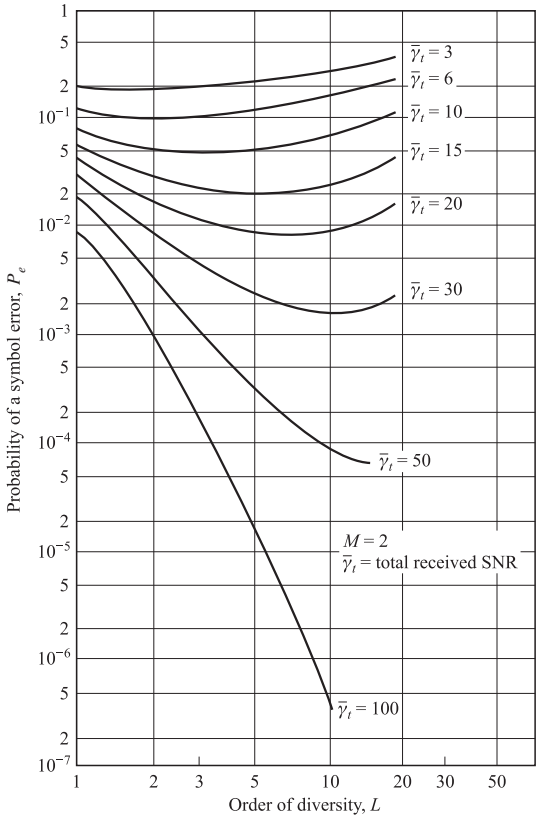

FIGURE 13.4–5
Performance of square-law-detected binary orthogonal signals as a function of diversity.

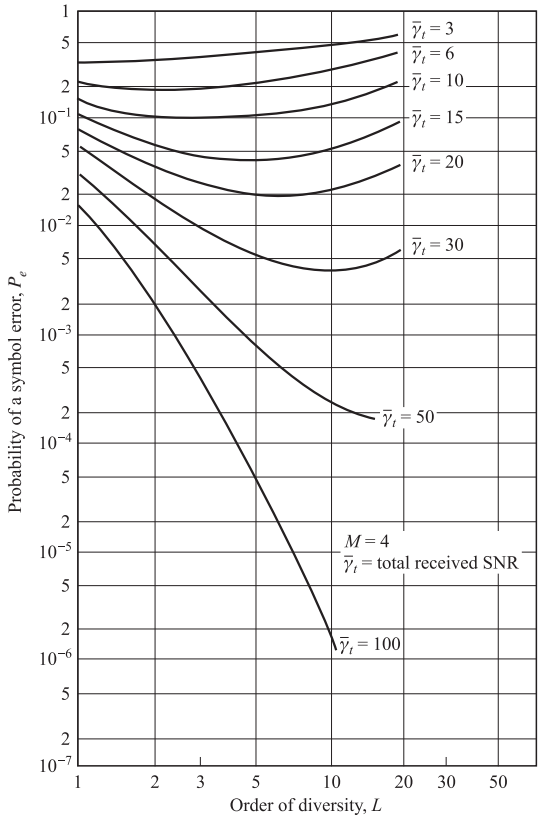

FIGURE 13.4–6
Performance of square-law-detected $M = 4$ orthogonal signals as a function of diversity.

in P_e is obtained when $\overline{\gamma}_c = \overline{\gamma}_t/L \approx 3$. This result appears to be independent of the alphabet size M.

Second, let us observe the error rate P_e as a function of the average SNR per bit, defined as $\overline{\gamma}_b = L\overline{\gamma}_c/k$. (If we interpret M-ary orthogonal FSK as a form of coding and the order of diversity as the number of times a symbol is repeated in a repetition code, then $\overline{\gamma}_b = \overline{\gamma}_c/R_c$, where $R_c = k/L$ is the code rate.) The graphs of P_e versus $\overline{\gamma}_b$ for $M = 2, 4, 8, 16, 32$ and $L = 1, 2, 4$ are shown in Figure 13.4–7. These results illustrate the gain in performance as M increases and L increases. First, we note that a significant gain in performance is obtained by increasing L. Second, we note that the gain in performance obtained with an increase in M is relatively small when L is small. However, as L increases, the gain achieved by increasing M also increases. Since an increase in either parameter results in an expansion of bandwidth, i.e.,

$$B_e = \frac{LM}{\log_2 M} \tag{13.4–51}$$

the results illustrated in Figure 13.4–7 indicate that an increase in L is more efficient than a corresponding increase in M. As we shall see in Chapter 14, coding is a bandwidth-effective means for obtaining diversity in the signal transmitted over the fading channel.

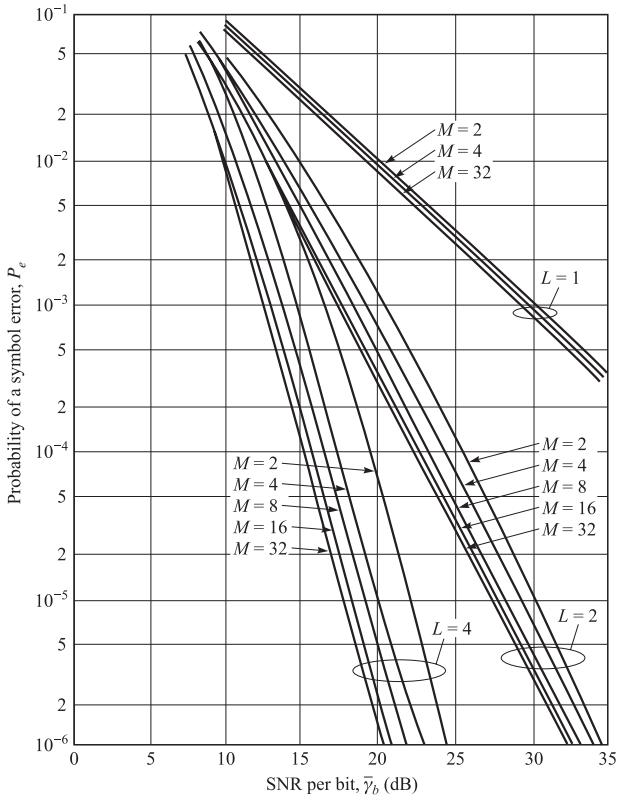

FIGURE 13.4–7
Performance of orthogonal signaling with M and L as parameters.

Chernov bound Before concluding this section, we develop a Chernov upper bound on the error probability of binary orthogonal signaling with Lth-order diversity, which will be useful in our discussion of coding for fading channels, the topic of Chapter 14. Our starting point is the expression for the two decision variables U_1 and U_2 given by Equation 13.4–29, where U_1 consists of the square-law-combined signal-plus-noise terms and U_2 consists of square-law-combined noise terms. The binary probability of error, denoted here by $P_b(L)$, is

$$\begin{aligned} P_b(L) &= P(U_2 - U_1 > 0) \\ &= P(X > 0) = \int_0^\infty p(x)\,dx \end{aligned} \tag{13.4–52}$$

where the random variable X is defined as

$$X = U_2 - U_1 = \sum_{k=1}^{L} \left(|N_{k2}|^2 - |2\mathcal{E}\alpha_k + N_{k1}|^2 \right) \tag{13.4–53}$$

The phase terms $\{\phi_k\}$ in U_1 have been dropped since they do not affect the performance of the square-law detector.

Using the Chernov bound, the error probability in 13.4–52 can be expressed in the form

$$P_b(L) \leq E(e^{\zeta X}) \tag{13.4–54}$$

where the parameter $\zeta > 0$ is optimized to yield a tight bound. Upon substituting for the random variable X from Equation 13.4–53 and noting that the random variables in the summation are mutually statistically independent, we obtain the result

$$P_b(L) \leq \prod_{k=1}^{L} E\left(e^{\zeta|N_{k2}|^2}\right) E\left(e^{-\zeta|2\mathcal{E}\alpha_k+N_{k1}|^2}\right) \tag{13.4–55}$$

But

$$E\left(e^{\zeta|N_{k2}|^2}\right) = \frac{1}{1-2\zeta\sigma_2^2}, \qquad \zeta < \frac{1}{2\sigma_2^2} \tag{13.4–56}$$

and

$$E\left(e^{-\zeta|2\mathcal{E}\alpha_k+N_{k1}|^2}\right) = \frac{1}{1+2\zeta\sigma_1^2}, \qquad \zeta > \frac{-1}{2\sigma_1^2} \tag{13.4–57}$$

where $\sigma_2^2 = 2\mathcal{E}N_0$, $\sigma_1^2 = 2\mathcal{E}N_0(1+\overline{\gamma}_c)$, and $\overline{\gamma}_c$ is the average SNR per diversity channel. Note that σ_1^2 and σ_2^2 are independent of k, i.e., the additive noise terms on the L diversity channels as well as the fading statistics are identically distributed. Consequently, Equation 13.4–55 reduces to

$$P_b(L) \leq \left[\frac{1}{\left(1-2\zeta\sigma_2^2\right)\left(1+2\zeta\sigma_1^2\right)}\right]^L, \qquad 0 \leq \zeta \leq \frac{1}{2\sigma_2^2} \tag{13.4–58}$$

By differentiating the right-hand side of Equation 13.4–58 with respect to ζ, we find that the upper bound is minimized when

$$\zeta = \frac{\sigma_1^2 - \sigma_2^2}{4\sigma_1^2\sigma_2^2} \tag{13.4–59}$$

Substitution of Equation 13.4–59 for ζ into Equation 13.4–58 yields the Chernov upper bound in the form

$$P_b(L) \leq \left[\frac{4(1+\overline{\gamma}_c)}{(2+\overline{\gamma}_c)^2}\right]^L \tag{13.4–60}$$

It is interesting to note that Equation 13.4–60 may also be expressed as

$$P_b(L) \leq [4p(1-p)]^L \tag{13.4–61}$$

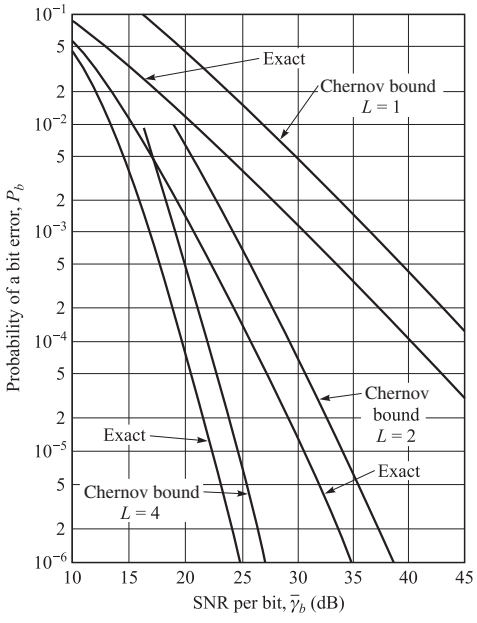

FIGURE 13.4–8
Comparison of Chernov bound with exact error probability.

where $p = 1/(2 + \overline{\gamma}_c)$ is the probability of error for binary orthogonal signaling on a fading channel without diversity.

A comparison of the Chernov bound in Equation 13.4–60 with the exact error probability for binary orthogonal signaling and square-law combining of the L diversity signals, which is given by the expression

$$\begin{aligned} P_b(L) &= \left(\frac{1}{2+\overline{\gamma}_c}\right)^L \sum_{k=0}^{L-1} \binom{L-1+k}{k} \left(\frac{1+\overline{\gamma}_c}{2+\overline{\gamma}_c}\right)^k \\ &= p^L \sum_{k=0}^{L-1} \binom{L-1+k}{k} (1-p)^k \end{aligned} \tag{13.4–62}$$

reveals the tightness of the bound. Figure 13.4–8 illustrates this comparison. We observe that the Chernov upper bound is approximately 6 dB from the exact error probability for $L = 1$, but, as L increases, it becomes tighter. For example, the difference between the bound and the exact error probability is about 2.5 dB when $L = 4$.

Finally we mention that the error probability for M-ary orthogonal signaling with diversity can be upper-bounded by means of the union bound

$$P_e \leq (M-1)P_2(L) \tag{13.4–63}$$

where we may use either the exact expression given in Equation 13.4–62 or the Chernov bound in Equation 13.4–60 for $P_b(L)$.

13.5
SIGNALING OVER A FREQUENCY-SELECTIVE, SLOWLY FADING CHANNEL: THE RAKE DEMODULATOR

When the spread factor of the channel satisfies the condition $T_m B_d \ll 1$, it is possible to select signals having a bandwidth $W \ll (\Delta f)_c$ and a signal duration $T \ll (\Delta t)_c$. Thus, the channel is frequency-nonselective and slowly fading. In such a channel, diversity techniques can be employed to overcome the severe consequences of fading.

When a bandwidth $W \gg (\Delta f)_c$ is available to the user, the channel can be subdivided into a number of frequency-division multiplexed (FDM) subchannels having a mutual separation in center frequencies of at least $(\Delta f)_c$. Then the same signal can be transmitted on the FDM subchannels, and, thus, frequency diversity is obtained. In this section, we describe an alternative method.

13.5–1 A Tapped-Delay-Line Channel Model

As we shall now demonstrate, a more direct method for achieving basically the same results is to employ a wideband signal covering the bandwidth W. The channel is still assumed to be slowly fading by virtue of the assumption that $T \ll (\Delta t)_c$. Now suppose that W is the bandwidth occupied by the real band-pass signal. Then the band occupancy of the equivalent low-pass signal $s_l(t)$ is $|f| \leq \frac{1}{2}W$. Since $s_l(t)$ is band-limited to $|f| \leq \frac{1}{2}W$, application of the sampling theorem results in the signal representation

$$s_l(t) = \sum_{n=-\infty}^{\infty} s_l\left(\frac{n}{W}\right) \frac{\sin[\pi W(t - n/W)]}{\pi W(t - n/W)} \tag{13.5–1}$$

The Fourier transform of $s_l(t)$ is

$$S_l(f) = \begin{cases} \dfrac{1}{W} \displaystyle\sum_{n=-\infty}^{\infty} s_l(n/W) e^{-j2\pi fn/W} & |f| \leq \frac{1}{2}W \\ 0 & |f| > \frac{1}{2}W \end{cases} \tag{13.5–2}$$

The noiseless received signal from a frequency-selective channel was previously expressed in the form

$$r_l(t) = \int_{-\infty}^{\infty} C(f; t) S_l(f) e^{j2\pi ft}\, df \tag{13.5–3}$$

where $C(f;t)$ is the time-variant transfer function. Substitution for $S_l(f)$ from Equation 13.5–2 into 13.5–3 yields

$$\begin{aligned} r_l(t) &= \frac{1}{W}\sum_{n=-\infty}^{\infty} s_l(n/W)\int_{-\infty}^{\infty} C(f;t)e^{j2\pi f(t-n/W)}\,df \\ &= \frac{1}{W}\sum_{n=-\infty}^{\infty} s_l(n/W)c(t-n/W;t) \end{aligned} \tag{13.5–4}$$

where $c(\tau;t)$ is the time-variant impulse response. We observe that Equation 13.5–4 has the form of a convolution sum. Hence, it can also be expressed in the alternative form

$$r_l(t) = \frac{1}{W}\sum_{n=-\infty}^{\infty} s_l(t-n/W)c(n/W;t) \tag{13.5–5}$$

It is convenient to define a set of time-variable channel coefficients as

$$c_n(t) = \frac{1}{W}c\left(\frac{n}{W};t\right) \tag{13.5–6}$$

Then Equation 13.5–5 expressed in terms of these channel coefficients becomes

$$r_l(t) = \sum_{n=-\infty}^{\infty} c_n(t)s_l(t-n/W) \tag{13.5–7}$$

The form for the received signal in Equation 13.5–7 implies that the time-variant frequency-selective channel can be modeled or represented as a tapped delay line with tap spacing $1/W$ and tap weight coefficients $\{c_n(t)\}$. In fact, we deduce from Equation 13.5–7 that the low-pass impulse response for the channel is

$$c(\tau;t) = \sum_{n=-\infty}^{\infty} c_n(t)\delta(\tau-n/W) \tag{13.5–8}$$

and the corresponding time-variant transfer function is

$$C(f;t) = \sum_{n=-\infty}^{\infty} c_n(t)e^{-j2\pi fn/W} \tag{13.5–9}$$

Thus, with an equivalent low-pass-signal having a bandwidth $\frac{1}{2}W$, where $W \gg (\Delta f)_c$, we achieve a resolution of $1/W$ in the multipath delay profile. Since the total multipath spread is T_m, for all practical purposes the tapped delay line model for the channel can be truncated at $L = \lfloor T_m W \rfloor + 1$ taps. Then the noiseless received signal can be expressed in the form

$$r_l(t) = \sum_{n=1}^{L} c_n(t)s_l\left(t-\frac{n}{W}\right) \tag{13.5–10}$$

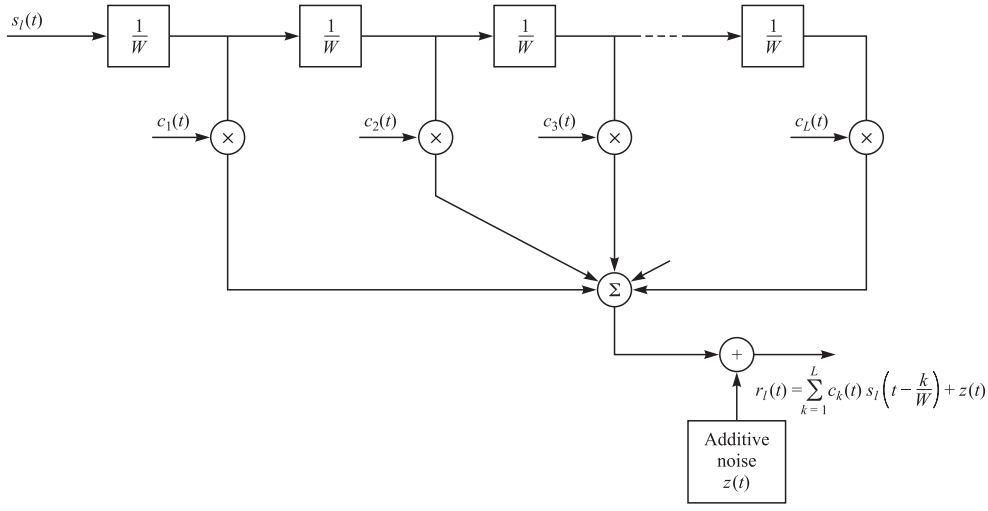

FIGURE 13.5–1
Trapped delay line model of frequency-selective channel.

The truncated tapped delay line model is shown in Figure 13.5–1. In accordance with the statistical characterization of the channel presented in Section 13.1, the time-variant tap weights $\{c_n(t)\}$ are complex-valued stationary random processes. In the special case of Rayleigh fading, the magnitudes $|c_n(t)| \equiv \alpha_n(t)$ are Rayleigh-distributed and the phases $\phi_n(t)$ are uniformly distributed. Since the $\{c_n(t)\}$ represent the tap weights corresponding to the L different delays $\tau = n/W, n = 1, 2, \ldots, L$, the uncorrelated scattering assumption made in Section 13.1 implies that the $\{c_n(t)\}$ are mutually uncorrelated. When the $\{c_n(t)\}$ are Gaussian random processes, they are statistically independent.

13.5–2 The RAKE Demodulator

We now consider the problem of digital signaling over a frequency-selective channel that is modeled by a tapped delay line with statistically independent time-variant tap weights $\{c_n(t)\}$. It is apparent at the outset, however, that the tapped delay line model with statistically independent tap weights provides us with L replicas of the same transmitted signal at the receiver. Hence, a receiver that processes the received signal in an optimum manner will achieve the performance of an equivalent Lth-order diversity communication system.

Let us consider binary signaling over the channel. We have two equal-energy signals $s_{l1}(t)$ and $s_{l2}(t)$, which are either antipodal or orthogonal. Their time duration T is selected to satisfy the condition $T \gg T_m$. Thus, we may neglect any intersymbol interference due to multipath. Since the bandwidth of the signal exceeds the coherent

bandwidth of the channel, the received signal is expressed as

$$\begin{aligned} r_l(t) &= \sum_{k=1}^{L} c_k(t) s_{li}(t - k/W) + z(t) \\ &= v_i(t) + z(t), \qquad 0 \le t \le T, \qquad i = 1, 2 \end{aligned} \tag{13.5–11}$$

where $z(t)$ is a complex-valued zero-mean white Gaussian noise process. Assume for the moment that the channel tap weights are known. Then the optimum demodulator consists of two filters matched to $v_1(t)$ and $v_2(t)$. The demodulator output is sampled at the symbol rate and the samples are passed to a decision circuit that selects the signal corresponding to the largest output. An equivalent optimum demodulator employs cross correlation instead of matched filtering. In either case, the decision variables for coherent detection of the binary signals can be expressed as

$$\begin{aligned} U_m &= \text{Re}\left[\int_0^T r_l(t) v_m^*(t)\, dt\right] \\ &= \text{Re}\left[\sum_{k=1}^{L} \int_0^T r_l(t) c_k^*(t) s_m^*(t - k/W)\, dt\right], \qquad m = 1, 2 \end{aligned} \tag{13.5–12}$$

Figure 13.5–2 illustrates the operations involved in the computation of the decision variables. In this realization of the optimum receiver, the two reference signals are delayed and correlated with the received signal $r_l(t)$.

An alternative realization of the optimum demodulator employs a single delay line through which is passed the received signal $r_l(t)$. The signal at each tap is correlated with $c_k^*(t)s_{lm}^*(t)$, where $k = 1, 2, \ldots, L$ and $m = 1, 2$. This receiver structure is shown in Figure 13.5–3. In effect, the tapped delay line demodulator attempts to collect the signal energy from all the received signal paths that fall within the span of the delay line and carry the same information. Its action is somewhat analogous to an ordinary garden rake and, consequently, the name "RAKE demodulator" has been coined for this demodulator structure by Price and Green (1958). The taps on the RAKE demodulator are often called "RAKE fingers."

13.5–3 Performance of RAKE Demodulator

We shall now evaluate the performance of the RAKE demodulator under the condition that the fading is sufficiently slow to allow us to estimate $c_k(t)$ perfectly (without noise). Furthermore, within any one signaling interval, $c_k(t)$ is treated as a constant and denoted as c_k. Thus the decision variables in Equation 13.5–12 may be expressed in the form

$$U_m = \text{Re}\left[\sum_{k=1}^{L} c_k^* \int_0^T r(t) s_{lm}^*(t - k/W)\, dt\right], \qquad m = 1, 2 \tag{13.5–13}$$

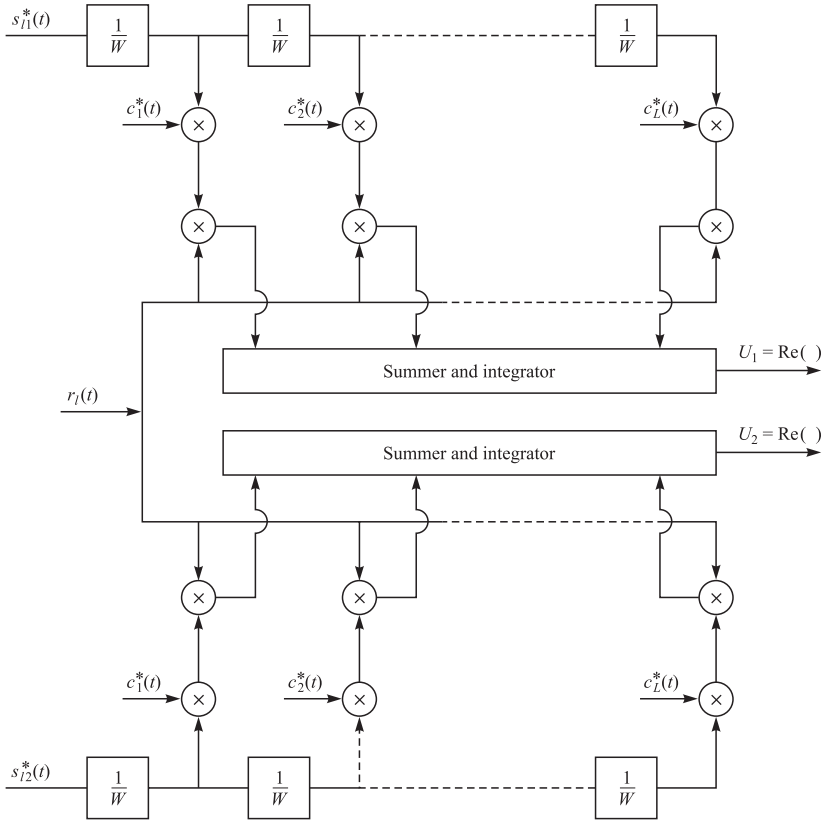

FIGURE 13.5–2
Optimum demodulator for wideband binary signals (delayed reference configuration).

Suppose the transmitted signal is $s_{l1}(t)$; then the received signal is

$$r_l(t) = \sum_{n=1}^{L} c_n s_{l1}(t - n/W) + z(t), \qquad 0 \le t \le T \tag{13.5–14}$$

Substitution of Equation 13.5–14 into Equation 13.5–13 yields

$$\begin{aligned} U_m = \text{Re}\left[\sum_{k=1}^{L} c_k^* \sum_{n=1}^{L} c_n \int_0^T s_{l1}(t - n/W) s_{lm}^*(t - k/W)\, dt\right] \\ + \text{Re}\left[\sum_{k=1}^{L} c_k^* \int_0^T z(t) s_{lm}^*(t - k/W)\, dt\right], \qquad m = 1, 2 \end{aligned} \tag{13.5–15}$$

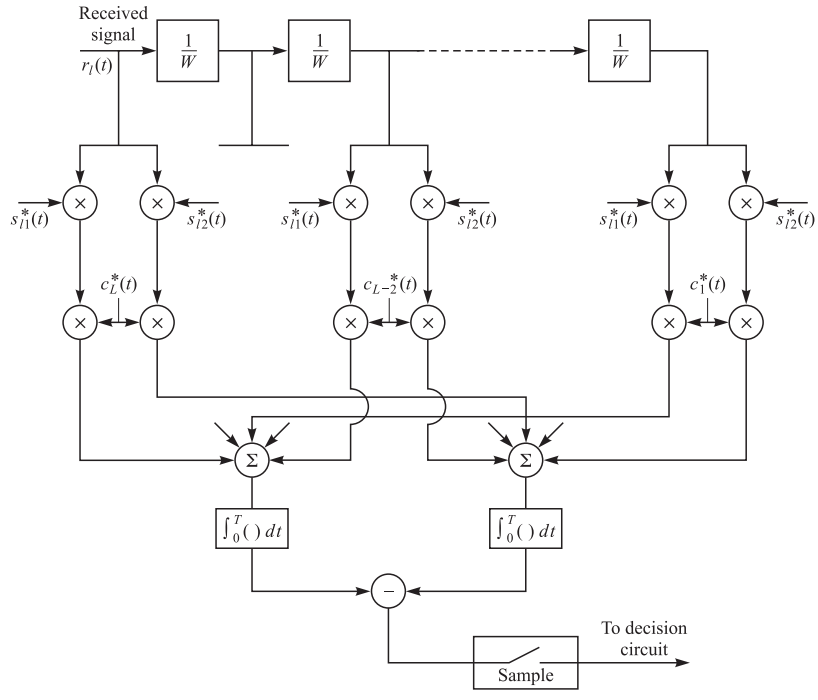

FIGURE 13.5–3
Optimum demodulator for wideband binary signals (delayed received signal configuration).

Usually the wideband signals $s_{l1}(t)$ and $s_{l2}(t)$ are generated from pseudorandom sequences, which result in signals that have the property

$$\int_0^T s_{li}(t - n/W)s_{li}^*(t - k/W)\,dt \approx 0, \qquad k \neq n, \qquad i = 1, 2 \tag{13.5–16}$$

If we assume that our binary signals are designed to satisfy this property, then Equation 13.5–15 simplifies to†

$$\begin{aligned} U_m = \text{Re}\left[\sum_{k=1}^{L} |c_k|^2 \int_0^T s_{l1}(t - k/W)s_{lm}^*(t - k/W)\,dt\right] \\ + \text{Re}\left[\sum_{k=1}^{L} c_k^* \int_0^T z(t)s_{lm}^*(t - k/W)\,dt\right], \qquad m = 1, 2 \end{aligned} \tag{13.5–17}$$

†Although the orthogonality property specified by Equation 13.5–16 can be satisfied by proper selection of the pseudorandom sequences, the cross correlation of $s_{l1}(t - n/W)$ with $s_{li}^*(t - k/W)$ gives rise to a signal-dependent self-noise, which ultimately limits the performance. For simplicity, we do not consider the self-noise term in the following calculations. Consequently, the performance results presented below should be considered as lower bounds (ideal RAKE). An approximation to the performance of the RAKE can be obtained by treating the self-noise as an additional Gaussian noise component with noise power equal to its variance.

When the binary signals are antipodal, a single decision variable suffices. In this case, Equation 13.5–17 reduces to

$$U_1 = \text{Re}\left(2\mathcal{E}\sum_{k=1}^{L}\alpha_k^2 + \sum_{k=1}^{L}\alpha_k N_k\right) \tag{13.5–18}$$

where $\alpha_k = |c_k|$ and

$$N_k = e^{-j\phi_k}\int_0^T z(t)s_l^*(t - k/W)\,dt \tag{13.5–19}$$

But Equation 13.5–18 is identical to the decision variable given in Equation 13.4–4, which corresponds to the output of a maximal ratio combiner in a system with Lth-order diversity. Consequently, the RAKE demodulator with perfect (noiseless) estimates of the channel tap weights is equivalent to a maximal ratio combiner in a system with Lth-order diversity. Thus, when all the tap weights have the same mean-square value, i.e., $E(\alpha_k^2)$ is the same for all k, the error rate performance of the RAKE demodulator is given by Equations 13.4–15 and 13.4–16. On the other hand, when the mean-square values $E(\alpha_k^2)$ are not identical for all k, the derivation of the error rate performance must be repeated since Equation 13.4–15 no longer applies.

We shall derive the probability of error for binary antipodal and orthogonal signals under the condition that the mean-square values of $\{\alpha_k\}$ are distinct. We begin with the conditional error probability

$$P_b(\gamma_b) = Q\left(\sqrt{\gamma_b(1-\rho_r)}\right) \tag{13.5–20}$$

where $\rho_r = -1$ for antipodal signals, $\rho_r = 0$ for orthogonal signals, and

$$\gamma_b = \frac{\mathcal{E}}{N_0}\sum_{k=1}^{L}\alpha_k^2 = \sum_{k=1}^{L}\gamma_k \tag{13.5–21}$$

Each of the $\{\gamma_k\}$ is distributed according to a chi-squared distribution with two degrees of freedom. That is,

$$p(\gamma_k) = \frac{1}{\overline{\gamma}_k}e^{-\gamma_k/\overline{\gamma}_k} \tag{13.5–22}$$

where $\overline{\gamma}_k$ is the average SNR for the kth path, defined as

$$\overline{\gamma}_k = \frac{\mathcal{E}}{N_0}E\left(\alpha_k^2\right) \tag{13.5–23}$$

Furthermore, from Equation 13.4–10 we know that the characteristic function of γ_k is

$$\Phi_{\gamma_k}(v) = \frac{1}{1 - jv\overline{\gamma}_k} \tag{13.5–24}$$

Since γ_b is the sum of L statistically independent components $\{\gamma_k\}$, the characteristic function of γ_b is

$$\Phi_{\gamma_b}(v) = \prod_{k=1}^{L} \frac{1}{1 - jv\overline{\gamma}_k} \tag{13.5–25}$$

The inverse Fourier transform of the characteristic function in Equation 13.5–25 yields the probability density function of γ_b in the form

$$p(\gamma_b) = \sum_{k=1}^{L} \frac{\pi_k}{\overline{\gamma}_k} e^{-\gamma_b/\overline{\gamma}_k}, \qquad \gamma_b \geq 0 \tag{13.5–26}$$

where π_k is defined as

$$\pi_k = \prod_{\substack{i=1 \\ i \neq k}}^{L} \frac{\overline{\gamma}_k}{\overline{\gamma}_k - \overline{\gamma}_i} \tag{13.5–27}$$

When the conditional error probability in Equation 13.5–20 is averaged over the probability density function given in Equation 13.5–26, the result is

$$P_b = \tfrac{1}{2} \sum_{k=1}^{L} \pi_k \left[1 - \sqrt{\frac{\overline{\gamma}_k(1 - \rho_r)}{2 + \overline{\gamma}_k(1 - \rho_r)}} \right] \tag{13.5–28}$$

This error probability can be approximated as ($\overline{\gamma}_k \gg 1$)

$$P_b \approx \binom{2L - 1}{L} \prod_{k=1}^{L} \frac{1}{2\overline{\gamma}_k(1 - \rho_r)} \tag{13.5–29}$$

By comparing Equation 13.5–29 for $\rho_r = -1$ with Equation 13.4–18, we observe that the same type of asymptotic behavior is obtained for the case of unequal SNR per path and the case of equal SNR per path.

In the derivation of the error rate performance of the RAKE demodulator, we assumed that the estimates of the channel tap weights are perfect. In practice, relatively good estimates can be obtained if the channel fading is sufficiently slow, e.g., $(\Delta t)_c/T \geq 100$, where T is the signaling interval. Figure 13.5–4 illustrates a method for estimating the tap weights when the binary signaling waveforms are orthogonal. The estimate is the output of the low-pass filter at each tap. At any one instant in time, the incoming signal is either $s_{l1}(t)$ or $s_{l2}(t)$. Hence, the input to the low-pass filter used to estimate $c_k(t)$ contains signal plus noise from one of the correlators and noise only from the other correlator. This method for channel estimation is not appropriate for antipodal signals, because the addition of the two correlator outputs results in signal cancellation. Instead, a single correlator can be employed for antipodal signals. Its output is fed to the input of the low-pass filter after the information-bearing signal is removed. To accomplish this, we must introduce a delay of one signaling interval into the channel estimation procedure, as illustrated in Figure 13.5–5. That is, first the receiver must decide whether the information in the received signal is $+1$ or -1 and, then, it uses the

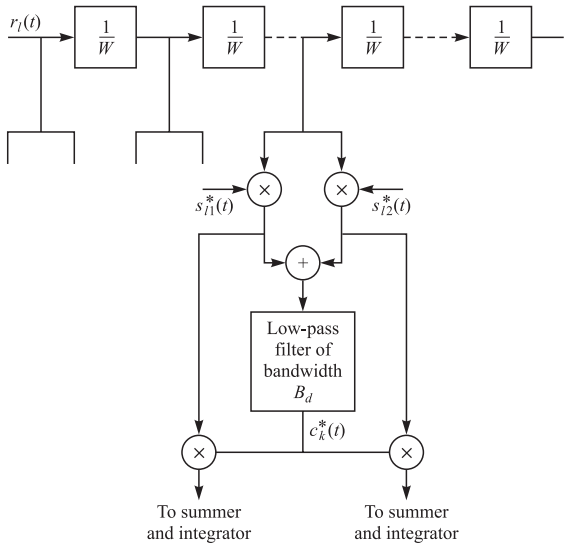

FIGURE 13.5–4
Channel tap weight estimation with binary orthogonal signals.

decision to remove the information from the correlator ouput prior to feeding it to the low-pass filter.

If we choose not to estimate the tap weights of the frequency-selective channel, we may use either DPSK signaling or noncoherently detected orthogonal signaling. The RAKE demodulator structure for DPSK is illustrated in Figure 13.5–6. It is apparent that when the transmitted signal waveform $s_l(t)$ satisfies the orthogonality property given in Equation 13.5–16, the decision variable is identical to that given in Equation 13.4–23 for an Lth-order diversity system. Consequently, the error rate performance of the RAKE demodulator for a binary DPSK is identical to that given in Equation 13.4–15 with $\mu = \overline{\gamma}_c/(1+\overline{\gamma}_c)$, when all the signal paths have the same SNR $\overline{\gamma}_c$. On the other hand, when the SNRs $\{\overline{\gamma}_k\}$ are distinct, the error probability can be obtained by averaging Equation 13.4–24, which is the probability of error conditioned on a time-invariant channel, over the probability density function of γ_b given by Equation 13.5–26. The result of this integration is

$$P_b = \left(\tfrac{1}{2}\right)^{2L-1} \sum_{m=0}^{L-1} m! b_m \sum_{k=1}^{L} \frac{\pi_k}{\overline{\gamma}_k} \left(\frac{\overline{\gamma}_k}{1+\overline{\gamma}_k}\right)^{m+1} \tag{13.5–30}$$

where π_k is defined in Equation 13.5–27 and b_m in Equation 13.4–25.

Finally, we consider binary orthognal signaling over the frequency-selective channel with square-law detection at the receiver. This type of signal is appropriate when the fading is rapid enough to preclude a good estimate of the channel tap weights. The RAKE demodulator with square-law combining of the signal from each tap is illustrated in Figure 13.5–7. In computing its performance, we again assume that the orthogonality property given in Equation 13.5–16 holds. Then the decision variables at

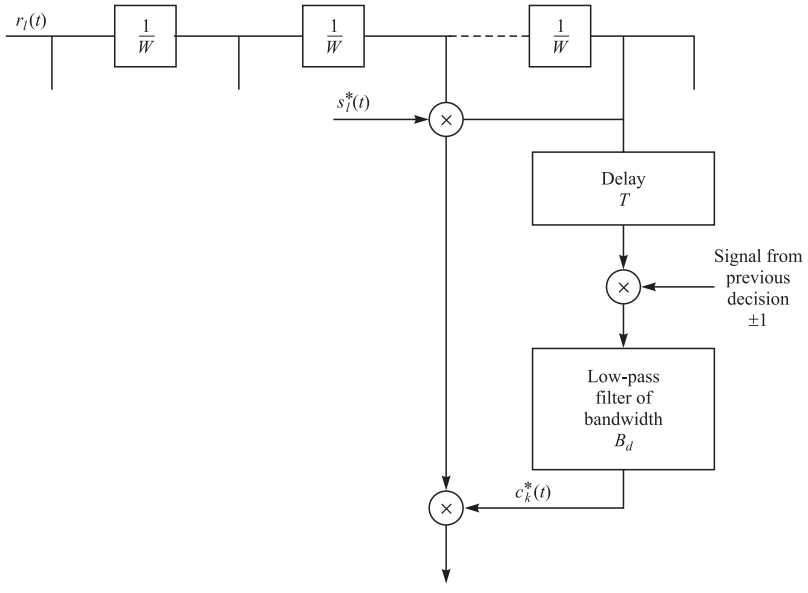

FIGURE 13.5–5
Channel tap weight estimation with binary antipodal signals.

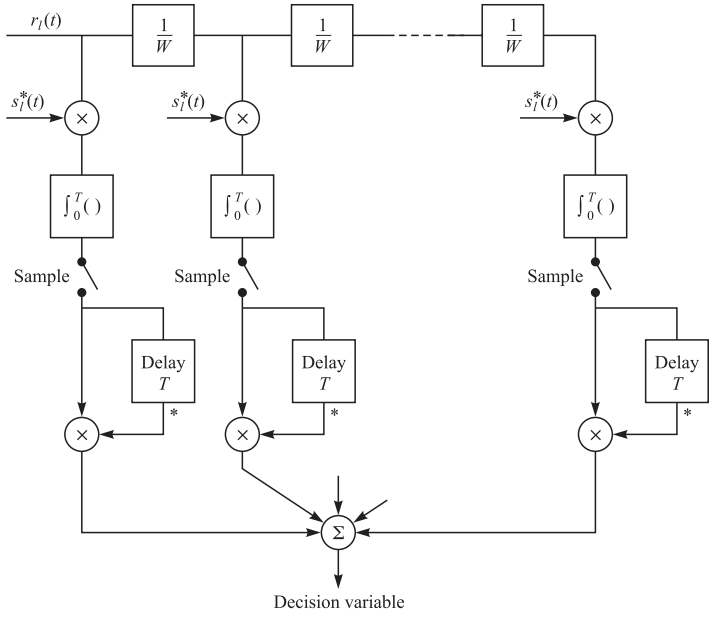

FIGURE 13.5–6
RAKE demodulator for DPSK signals.

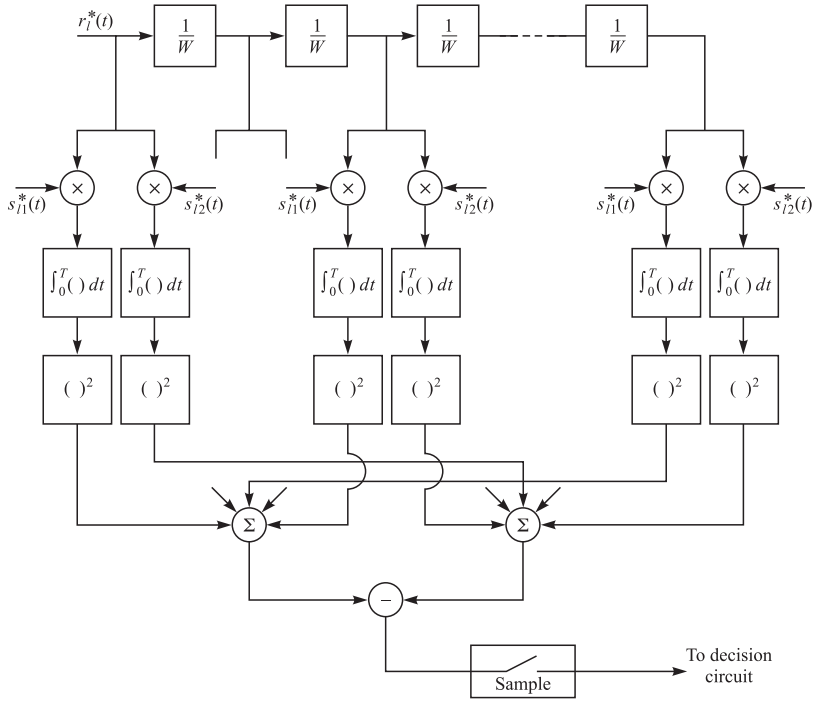

FIGURE 13.5–7
RAKE demodulator for square-law combination of orthogonal signals.

the output of the RAKE are

$$U_1 = \sum_{k=1}^{L} |2\mathcal{E}c_k + N_{k1}|^2$$
$$U_2 = \sum_{k=1}^{L} |N_{k2}|^2 \tag{13.5–31}$$

where we have assumed that $s_{l1}(t)$ was the transmitted signal. Again we observe that the decision variables are identical to the ones given in Equation 13.4–29, which apply to orthogonal signals with Lth-order diversity. Therefore, the performance of the RAKE demodulator for square-law-detected orthogonal signals is given by Equation 13.4–15 with $\mu = \bar{\gamma}_c/(2 + \gamma_c^-)$ when all the signal paths have the same SNR. If the SNRs are distinct, we can average the conditional error probability given by Equation 13.4–24, with γ_b replaced by $\frac{1}{2}\gamma_b$, over the probability density function $p(\gamma_b)$ given in Equation 13.5–26. The result of this averaging is given by Equation 13.5–30, with $\overline{\gamma}_k$ replaced by $\frac{1}{2}\overline{\gamma}_k$.

In the above analysis, the RAKE demodulator shown in Figure 13.5–7 for square-law combining of orthogonal signals is assumed to contain a signal component at each delay. If that is not the case, its performance will be degraded, since some of the tap

correlators will contribute only noise. Under such conditions, the low-level, noise-only contributions from the tap correlators should be excluded from the combiner, as shown by Chyi et al. (1988).

The configurations of the RAKE demodulator presented in this section can be easily generalized to multilevel signaling. In fact, if M-ary PSK or DPSK is chosen, the RAKE structures presented in this section remain unchanged. Only the PSK and DPSK detectors that follow the RAKE correlator are different.

Generalized RAKE Demodulator

The RAKE demodulator described above is the optimum demodulator when the additive noise is white and Gaussian. However, there are communication scenarios in which additive interference from other users of the channel results in colored additive noise. This is the case, for example, in the downlink of a cellular communication system employing CDMA as a multiple access method. In this case, the spread spectrum signals transmitted from a base station to the mobile receivers carry information on synchronously transmitted orthogonal spreading codes. However, in transmission over a frequency-selective channel, the orthogonality of the code sequences is destroyed by the channel time dispersion due to multipath. As a consequence, the RAKE demodulator for any given mobile receiver must demodulate its desired signal in the presence of additional additive interference resulting from the cross-correlations of its desired spreading code sequence with the multipath corrupted code sequences that are assigned to the other mobile users. This additional interference is generally characterized as colored Gaussian noise, as shown by Bottomley (1993) and Klein (1997).

A model for the downlink transmission in a CDMA cellular communication system is illustrated in Figure 13.5–8. The base station transmits the combined signal.

$$s(t) = \sum_{k=1}^{K} s_k(t) \tag{13.5–32}$$

to the K mobile terminals, where each $s_k(t)$ is a spread spectrum signal intended for the kth user and the corresponding spreading code for the kth user is orthogonal with each of the spreading codes of the other $K - 1$ users. We assume that the signals propagate through a channel characterized by the baseband equivalent lowpass, time-invariant

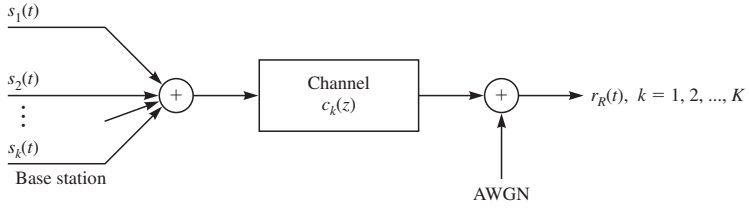

FIGURE 13.5–8
Model for the downlink transmission of a CDMA cellular communication system.

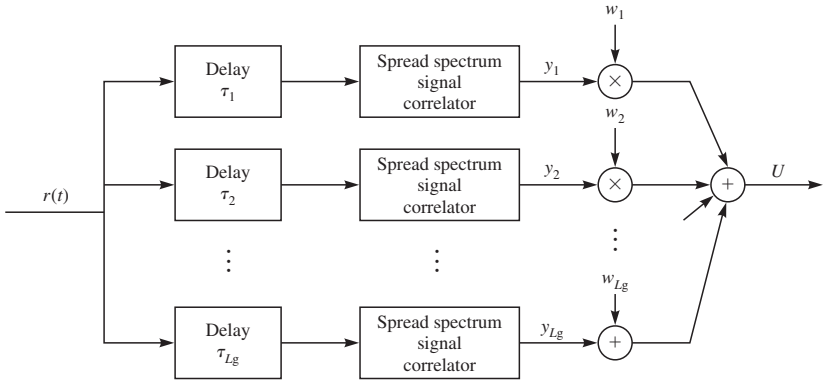

FIGURE 13.5–9
Structure of generalized RAKE demodulator.

impulse response

$$c_k(\tau) = \sum_{i=1}^{L_k} c_{ki}\,\delta(\tau - \tau_{ki}), \qquad k = 1, 2, \ldots, K \tag{13.5–33}$$

where L_k is the number of resolvable multipath components, $\{c_{ki}\}$ are the complex-valued coefficients, and $\{\tau_{ki}\}$ are the corresponding time delays. To simplify this presentation, we focus on the processing at the receiver of the first user ($k = 1$) and drop the index k. In a CDMA cellular system, an unmodulated spread spectrum signal, say $s_0(t)$, is transmitted along with the information-bearing signals and serves as a pilot signal that is used by each mobile receiver to estimate the channel coefficients $\{c_i\}$ and the time delays $\{\tau_i\}$.

A conventional RAKE demodulator would consist of L "fingers" with each finger corresponding to one of the L channel delays, and the weights at the L fingers would be $\{c_i^*\}$, the complex conjugates of the corresponding channel coefficients. In contrast, a generalized RAKE demodulator consists of $L_g > L$ RAKE fingers, and the weights at the L_g fingers, denoted as $\{w_i\}$, are different from $\{c_i^*\}$. The structure of the generalized RAKE demodulator is illustrated in Figure 13.5–9 for phase coherent modulation such as PSK or QAM. The decision variable U at the detector may be expressed as

$$U = \boldsymbol{w}^H \boldsymbol{y} \tag{13.5–34}$$

It is convenient to express the received vector $\boldsymbol{y}$ at the output of the cross-correlators as

$$\boldsymbol{y} = \boldsymbol{g}b + \boldsymbol{z} \tag{13.5–35}$$

where $\boldsymbol{g}$ is a vector of complex-valued elements which result from the cross-correlations of the desired received signal, say $s_1(t) * c_1(t)$, with the corresponding spreading sequence at the L_g delays, b is the desired symbol to be detected, and $\boldsymbol{z}$ represents the vector of additive Gaussian noise plus interference resulting from the cross-correlations of the spreading sequence with the received signals of the other users and intersymbol

interference due to channel multipath. For a sufficiently large number of users and channel multipath components, the vector $\boldsymbol{z}$ may be characterized as complex-valued Gaussian with zero mean and covariance matrix $\boldsymbol{R}_z = E[\boldsymbol{z}\boldsymbol{z}^H]$. Based on this statistical characterization of $\boldsymbol{z}$, the RAKE finger weight vector for maximum-likelihood detection is given as

$$\boldsymbol{w} = \boldsymbol{R}_z^{-1}\boldsymbol{g} \tag{13.5–36}$$

Given the channel impulse response, the implementation of the maximum-likelihood detector requires the evaluation of the covariance matrix $\boldsymbol{R}_z$ and the desired signal vector $\boldsymbol{g}$. The procedure for evaluation of these parameters has been described in a paper by Bottomley et al. (2000). Also investigated in this paper is the selection of the number of RAKE fingers and the selection of the corresponding delays for different channel characteristics.

In the description of the generalized RAKE demodulator given above, we assumed that the channel is time-invariant. In a randomly time-variant channel, the position of the RAKE fingers and the weights $\{w_i\}$ must be varied according to the characteristics of the channel impulse response. The pilot signal transmitted by the base station to the mobile receivers is used to estimate the channel impulse response, from which the finger placement and weights $\{w_i\}$ can be determined adaptively. The interested reader is referred to the paper by Bottomley et al. (2000) for a detailed description of the performance of the generalized RAKE demodulator for some channel models.

13.5–4 Receiver Structures for Channels with Intersymbol Interference

As described above, the wideband signal waveforms that are transmitted through the multipath channels resolve the multipath components with a time resolution of $1/W$, where W is the signal bandwidth. Usually, such wideband signals are generated as direct sequence spread spectrum signals, in which the PN spreading sequences are the outputs of linear feedback shift registers, e.g., maximum-length linear feedback shift registers. The modulation impressed on the sequences may be binary PSK, QPSK, DPSK, or binary orthogonal. The desired bit rate determines the bit interval or symbol interval.

The RAKE demodulator that we described above is the optimum demodulator based on the condition that the bit interval $T_b \gg T_m$, i.e., there is negligible ISI. When this condition is not satisfied, the RAKE demodulator output is corrupted by ISI. In such a case, an equalizer is required to suppress the ISI.

To be specific, we assume that binary PSK modulation is used and spread by a PN sequence. The bandwidth of the transmitted signal is sufficiently broad to resolve two or more multipath components. At the receiver, after the signal is demodulated to baseband, it may be processed by the RAKE, which is the matched filter to the channel response, followed by an equalizer to suppress the ISI. The RAKE output is sampled at the bit rate, and these samples are passed to the equalizer. An appropriate equalizer, in this case, would be a maximum-likelihood sequence estimator implemented by use

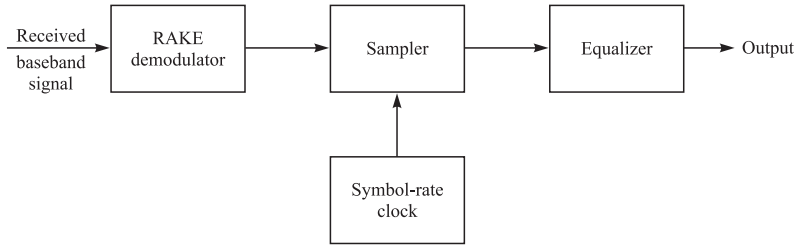

FIGURE 13.5–10
Receiver structure for processing wideband signal corrupted by ISI.

of the Viterbi algorithm or a decision feedback equalizer (DFE). This demodulator structure is shown in Figure 13.5–10.

Other receiver structures are also possible. If the period of the PN sequence is equal to the bit interval, i.e., $LT_c = T_b$, where T_c is the chip interval and L is the number of chips per bit, a fixed filter matched to the spreading sequence may be used to process the received signal and followed by an adaptive equalizer, such as a fractionally spaced DFE, as shown in Figure 13.5–11. In this case, the matched filter output is sampled at some multiple of the chip rate, e.g., twice the chip rate, and fed to the fractionally spaced DFE. The feedback filter in the DFE would have taps spaced at the bit interval. The adaptive DFE would require a training sequence for adjustment of its coefficients to the channel multipath structure.

An even simpler receiver structure is one in which the spread spectrum matched filter is replaced by a low-pass filter whose bandwidth is matched to the transmitted signal bandwidth. The output of such a filter may be sampled at an integer multiple of the chip rate and the samples are passed to an adaptive fractionally spaced DFE. In this case, the coefficients of the feedback filter in the DFE, with the aid of a training sequence, will adapt to the combination of the spreading sequence and the channel multipath. Abdulrahman et al. (1994) consider the use of a DFE to suppress ISI in a CDMA system in which each user employs a wideband direct sequence spread spectrum signal.

The paper by Taylor et al. (1998) provides a broad survey of equalization techniques and their performance for wireless channels.

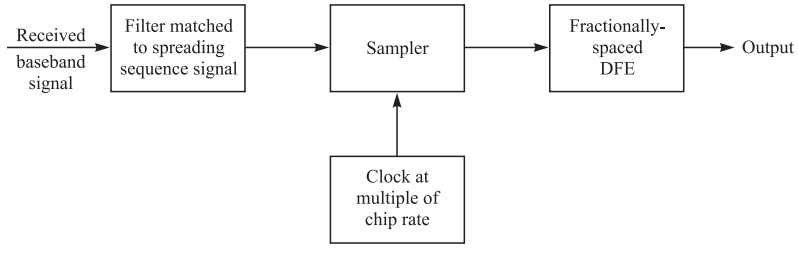

FIGURE 13.5–11
Alternative receiver structure for processing wideband signal corrupted by ISI.

13.6 MULTICARRIER MODULATION (OFDM)

Multicarrier modulation was introduced in Chapter 11 (Section 11.2), and a special form of multicarrier transmission, called orthogonal frequency-division multiplexing (OFDM), was treated in detail. In this section, we consider the use of OFDM for digital transmission on fading multipath channels.

From our previous discussion, we have observed that OFDM is an attractive alternative to single-carrier modulation for use in time-dispersive channels. By selecting the symbol duration in an OFDM system to be significantly larger than the channel dispersion, intersymbol interference (ISI) can be rendered negligible and completely eliminated by use of a time guard band or, equivalently, by the use of a cyclic prefix embedded in the OFDM signal. The elimination of ISI due to multipath dispersion, without the use of complex equalizers, is a basic motivation for use of OFDM for digital communication in fading multipath channels. However, OFDM is especially vulnerable to Doppler spread resulting from time variations in the channel impulse response, as is the case in mobile communication systems. The Doppler spreading destroys the orthogonality of the OFDM subcarriers and results in intercarrier interference (ICI) which can severely degrade the performance of the OFDM system. In the following section we evaluate the effect of a Doppler spread on the performance of OFDM.

13.6–1 Performance Degradation of an OFDM System due to Doppler Spreading

Let us consider an OFDM system with N subcarriers $\{e^{j2\pi f_k t}\}$, where each subcarrier employs either M-ary QAM or PSK modulation. The subcarriers are orthogonal over the symbol duration T, i.e., $f_k = k/T, k = 1, 2, \ldots, N$, so that

$$\frac{1}{T}\int_0^T e^{j2\pi f_i t}\, e^{-j2\pi f_k t}\, dt = \begin{cases} 1 & k = i \\ 0 & k \neq i \end{cases} \tag{13.6–1}$$

The channel is modeled as a frequency-selective randomly varying channel with impulse response $c(\tau; t)$. Within the frequency band of each subcarrier, the channel is modeled as a frequency-nonselective Rayleigh fading channel with impulse response.

$$c_k(\tau; t) = \alpha_k(t)\delta(t), \qquad k = 0, 1, \ldots, N-1 \tag{13.6–2}$$

It is assumed that the processes $\{\alpha_k(t), k = 0, 1, \ldots, N-1\}$ are complex-valued, jointly stationary, and jointly Gaussian with zero means and cross-covariance function

$$R_{\alpha_k\alpha_i}(\tau) = E[\alpha_k(t+\tau)\alpha_i^*(t)], \qquad k, i = 0, 1, \ldots, N-1 \tag{13.6–3}$$

For each fixed k, the real and imaginary parts of the process $\alpha_k(t)$ are assumed independent with identical covariance function. It is further assumed that the covariance function $R_{\alpha_k\alpha_i}(\tau)$ has the following factorable form

$$R_{\alpha_k\alpha_i}(\tau) = R_1(\tau)R_2(k-i) \tag{13.6–4}$$

which is sufficient to represent the frequency selectivity and the time-varying effects of the channel. $R_1(\tau)$ represents the temporal correlation of the process $\alpha_k(t)$, which is identical for all $k = 0, 1, \ldots, N-1$, and $R_2(k)$ represents the correlation in frequency across subcarriers.

To obtain numerical results, we assume that the power spectral density corresponding to $R_1(\tau)$ is modeled as in Jakes (1974) and given by (see Figure 13.1–8)

$$\mathcal{S}(f) = \begin{cases} \dfrac{1}{\pi f_m \sqrt{1-(f/f_m)^2}} & |f| \le f_m \\ 0 & \text{otherwise} \end{cases} \tag{13.6–5}$$

where F_d is the maximum Doppler frequency. We note that

$$R_1(\tau) = J_0(2\pi f_m \tau) \tag{13.6–6}$$

where $J_0(\tau)$ is the zero-order Bessel function of the first kind. To specify the correlation in frequency across the subcarriers, we model the multipath power intensity profile as an exponential of the form

$$R_c(\tau) = \beta e^{-\beta\tau}, \qquad \tau > 0, \quad \beta > 0 \tag{13.6–7}$$

where β is a parameter that controls the coherence bandwidth of the channel. The Fourier transform of $R_c(\tau)$ yields

$$R_C(f) = \frac{\beta}{\beta + j2\pi f} \tag{13.6–8}$$

which provides a measure of the correlation of the fading across the subcarriers, as shown in Figure 13.6–1. Hence, $R_2(k) = R_C(k/T)$ is the frequency separation between two adjacent subcarriers. The 3-dB bandwidth of $R_C(f)$ may be defined as the coherence bandwidth of the channel and is easily shown to be $\sqrt{3}\beta/2\pi$.

The channel model described above is suitable for modeling OFDM signal transmission in mobile radio systems, such as cellular systems and radio broadcasting systems. Since the symbol duration T is usually selected to be much larger than the channel multipath spread, it is reasonable to model the signal fading as flat over each subcarrier. However, compared with the entire OFDM system bandwidth W, the coherence bandwidth of the channel is usually smaller. Hence, the channel is frequency-selective over the entire OFDM signal bandwidth.

Let us now model the time variations of the channel within an OFDM symbol interval T. For mobile radio channels of practical interest, the channel coherence time is significantly larger than T. For such slow fading channels, we may use the two-term Taylor series expansion, first introduced by Bello (1963), to represent the time-varying channel variations $\alpha_k(t)$ as

$$\alpha_k(t) = \alpha_k(t_0) + \alpha_k'(t_0)(t - t_0), \qquad t_0 = \frac{T}{2}, \quad 0 \le t \le T \tag{13.6–9}$$

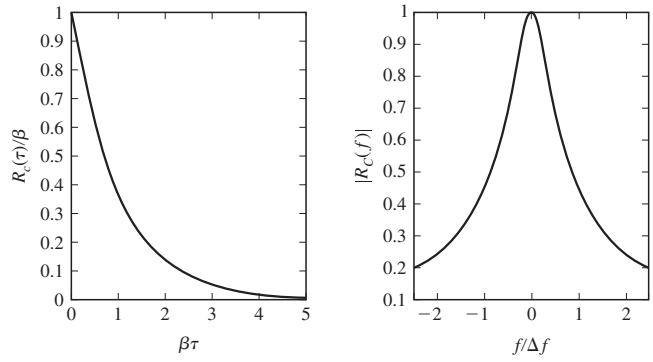

FIGURE 13.6–1
Multipath delay profile and frequency correlation function.

Therefore, the impulse response of the kth subchannel within a symbol interval is given as

$$c_k(\tau; t) = \alpha_k(t_0)\delta(\tau) + (t - t_0)\alpha_k'(t_0)\delta(\tau) \tag{13.6–10}$$

Since $R_1(\tau)$ given by Equation 13.6–6 is infinitely differentiable, all mean-square derivatives exist and hence the differentiation of $\alpha_k(t)$ is justified.

Based on the channel model described above, we determine the ICI term at the detector and evaluate its power. The baseband signal transmitted over the channel is expressed as

$$s(t) = \frac{1}{\sqrt{T}} \sum_{k=0}^{N-1} s_k \, e^{j2\pi f_k t}, \qquad 0 \le t \le T \tag{13.6–11}$$

where $f_k = k/T$ and $s_k,\ k = 0, 1, \ldots, N-1$, represents the complex-valued signal constellation points. We assume that

$$E\left[|s_k|^2\right] = 2\mathcal{E}_{\text{avg}} \tag{13.6–12}$$

where $2\mathcal{E}_{\text{avg}}$ denotes the average symbol energy of each s_k.

The received baseband signal may be expressed as

$$r(t) = \frac{1}{\sqrt{T}} \sum_{k=0}^{N-1} \alpha_k(t) s_k \, e^{j2\pi f_k t} + n(t) \tag{13.6–13}$$

where $n(t)$ is the additive noise, which is modeled as a complex-valued, zero-mean Gaussian process that is spectrally flat within the signal bandwidth with spectral density $2N_0$ W/Hz. By using the two-term Taylor series expansion for $a_k(t)$, $r(t)$ may be expressed as

$$r(t) = \frac{1}{\sqrt{T}} \sum_{k=0}^{N-1} \alpha_k\,(t_0) s_k e^{j2\pi f_k t} + \frac{1}{\sqrt{T}} \sum_{k=0}^{N-1} (t - t_0)\alpha_k'(t_0) s_k \, e^{j2\pi f_k t} + n(t) \tag{13.6–14}$$

The received signal in a symbol interval is passed through a parallel bank of N correlators, where each correlator is tuned to one of the N subcarrier frequencies. The output of the ith correlator at the sampling instant is

$$\begin{aligned}\hat{s}_i &= \frac{1}{\sqrt{T}} \int_0^T r(t)\, e^{-j2\pi f_i t}\, dt \\ &= \alpha_i(t_0)s_i + \frac{T}{2\pi j} \sum_{\substack{k=0 \\ k\neq i}}^{N-1} \frac{\alpha'_k(t_0)s_k}{k-i} + n_i\end{aligned} \tag{13.6–15}$$

The first term in Equation 13.6–15 represents the desired signal, the second term represents the ICI, and the third term is the additive noise component.

The mean-square value of the desired signal component is

$$\begin{aligned}S &= E\left[|\alpha_i(t_0)s_i|^2\right] \\ &= E\left[|\alpha_i(t_0)|^2\right] E\left[|s_i|^2\right] = 2\mathcal{E}_{\text{avg}}\end{aligned} \tag{13.6–16}$$

where the average channel gain is normalized to unity. The mean-square value of the ICI term is evaluated as follows. Since $R_{\alpha_s a_k}(\tau) = R_1(\tau)$ is infinitely differentiable, all (mean-square) derivatives of the process $\alpha_k(t)$, $-\infty < t < \infty$, exist. In particular, the first derivative $\alpha'_k(t)$ is a zero-mean, complex-valued Gaussian process with correlation function

$$E\left[\alpha'_k(t+\tau)(\alpha'_k(t)^*)\right] = -R''_1(\tau) \tag{13.6–17}$$

with corresponding spectral density $(2\pi f)^2\mathcal{S}(f)$. Hence,

$$E\left[|\alpha'_k(t)|^2\right] = \int_{-f_m}^{f_m} (2\pi f)^2 \mathcal{S}(f)\, df = 2\pi^2 f_m^2 \tag{13.6–18}$$

The power in the ICI term is

$$\begin{aligned}I &= E\left[\left|\frac{T}{2\pi j} \sum_{\substack{k=0 \\ k\neq i}}^{N-1} \frac{a'_k(t_0)s_k}{k-i}\right|^2\right] \\ &= \left(\frac{T}{2\pi}\right)^2 \sum_{\substack{k=0 \\ k\neq i}}^{N-1} \sum_{\substack{l=0 \\ l\neq i}}^{N-1} \frac{1}{(k-i)(l-i)} E\left[\alpha'_k(t_0)s_k\,(\alpha'_l(t_0)s_l)^*\right] \\ &\quad + \left(\frac{T}{2\pi}\right)^2 \sum_{\substack{k=0 \\ k\neq i}}^{N-1} \frac{1}{(k-i)^2} E\left[|\alpha'_k(t_0)s_k|^2\right]\end{aligned} \tag{13.6–19}$$

We note that the pair $(\alpha'_k(t_0), \alpha'_l(t_0))$ is statistically independent of (s_k, s_l). Furthermore, the $\{s_k\}$ are iid with zero means. Hence, the first term of the right-hand side of

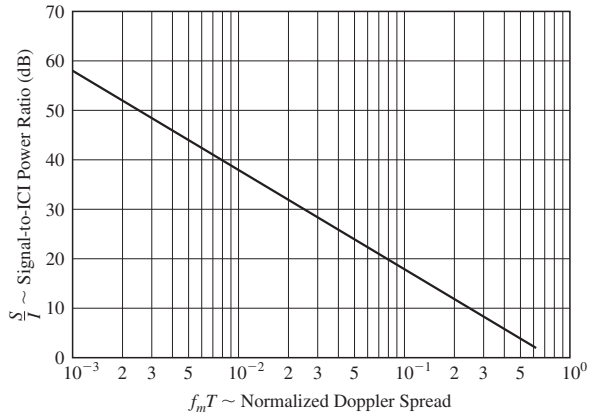

FIGURE 13.6–2
Signal-to-ICI power ratio versus normalized Doppler spread.

Equation 13.6–19 is zero. Therefore, by using the result from Equation 13.6–18 in Equation 13.6–19, the power of the ICI component is

$$I = \frac{(Tf_m)^2}{2} \sum_{\substack{k=0 \\ k\neq i}}^{N-1} \frac{2\mathcal{E}_s}{(k-i)^2} \tag{13.6–20}$$

Consequently, the signal-to-interference ratio S/I is given by

$$\frac{S}{I} = \frac{1}{\dfrac{(Tf_m)^2}{2} \displaystyle\sum_{\substack{k=0 \\ k\neq 1}}^{N-1} \frac{1}{(k-i)^2}} \tag{13.6–21}$$

Graphs of S/I versus Tf_m are shown in Figure 13.6–2 for $N = 256$ subcarriers and $i = N/2$, the interference on the middle subcarrier.

The evaluation of the effect of the ICI on the error rate performance of an OFDM system requires knowledge of the PDF of the ICI which, in general, is a mixture of Gaussian PDFs. However, when the number of subcarriers is large, the distribution of the ICI can be approximated by a Gaussian distribution, and thus the evaluation of the error rate performance is straightforward.

Figure 13.6–3 illustrates the symbol error probability for an OFDM system having $N = 256$ subcarriers and 16-QAM, where the error probability is evaluated analytically based on the Gaussian model for the ICI and by Monte Carlo simulation. We observe that the ICI severely degrades the performance of the OFDM system. In the following section we describe a method for suppressing the ICI and, thus, improving the performance of the OFDM system.

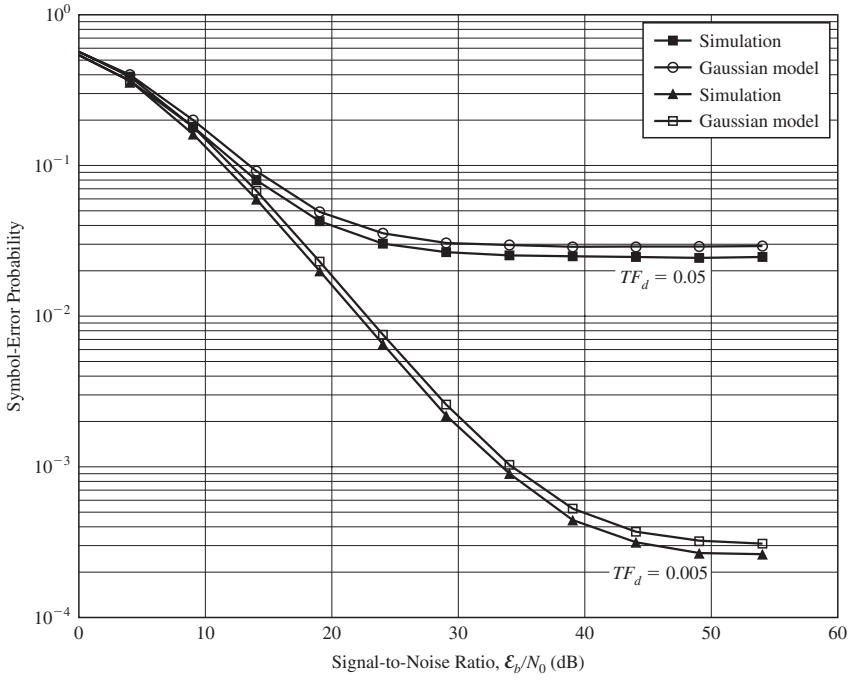

FIGURE 13.6–3
Symbol error probability for 16-QAM OFDM system with $N = 256$ subcarriers.

13.6–2 Suppression of ICI in OFDM Systems

The distortion caused by ICI in an OFDM system is akin to the distortion caused by ISI in a single-carrier system. Recall that a linear time-domain equalizer based on the minimum mean-square-error (MMSE) criterion is an effective method for suppressing ISI. In a similar manner, we may apply the MMSE criterion to suppress the ICI in the frequency domain. Thus, we begin with the N frequency samples at the output of the discrete Fourier transform (DFT) processor, which we denote by the vector $\boldsymbol{R}(m)$ for the mth frame. Then we form the estimate of the symbol $s_k(m)$ as

$$\hat{s}_k(m) = \boldsymbol{b}_k^H(m)\boldsymbol{R}(m), \qquad k = 0, 1, \ldots, N-1 \tag{13.6–22}$$

where $\boldsymbol{b}_k(m)$ is the coefficient vector of size $N \times 1$. This vector is selected to minimize the MSE

$$E\left[|s_k(m) - \hat{s}_k(m)|^2\right] = E\left[|s_k(m) - \boldsymbol{b}_k^H(m)\boldsymbol{R}(m)|^2\right] \tag{13.6–23}$$

where the expectation is taken with respect to the signal and noise statistics. By applying the orthogonality principle, the optimum coefficient vector is obtained as

$$\boldsymbol{b}_k(m) = \left[\boldsymbol{G}(m)\boldsymbol{G}^H(m) + \sigma^2\boldsymbol{I}_N\right]^{-1}\boldsymbol{g}_k(m), \qquad k = 0, 1, \ldots, N-1 \tag{13.6–24}$$

where

$$E\left[\boldsymbol{R}(m)\boldsymbol{R}^H(m)\right] = \boldsymbol{G}(m)\boldsymbol{G}^H(m) + \sigma^2\boldsymbol{I}_N$$
$$E\left[\boldsymbol{R}(m)s_k^H(m)\right] = \boldsymbol{g}_k(m) \tag{13.6–25}$$

and $\boldsymbol{G}(m)$ is related to the channel impulse response matrix $\boldsymbol{H}(m)$ through the DFT relation (see Problem 13.16)

$$\boldsymbol{G}(m) = \boldsymbol{W}^H\boldsymbol{H}(m)\boldsymbol{W} \tag{13.6–26}$$

where $\boldsymbol{W}$ is the orthonormal (IDFT) transformation matrix. The vector $\boldsymbol{g}_k(m)$ is the kth column of the matrix $\boldsymbol{G}(m)$, and σ^2 is the variance of the additive noise component. It is easily shown that the minimum MSE for the signal on the kth subcarrier may be expressed as

$$E\left[|s_k(m) - \hat{s}_k(m)|^2\right] = 1 - \boldsymbol{g}_k^H(m)(\boldsymbol{G}(m)\boldsymbol{G}^H(m) + \sigma^2\boldsymbol{I}_N)^{-1}\boldsymbol{g}_k(m) \tag{13.6–27}$$

We observe that the optimum weight vectors $\{\boldsymbol{b}_k(m)\}$ require knowledge of the channel impulse response. In practice, the channel response may be estimated by periodically transmitting pilot signals on each of the subcarriers and by employing a decision-directed method when data are transmitted on the N subcarriers. In a slowly fading channel, the coefficient vectors $\{\boldsymbol{b}_k(m)\}$ may also be adjusted recursively by employing either an LMS- or an RLS-type algorithm, as previously described in the context of equalization for suppression of ISI.

13.7 BIBLIOGRAPHICAL NOTES AND REFERENCES

In this chapter, we have considered a number of topics concerned with digital communications over a fading multipath channel. We began with a statistical characterization of the channel and then described the ramifications of the channel characteristics on the design of digital signals and on their performance. We observed that the reliability of the communication system is enhanced by the use of diversity transmission and reception. We also considered the transmission of digital information through time-dispersive channels and described the RAKE demodulator, which is the matched filter for the channel. Finally, we considered the use of OFDM for mobile communications and on the performance of an OFDM system, described the effect of ICI caused by Doppler frequency spreading.

The pionerring work on the characterization of fading multipath channels and on signal and receiver design for reliable digital communciations over such channels was done by Price (1954, 1956). This work was followed by additional significant contributions from Price and Green (1958, 1960), Kailath (1960, 1961), and Green (1962). Diversity transmission and diversity combining techniques under a variety of channel conditions have been considered in the papers by Pierce (1958), Brennan (1959), Turin (1961, 1962), Pierce and Stein (1960), Barrow (1963), Bello and Nelin (1962a, b, 1963), Price (1962a, b), and Lindsey (1964).

Our treatment of digital communications over fading channels focused primarily on the Rayleigh fading channel model. For the most part, this is due to the wide acceptance of this model for describing the fading effects on many radio channels and to its mathematical tractability. Although other statistical models, such as the Ricean fading model or the Nakagami fading model may be more appropriate for characterizing fading on some real channels, the general approach in the design of reliable communications presented in this chapter carries over. Alouini and Goldsmith (1998), Simon and Alouini (1988, 2000), and Annamalai et al. (1998, 1999) have presented a unified approach to evaluating the error rate performance of digital communication systems for various fading channel models. The effect of ICI in OFDM for mobile communications has been extensively treated in the literature, e.g., the papers by Robertson and Kaiser (1999), Li and Kavehrad (1999), Ciavaccini and Vitetta (2000), Li and Cimini (2001), Stamoulis et al. (2002), and Wang et al. (2006). A general treatment of wireless communications is given in the books by Rappaport (1996) and Stuber (2000).

PROBLEMS

13.1 The scattering function $S(\tau; \lambda)$ for a fading multipath channel is nonzero for the range of values $0 \leq \tau \leq 1$ ms and $-0.1\,\text{Hz} \leq \lambda \leq 0.1\,\text{Hz}$. Assume that the scattering function is approximately uniform in the two variables.

a. Give numerical values for the following parameters:
   (i) The multipath spread of the channel.
   (ii) The Doppler spread of the channel.
   (iii) The coherence time of the channel.
   (iv) The coherence bandwidth of the channel.
   (v) The spread factor of the channel.

b. Explain the meaning of the following, taking into consideration the answers given in (a):
   (i) The channel is frequency-nonselective.
   (ii) The channel is slowly fading.
   (iii) The channel is frequency-selective.

c. Suppose that we have a frequency allocation (bandwidth) of 10 kHz and we wish to transmit at a rate of 100 bits over this channel. Design a binary communication system with frequency diversity. In particular, specify
   (i) The type of modulation.
   (ii) The number of subchannels.
   (iii) The frequency separation between adjacent carriers.
   (iv) The signaling interval used in your design.
   Justify your choice of parameters.

13.2 Consider a binary communication system for transmitting a binary sequence over a fading channel. The modulation is orthogonal FSK with third-order frequency diversity ($L = 3$). The demodulator consists of matched filters followed by square-law detectors. Assume that the FSK carriers fade independently and identically according to a Rayleigh envelope

distribution. The additive noises on the diversity signals are zero-mean Gaussian with autocorrelation functions $E[z_k^*(t)z_k(t+\tau)] = 2N_0\delta(\tau)$. The noise processes are mutually statistically independent.

a. The transmitted signal may be viewed as binary FSK with square-law detection, generated by a repetition code of the form

$$1 \rightarrow \boldsymbol{c}_1 = [1 \quad 1 \quad 1], \qquad 0 \rightarrow \boldsymbol{c}_0 = [0 \quad 0 \quad 0]$$

Determine the error rate performance P_{bh} for a hard-decision decoder following the square-law-detected signals.

b. Evaluate P_{bh} for $\overline{\gamma}_c = 100$ and 1000.

c. Evaluate the error rate P_{bs} for $\overline{\gamma}_c = 100$ and 1000 if the decoder employs soft-decision decoding.

d. Consider the generalization of the result in (a). If a repetition code of block length L (L odd) is used, determine the error probability P_{bh} of the hard-decision decoder and compare that with P_{bs}, the error rate of the soft-decision decoder. Assume $\overline{\gamma} \gg 1$.

13.3 Suppose that the binary signal $\pm s_l(t)$ is transmitted over a fading channel and the received signal is

$$r_l(t) = \pm a s_l(t) + z(t), \qquad 0 \le t \le T$$

where $z(t)$ is zero-mean white Gaussian noise with autocorrelation function

$$R_{zz}(\tau) = 2N_0\delta(\tau)$$

The energy in the transmitted signal is $\mathcal{E} = \frac{1}{2}\int_0^T |s_l(t)|^2\, dt$. The channel gain a is specified by the probability density function

$$p(a) = 0.1\delta(a) + 0.9\delta(a-2)$$

a. Determine the average probability of error P_b for the demodulator that employs a filter matched to $s_l(t)$.

b. What value does P_b approach as $\mathcal{E}/N_0$ approaches infinity?

c. Suppose that the same signal is transmitted on two statistically *independently fading* channels with gains a_1 and a_2, where

$$p(a_k) = 0.1\delta(a_k) + 0.9\delta(a_k - 2), \qquad k = 1, 2$$

The noises on the two channels are statistically independent and identically distributed. The demodulator employs a matched filter for each channel and simply adds the two filter outputs to form the decision variable. Determine the average P_b.

d. For the case in (c) what value does P_b approach as $\mathcal{E}/N_0$ approaches infinity?

13.4 A multipath fading channel has a multipath spread of $T_m = 1$ s and a Doppler spread $B_d = 0.01$ Hz. The total channel bandwidth at bandpass available for signal transmission is $W = 5$ Hz. To reduce the effects of intersymbol interference, the signal designer selects a pulse duration $T = 10$ s.

a. Determine the coherence bandwidth and the coherence time.

b. Is the channel frequency selective? Explain.

c. Is the channel fading slowly or rapidly? Explain.

d. Suppose that the channel is used to transmit binary data via (antipodal) coherently detected PSK in a frequency diversity mode. Explain how you would use the available

channel bandwidth to obtain frequency diversity and determine how much diversity is available.

e. For the case in (d), what is the *approximate* SNR required per diversity to achieve an error probability of 10^{-6}?

f. Suppose that a wideband signal is used for transmission and a RAKE-type receiver is used for demodulation. How many taps would you use in the RAKE receiver?

g. Explain whether or not the RAKE receiver can be implemented as a coherent receiver with maximal ratio combining.

h. If binary orthogonal signals are used for the wideband signal with square-law post-detection combining in the RAKE receiver, what is the *approximate* SNR required to achieve an error probability of 10^{-6}? (Assume that all taps have the same SNR.)

13.5 In the binary communication system shown in Figure P13.5, $z_1(t)$ and $z_2(t)$ are statistically independent white Gaussian noise processes with zero-mean and identical autocorrelation functions $R_{zz}(\tau) = 2N_0\delta(\tau)$. The sampled values U_1 and U_2 represent the *real parts* of the matched filter outputs. For example, if $s_l(t)$ is transmitted, then we have

$$U_1 = 2\mathcal{E} + N_1$$
$$U_2 = N_1 + N_2$$

where $\mathcal{E}$ is the transmitted signal energy and

$$N_k = \text{Re}\left[\int_0^T s_l^*(t) z_k(t)\, dt\right], \qquad k = 1, 2$$

It is apparent that U_1 and U_2 are correlated Gaussian variables while N_1 and N_2 are independent Gaussian variables. Thus,

$$p(n_1) = \frac{1}{\sqrt{2\pi}\sigma} \exp\left(-\frac{n_1^2}{2\sigma^2}\right)$$
$$p(n_2) = \frac{1}{\sqrt{2\pi}\sigma} \exp\left(-\frac{n_2^2}{2\sigma^2}\right)$$

where the variance of N_k is $\sigma^2 = 2\mathcal{E}N_0$.

a. Show that the joint probability density function for U_1 and U_2 is

$$p(u_1, u_2) = \frac{1}{2\pi\sigma^2} \exp\left\{-\frac{1}{\sigma^2}\left[(u_2 - 2\mathcal{E})^2 - u_2(u_1 - 2\mathcal{E}) + \tfrac{1}{2}u_2^2\right]\right\}$$

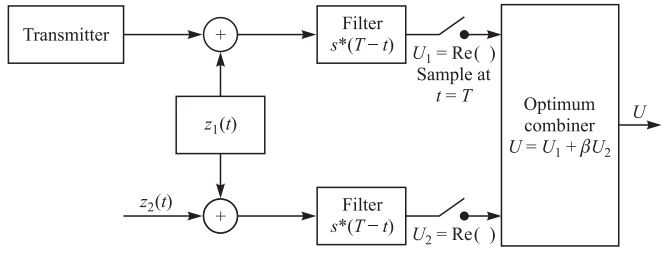

FIGURE P13.5

if $s(t)$ is transmitted and

$$p(u_1, u_2) = \frac{1}{2\pi\sigma^2} \exp\left\{-\frac{1}{\sigma^2}\left[(u_1 + 2\mathcal{E})^2 - u_2(u_1 + 2\mathcal{E}) + \tfrac{1}{2}u_2^2\right]\right\}$$

if $-s(t)$ is transmitted.

b. Based on the likelihood ratio, show that the optimum combination of U_1 and U_2 results in the decision variable

$$U = U_1 + \beta U_2$$

where β is a constant. What is the optimum value of β?

c. Suppose that $s(t)$ is transmitted. What is the probability density function of U?

d. What is the probability of error assuming that $s(t)$ was transmitted? Express your answer as a function for the SNR $\mathcal{E}/N_0$.

e. What is the loss in performance if only $U = U_1$ is the decision variable?

13.6 Consider the model for a binary communication system with diversity as shown in Figure P13.6. The channels have fixed attenuations and phase shifts. The $\{z_k(t)\}$ are complex-valued white Gaussian noise processes with zero-mean and autocorrelation functions

$$R_{zz}(t) = E\left[z_k^*(t)z_k(t+\tau)\right] = 2N_{0k}\delta(\tau)$$

(Note that the spectral densities $\{N_{0k}\}$ are all different.) Also, the noise processes $\{z_k(t)\}$ are mutually statistically independent. The $\{\beta_k\}$ are complex-valued weighting factors to be determined. The decision variable from the combiner is

$$U = \text{Re}\left(\sum_{k=1}^{L} \beta_k U_k\right) \underset{-1}{\overset{1}{\gtrless}} 0$$

a. Determine the PDF $p(u)$ when $+1$ is transmitted.

b. Determine the probability of error P_b as a function of the weights $\{\beta_k\}$.

c. Determine the values of $\{\beta_k\}$ that minimize P_b.

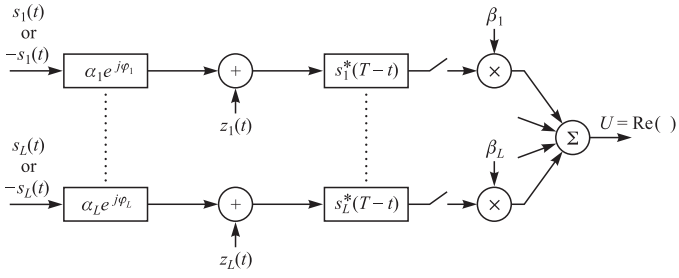

FIGURE P13.6

13.7 Determine the probability of error for binary orthogonal signaling with Lth-order diversity over a Rayleigh fading channel. The PDFs of the two decision variables are given by Equations 13.4–31 and 13.4–32.

13.8 A binary sequence is transmitted via binary antipodal signaling over a Rayleigh fading channel with Lth-order diversity. When $s_l(t)$ is transmitted, the received equivalent low-pass signals are

$$r_k(t) = \alpha_k e^{j\phi_k} s_l(t) + z_k(t), \qquad k = 1, 2, \ldots, L$$

The fading among the L subchannels is statistically independent. The additive noise terms $\{z_k(t)\}$ are zero-mean, statistically independent, and identically distributed white Gaussian noise processes with autocorrelation function $R_{zz}(\tau) = 2N_0\delta(\tau)$. Each of the L signals is passed through a filter matched to $s_l(t)$ and the output is phase-corrected to yield

$$U_k = \text{Re}\left[e^{-j\phi_k} \int_0^T r_k(t) s_l^*(t)\, dt\right], \qquad k = 1, 2, \ldots, L$$

The $\{U_k\}$ are combined by a linear combiner to form the decision variable

$$U = \sum_{k=1}^{L} U_k$$

a. Determine the PDF of U conditional on fixed values for the $\{a_k\}$.
b. Determine the expression for the probability of error when the $\{a_k\}$ are statistically independent and identically distributed Rayleigh random variables.

13.9 The Chernov bound for the probability of error for binary FSK with diversity L in Rayleigh fading was shown to be

$$P_2(L) < [4p(1-p)]^L = \left[4\frac{1+\overline{\gamma}_c}{(2+\overline{\gamma}_c)^2}\right]^L$$
$$< 2^{-\overline{\gamma}_b g(\overline{\gamma}_c)}$$

where

$$g(\overline{\gamma}_c) = \frac{1}{\overline{\gamma}_c} \log_2\left[\frac{(2+\overline{\gamma}_c)^2}{4(1+\overline{\gamma}_c)}\right]$$

a. Plot $g(\overline{\gamma}_c)$ and determine its approximate maximum value and the value of $\overline{\gamma}_c$ where the maximum occurs.
b. For a given $\overline{\gamma}_b$, determine the optimal order of diversity.
c. Compare $P_2(L)$, under the condition that $g(\overline{\gamma}_c)$ is maximized (optimal diversity), with the error probability for binary FSK and AWGN with no fading, which is

$$P_2 = \tfrac{1}{2}e^{-\gamma_b/2}$$

and determine the penalty in SNR due to fading and noncoherent (square-law) combining.

13.10 A DS spread spectrum system is used to resolve the multipath signal components in a two-path radio signal propagation scenario. If the path length of the secondary path is 300 m longer than that of the direct path, determine the minimum chip rate necessary to resolve the multipath components.

13.11 A baseband digital communication system employs the signals shown in Figure P13.11(a) for the transmission of two equiprobable messages. It is assumed that the communication problem studied here is a "one-shot" communication problem; that is, the above messages are transmitted just once and no transmission takes place afterward. The channel has no attenuation ($\alpha = 1$), and the noise is AWGN with power spectral density $\frac{1}{2}N_0$.

a. Find an appropriate orthonormal basis for the representation of the signals.

b. In a block diagram, give the precise specifications of the optimum receiver using matched filters. Label the diagram carefully.

c. Find the error probability of the optimum receiver.

d. Show that the optimum receiver can be implemented by using just *one* filter (see the block diagram in Figure P13.11(b)). What are the characteristics of the matched filter, the sampler and decision device?

e. Now assume that the channel is not ideal but has an impulse response of $c(t) = \delta(t) + \frac{1}{2}\delta(t - \frac{1}{2}T)$. Using the same matched filter as in (d), design the optimum receiver.

f. Assuming that the channel impulse response is $c(t) = \delta(t) + a\delta(t - \frac{1}{2}T)$, where a is a random variable uniformly distributed on [0, 1], and using the same matched filter as in (d), design the optimum receiver.

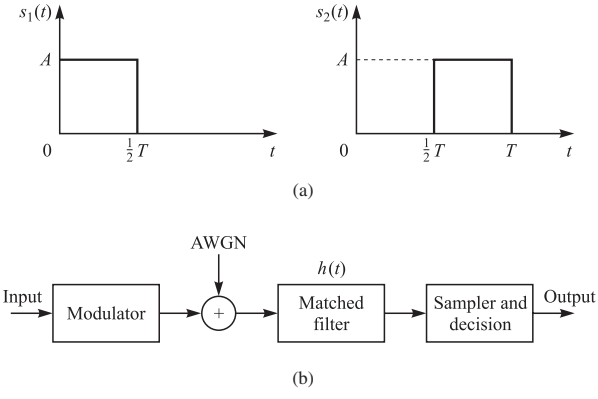

FIGURE P13.11

13.12 A communication system employs dual antenna diversity and binary orthogonal FSK modulation. The received signals at the two antennas are

$$r(t) = \alpha_1 s(t) + n_1(t)$$
$$r_2(t) = \alpha_2 s(t) + n_2(t)$$

where α_1 and α_2 are statistically iid Rayleigh random variables, and $n_1(t)$ and $n_2(t)$ are statistically independent, zero-mean and white Gaussian random processes with power-spectral density $\frac{1}{2}N_0$. The two signals are demodulated, squared, and then combined (summed) prior to detection.

a. Sketch the functional block diagram of the entire receiver, including the demodulator, the combiner, and the detector.

b. Plot the probability of error for the detector and compare the result with the case of no diversity.

13.13 The two equivalent lowpass signals shown in Figure P13.13 are used to transmit a binary sequence. The equivalent low-pass impulse response of the channel is $h(t) = 4\delta(t) - 2\delta(t-T)$. To avoid pulse overlap between successive transmissions, the transmission rate in bits/s is selected to be $R = 1/2T$. The transmitted signals are equally probable and are corrupted by additive zero-mean white Gaussian noise having an equivalent lowpass representation $z(t)$ with an autocorrelation function

$$R_{zz}(\tau) = E[z^*(t)z(t+\tau)] = 2N_0\delta(\tau)$$

a. Sketch the two possible equivalent lowpass noise-free *received* waveforms.
b. Specify the optimum receiver and sketch the equivalent lowpass impulse responses of all filters used in the optimum receiver. Assume *coherent detection* of the signals.

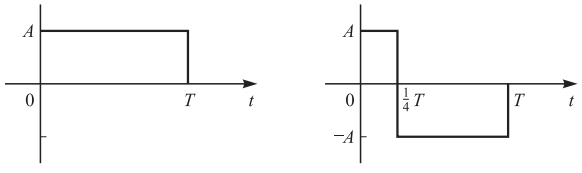

FIGURE P13.13

13.14 Verify the relation in Equation 13.3–14 by making the change of variable $\gamma = \alpha^2\mathcal{E}_b/N_0$ in the Nakagami-*m* distribution.

13.15 Consider a digital communication system that uses two transmitting antennas and one receiving antenna. The two transmitting antennas are sufficiently separated so as to provide dual spatial diversity in the transmission of the signal. The transmission scheme is as follows: If s_1 and s_2 represent a pair of symbols from either a one-dimensional or a two-dimensional signal constellation, which are to be transmitted by the two antennas, the signal from the first antenna over two signal intervals is (s_1, s_2^*) and from the second antenna the transmitted signal is $(s_2, -s_1^*)$. The signal received by the single receiving antenna over the two signal intervals is

$$r_1 = h_1 s_1 + h_2 s_2 + n_1$$
$$r_2 = h_1 s_2^* - h_2 s_1^* + n_2$$

where (h_1, h_2) represent the complex-valued channel path gains, which may be assumed to be zero-mean, complex Gaussian with unit variance and statistically independent. The channel path gains (h_1, h_2) are assumed to be constant over the two signal intervals and known to the receiver. The terms (n_1, n_2) represent additive white Gaussian noise terms that have zero-mean and variance σ^2 and uncorrelated.
a. Show how to recover the transmitted symbols (s_1, s_2) from (r_1, r_2) and achieve dual diversity reception.
b. If the energy in the pair (s_1, s_2) is $(\mathcal{E}_s, \mathcal{E}_s)$ and the modulation is binary PSK, determine the probability of error.
c. Repeat (b) if the modulation is QPSK.

13.16 In the suppression of ICI in on DFDM system, the received signal vector for the *m*th frame may be expressed as

$$\boldsymbol{r}(m) = \boldsymbol{H}(m)\boldsymbol{W}\boldsymbol{s}(m) + \boldsymbol{n}(m)$$

where $\boldsymbol{W}$ is the $N \times N$ IDFT transformation matrix, $\boldsymbol{s}(m)$ is the $N \times 1$ signal vector, $\boldsymbol{n}(m)$ is the zero-mean, Gaussian noise vector with iid components, and $\boldsymbol{H}(m)$ is the $N \times N$ channel impulse response matrix, defined as

$$\boldsymbol{H}(m) = [\boldsymbol{h}^H(0, m)\, \boldsymbol{h}^H(1, m) \cdots \boldsymbol{h}^H(N-1, m)]^H$$

where $\boldsymbol{h}(n, m)$ is the right cyclic shift by $n + 1$ positions of the zero-padded channel impulse response vector of dimension $N \times 1$.

By expressing the DFT of $\boldsymbol{r}(m)$ by $\boldsymbol{R}(m)$, derive the relations in Equations 13.6–24, 13.6–25, and 13.6–27, where $\boldsymbol{G}(m)$ is defined in Equation 13.6–26.

13.17 Prove the result given in Equation 13.6–17.

13.18 Prove the result given in Equation 13.6–18.